AN ABSTRACT OF THE DISSERTATION OF

Matthias C. Merzenich for the degree of Doctor of Philosophy in Mathematics presented on June 4, 2020.

Title: A Computational Method for Building Spherical Pictures and Theoretic Results from Explicit Constructions

Abstract approved: _____

William A. Bogley

Let H be a cyclically-presented group on n generators with a single defining relator. Attempts have been made to classify such groups by their order, their status as a 3-manifold group, and the asphericity status of their presentations. For groups with a defining relator of length 3 these classifications are nearly complete, with only two groups, $H(9,4)$ and $H(9,7)$, representing outstanding cases in each classification. We complete the asphericity classification for the presentations of these two groups and show that $H(9,4)$ is not a 3-manifold group. We also determine that $H(9,7)$ is a 3-manifold group if and only if it is cyclic of order 37.

We consider a relative presentation $\mathcal{P}$ for a natural degree-n split extension E of H, and apply a practical computational method to find reduced relative spherical pictures (a type of graph) over $\mathcal{P}$. Our method uses a depth-first search to construct pictures region-by-region (i.e., face-by-face) from a pre-chosen starting region. New regions are typically added directly adjacent to the newest and oldest regions with available edges. This gives a construction of relative picture in a spiral ordering centered on the initial region. The addition of regions outside of this spiral ordering is sometimes required, but is done only in a limited capacity. Some user-defined limitations are also applied to prevent the search

from continuing indefinitely down non-viable branches of the search graph. The method terminates when all edges have been connected–resulting in a complete picture–or when the search backs up and can no longer continue from the initial region.

We successfully apply our method to the split extensions arising from $H(9, 4)$ and $H(9, 7)$. In each case, the resulting symmetric picture reveals interesting relations in the group extension E. In particular, these relations can establish that the relative presentation $\mathcal{P}$ for E is not relatively aspherical, and hence the presentation for the cyclically-presented group H is not aspherical in each case. One of these two cyclically-presented groups, $H(9, 7)$, is also shown to contain a torsion element. The question of whether these groups are infinite remains unresolved.

A Computational Method for Building Spherical Pictures and Theoretic Results from
Explicit Constructions

by

Matthias C. Merzenich

A DISSERTATION

submitted to

Oregon State University

in partial fulfillment of
the requirements for the
degree of

Doctor of Philosophy

Presented June 4, 2020
Commencement June 2021

Doctor of Philosophy dissertation of Matthias C. Merzenich presented on June 4, 2020

APPROVED:

_____

Major Professor, representing Mathematics

_____

Head of the Department of Mathematics

_____

Dean of the Graduate School

I understand that my dissertation will become part of the permanent collection of Oregon State University libraries. My signature below authorizes release of my dissertation to any reader upon request.

_____

Matthias C. Merzenich, Author

ACKNOWLEDGEMENTS

TABLE OF CONTENTS

TABLE OF CONTENTS (Continued)

TABLE OF CONTENTS (Continued)

Page

LIST OF FIGURES

LIST OF FIGURES (Continued)

LIST OF TABLES

LIST OF APPENDIX FIGURES

NOTATION

Let k, m, n be integers with $n > 0$.

C_n	the finite cyclic group of order n
F_n	the free group on n generators
θ	the shift automorphism on F_n
$G_n(m, k)$	the groups of Fibonacci type with presentations $\mathcal{G}_n(m, k)$
$F(2, n)$	the Fibonacci groups with presentations $\mathcal{F}(2, n) = \mathcal{G}_n(1, 2)$
$H(n, m)$	the Gilbert-Howie groups with presentations $\mathcal{H}(n, m) = \mathcal{G}_n(m, 1)$
$S(2, n)$	the Sieradski groups with presentations $\mathcal{S}(2, n) = \mathcal{G}_n(2, 1)$

Let $w \in F_n$.

$G_n(w)$	the cyclically presented group with generator w
$E_n(w)$	the shift extension of $G_n(w)$

Let $\mathbf{x}$ be a set.

$F(\mathbf{x})$	the free group on $\mathbf{x}$
$\mathbf{x}^{-1}$	the set $\{x^{-1} : x \in \mathbf{x}\}$ of inverses of elements of $\mathbf{x}$
$|\mathbf{x}|$	the cardinality of $\mathbf{x}$

Let G and H be groups.

$G \times H$	the direct product
$G * H$	the free product
$G \rtimes H$	the split extension of G by H
$G \rtimes_\varphi H$	the split extension of G by H with H-action φ
$G \cong H$	G is isomorphic to H
G/H	the quotient of G by H
$K(G, 1)$	an Eilenberg-MacLane space

NOTATION (Continued)

Let $a, b \in G$ and $\mathbf{s} \subseteq G$.

$|a|$ the order of a

$[a, b]$ the commutator of a and b

$\langle\langle\mathbf{s}\rangle\rangle$ the least normal subgroup of G containing $\mathbf{s}$

Let $\mathbf{r} \subseteq G * F(\mathbf{x})$.

$\mathbf{r}^*$ the set of all cyclic permutations of elements of $\mathbf{r} \cup \mathbf{r}^{-1}$ that start with a symbol in $\mathbf{x} \cup \mathbf{x}^{-1}$

$\widetilde{\mathbf{r}}$ the set of lifted words

Let $R = Sg \in \mathbf{r}^*$ where $g \in G$ and S begins and ends with an element of $\mathbf{x} \cup \mathbf{x}^{-1}$.

$\overline{R}$ $S^{-1}g^{-1}$

$\lambda(R)$ g^{-1}

Let $\mathcal{P} = \langle G, \mathbf{x} \mid \mathbf{r} \rangle$ be a relative presentation.

$G(\mathcal{P})$ the group defined by $\mathcal{P}$

$L(\mathcal{P})$ the relative cellular model of $\mathcal{P}$

$\widetilde{\mathcal{P}}$ a lifted presentation

$\mathcal{P}^{\mathrm{st}}$ the star graph

Let $w = (R_1, R_2 \ldots, R_n)$ be a walk in $\mathcal{P}^{\mathrm{st}}$ where $R_1, R_2, \ldots, R_n \in \mathbf{r}^*$.

$\lambda(w)$ $\lambda(R_1)\lambda(R_2) \cdots \lambda(R_n)$

Let L and K be path-connected topological spaces with $K \subseteq L$.

$\pi_n(L)$ the nth homotopy group of L

$\pi_n(L, K)$ the nth relative homotopy group of the pair (L, K)

NOTATION (Continued)

Let $\mathbb{P}$ be a picture over $\mathcal{P}$.

$\widetilde{\mathbb{P}}$ a lifted picture over $\widetilde{\mathcal{P}}$

$\partial\mathbb{P}$ the boundary of $\mathbb{P}$

Let κ be a corner of $\mathbb{P}$.

$W(\kappa)$ the element of $\mathbf{r}^*$ obtained by reading counterclockwise around the disc associated to κ

Let M and N be manifolds.

$M\#N$ the connected sum

DEDICATION

This work is dedicated to the memory of John Horton Conway, who inspired my lifelong love of mathematics. It was his simple question that sparked the study of cyclically-presented groups on which this work is based.

A COMPUTATIONAL METHOD FOR BUILDING SPHERICAL PICTURES AND THEORETIC RESULTS FROM EXPLICIT CONSTRUCTIONS

1 INTRODUCTION

1.1 Background

In 1965, John Horton Conway [17] asked whether the group on 5 generators a, b, c, d, e subject only to the relations $ab = c$, $bc = d$, $cd = e$, $de = a$, $ea = b$ is cyclic of order 11. This question generated significant interest [18], as the group naturally generalizes to groups on n generators. These groups are now known as the **Fibonacci groups** $F(2, n)$ with presentations

$$\mathcal{F}(2, n) = \langle x_0, \ldots, x_{n-1} \mid x_i x_{i+1} = x_{i+2} \ (0 \leq i < n) \rangle$$

where all indices are reduced mod n. The most studied question regarding these groups is whether they are finite or infinite. By 1974 this question had been answered for all these groups except $F(2, 9)$, with $F(2, n)$ being infinite for $n = 6, 8$ and $n \geq 10$ [11]. $F(2, 9)$ was finally shown to be infinite in 1990 by Newman [51] based on computational results from various authors. While the finiteness question has been a major driver of interest in these groups, many other questions have arisen about their structure.

We consider a natural generalization of the Fibonacci groups. Let w be a word in the free group F_n with generators $x_0, \ldots x_{n-1}$, and let $\theta \colon F_n \to F_n$ be the **shift automorphism** defined by $x_i \mapsto x_{i+1}$ (subscripts mod n). The **cyclic presentation**

$$\mathcal{G}_n(w) = \langle x_0, \ldots, x_{n-1} \mid w, \theta(w), \ldots, \theta^{n-1}(w) \rangle.$$

defines the **cyclically presented group** $G_n(w)$.

We are concerned with the **groups of Fibonacci type**, that is, the 3-parameter family $G_n(m, k) = G_n(x_0 x_m x_k^{-1})$. This family was first considered in [43] and generalizes the Fibonacci groups $F(2, n) = G_n(1, 2)$, as well as the **Sieradski groups** $S(2, n) = G_n(2, 1)$ of [57] and the **Gilbert-Howie groups** $H(n, m) = G_n(m, 1)$ of [25] (we write

$\mathcal{G}_n(m,k)$, $\mathcal{S}(2,n)$, and $\mathcal{H}(n,m)$ for the presentations of these groups). Many results about these groups were collected in [40, 61] and in most cases, two groups stand out. $H(9,4)$ and $H(9,7)$ have proven difficult to study, and several classification results note these as the only exceptional unsolved cases. These two groups, and their presentations $\mathcal{H}(9,4)$ and $\mathcal{H}(9,7)$, are the primary focus of this dissertation. The finiteness question for these groups is still unresolved [40].

Of particular interest to us are two topological questions. The first concerns group presentations. Given a group H with presentation $\mathcal{P}$, it is possible to build a 2-dimensional CW-complex L based on $\mathcal{P}$ with fundamental group H. If the higher homotopy groups $\pi_i(L)$ are trivial, then L is an aspherical space (since L is 2-dimensional, we only need to consider $\pi_2(L)$). A classical result of CW topology gives that the fundamental group of a finite-dimensional aspherical CW-complex is torsion free [30, Proposition 2.45]. This has immediate bearing on the finiteness question. Indeed, showing that a group presentation defines an aspherical complex is the route by which many groups have been shown to be infinite [55, 15, 5, 22].

It is natural to ask whether a presentation $\mathcal{P}$ defines an aspherical CW-complex. We call this the **asphericity question** for $\mathcal{P}$. One of the primary approaches for resolving this question is the theory of pictures. For many presentations, generators of $\pi_2(L)$ can be constructed combinatorially as certain labeled planar graphs called spherical pictures. If it can shown that every spherical picture represents the identity in $\pi_2(L)$, then this suffices to prove asphericity.

We approach the asphericity question of $\mathcal{G}_n(w)$ by considering a natural extension for the group $G_n(w)$. The shift automorphism θ defined on F_n descends to an automorphism on $G_n(w)$. By letting $x_i = g^i x g^{-i}$ we can construct the **shift extension** $E_n(w) = G_n(w) \rtimes_\theta C_n$ with a two-generator two-relator presentation of the form $\mathcal{E}_n(w) = \langle g, x \mid g^n, W \rangle$ where $W \in \langle g \rangle * \langle x \rangle$. This extension suggests the more general

notion of a relative group presentation $\langle G, x \mid W \rangle$ where G is a group and $W \in G * \langle x \rangle$. The groups $E_n(w)$ then have a relative presentation $\langle G, x \mid W \rangle$ with G cyclic of order n. A recent treatment of relative presentations is given in [10].

Associated to relative presentations is the concept of relative asphericity and relative pictures. These concepts have been explored directly in [7, 21, 4, 5, 22] (see the references in [10] for further examples). Not surprisingly, there is a direct connection between the asphericity question for cyclically presented groups and the relative asphericity question for their extensions. We develop a method to search for relative spherical pictures which we implement as a computer program. In this way, our work extends beyond cyclically presented groups.

The (ordinary) asphericity question had previously been answered for presentations of the form $\mathcal{G}_n(m, k)$ that are not in some sense equivalent to $\mathcal{H}(9, 4)$ or $\mathcal{H}(9, 7)$ [25][60] (see also [61, Theorems 25 and 26]). In this dissertation we resolve the asphericity question for $\mathcal{H}(9, 4)$ and $\mathcal{H}(9, 7)$, completing the asphericity classification for prestentations of Fibonacci type. In both cases, the presentation is not aspherical, so this does not appear to be an immediate avenue towards a resolution of the finiteness question for $H(9, 4)$ or $H(9, 7)$.

Our second topological question, the **3-manifold question,** asks whether a given group is the fundamental group of a 3-manifold. Helling, Kim, and Mennicke [48] found that for even $n \geq 8$, $F(2, n)$ is the fundamental group of a hyperbolic 3-manifold. Since hyperbolic 3-manifolds are covered by the contractible space $\mathbb{H}^3$, they are aspherical, so their fundamental groups are torsion-free. Cavicchioli, Repovš, and Spaggiari [13, Corollary 3.5], expanding on the ideas of Maclachlan [45], proved that many cyclically presented groups with an odd number of generators could not be the fundamental group of a closed, oriented, hyperbolic 3-manifold with finite volume, among them $H(9, 4)$ and $H(9, 7)$.

Howie and Williams [40] considered the general 3-manifold question for groups of Fibonacci type, and produced a classification that omitted groups isomorphic to $H(9,4)$ or $H(9,7)$ as the only unsolved cases. We prove that $H(9,4)$ is not a 3-manifold group and that $H(9,7)$ is a 3-manifold group if and only if it is cyclic of order 37, very nearly completing this classification. Our proof makes use of the Elliptization Theorem–a consequence of the Geometrization Theorem proved by Perelman [52, 53, 54] based on the earlier work of Hamilton [27, 28, 29]–which places significant restrictions on the structure of finite 3-manifold groups.

1.2 Main Results

Our first result is the development and implementation of a method for searching for spherical pictures over certain relative group presentations. Despite the limitations discussed in Section 3.5, it has proven sufficient for discovering pictures in some previously unresolved cases. The structures of these pictures form the basis for the series of theorems given below.

The relative asphericity question for presentations of the form $\langle G, x \mid xaxbx^{-1}c \rangle$ was largely answered by Edjvet in [21]. Three exceptional cases were identified, one of which was solved by Bardakov and Vesnin in [3]. We answer this question for the remaining two cases, the results being given in Theorems A and B. This naturally yields answers to the ordinary asphericity question in the two unsolved cases listed in [61, Theorem 25] (see also [25, Theorem 3.2]), as captured in Corollaries A.1 and B.2. We additionally show that the group in Theorem B has interesting torsion.

Theorem A. *Let* $G = \langle g \mid g^9 \rangle$. *Then the relative presentation* $\mathcal{P} = \langle G, x \mid x^2 g x^{-1} g^3 \rangle$ *is not aspherical.*

Corollary A.1. *The presentation* $\mathcal{H}(9,4)$ *is not aspherical.*

Theorem B. *Let $G = \langle g \mid g^9 \rangle$. Then the group generated by the relative presentation $\mathcal{P} = \langle G, x \mid x^2 g x^{-1} g^{-3} \rangle$ contains a finite subgroup that is not isomorphic (and hence not conjugate) to a subgroup of G. In particular, $\mathcal{P}$ is not aspherical.*

Corollary B.1. *$H(9,7)$ has nontrivial torsion.*

Corollary B.2. *The presentation $\mathcal{H}(9,7)$ is not aspherical.*

The complete classification of relative asphericity for the cases considered in [21] is given by Theorem C. While the presentations in [21] have a more general form, they each reduce to one of those given here by a series of Tietze transformations, and these reductions preserve the answer to the asphericity question. Our contribution is in the resolution of cases (k) and (l).

Theorem C. *Let $\mathcal{P} = \langle G, x \mid x^2 g x^{-1} h \rangle$ where $g, h \in G$ and $|g| \geq |h| > 1$. Then $\mathcal{P}$ is not aspherical if and only if $|g| < \infty$ and at least one of the following holds.*

(a) $\dfrac{1}{|g|} + \dfrac{1}{|h|} + \dfrac{1}{|gh^{-1}|} > 1,$

(b) $h = g^{-1},$

(c) $h = g^{-2}$ *or* $g = h^{-2},$

(d) $|h| = 2$ *and* $[g, h] = 1,$

(e) $|g| = 3$, $|h| = 2$, *and* $(gh)^2 = (hg)^2,$

(f) $|g| = |h| = 3$ *and* $[g, h] = 1,$

(g) $|g| = 6$ *and* $h = g^2,$

(h) $|g| = 7$, *and* $h = g^2$ *or* $g = h^2,$

(i) $|g| = 8$, *and* $h = g^2,$

(j) $|g| = 9$, and $h = g^2$ or $g = h^2$,

(k) $|g| = 9$ and $h = g^3$,

(l) $|g| = 9$ and $h = g^{-3}$.

We next consider which obstructions to asphericity are present in the exceptional cases of Theorem C. Two obstructions suffice to establish nonasphericity in the cases (a)–(j) and (l). The following theorem is due to William Bogley, except as it regards cases (k) and (l) of Theorem C.

Theorem D. *Let $\mathcal{P} = \langle G, x \mid x^2 g x^{-1} h \rangle$ where $G = \langle g, h \rangle$ and $|g| \geq |h| > 1$. Then at least one of the following conditions holds:*

(i) *$\mathcal{P}$ is aspherical.*

(ii) *There exists a finite subgroup of $G(\mathcal{P})$ that is not conjugate to a subgroup of G.*

(iii) *The natural map $G \to G(\mathcal{P})$ is split by a retraction $G(\mathcal{P}) \to G$ whose kernel is a nontrivial 3-manifold group.*

(iv) *$|g| = 9$, and $h = g^3$.*

Moreover, $\mathcal{P}$ is not aspherical in cases (ii)–(iv).

We wonder if the statement of Theorem D is still true with (iv) removed–that is, if case (k) of Theorem C satisfies (ii) or (iii). Theorem F shows that (k) does not satisfy (iii), but it is not known whether (k) satisfies (ii). We may consider relaxing (iii) as follows.

(iii)$'$ The natural map $G \to G(\mathcal{P})$ is split by a retraction $G(\mathcal{P}) \to G$ that is not an isomorphism, and $G(\mathcal{P})$ is a virtual 3-manifold group.

It may then be possible that (k) satisfies (iii)$'$, however Corollary E.1 shows that if (k) does not satisfy (ii), then it also does not satisfy (iii)$'$. Thus, even in this relaxed form, the possibility of removing (iv) from Theorem D is dependent on its inclusion in case (ii).

Theorem E. *Let* $\mathcal{P} = \langle G, x \mid x^2 g x^{-1} g^3 \rangle$ *where* $G = \langle g \mid g^9 \rangle$. *If every finite subgroup of* $G(\mathcal{P})$ *has order dividing* 18, *then* $G(\mathcal{P})$ *is not a virtual 3-manifold group.*

Corollary E.1. *Let* $\mathcal{P} = \langle G, x \mid x^2 g x^{-1} g^3 \rangle$ *where* $G = \langle g \mid g^9 \rangle$. *If every finite subgroup of* $G(\mathcal{P})$ *is conjugate to a subgroup of* G, *then* $G(\mathcal{P})$ *is not a virtual 3-manifold group.*

In [40, Theorem A] Howie and Williams identified, with the exception of those groups that are isomorphic to $H(9,4)$ or $H(9,7)$, precisely which groups of Fibonacci type are the fundamental groups of 3-manifolds. We contribute to this classification by showing that $H(9,4)$ is not a 3-manifold group. We additionally show that if $H(9,7)$ is a 3-manifold group, then it must be isomorphic to the cyclic group C_{37}.

Theorem F. $H(9,4)$ *is not a 3-manifold group.*

Theorem G. $H(9,7)$ *is a 3-manifold group if and only if* $H(9,7) \cong C_{37}$.

Finally, we successfully apply our picture searching method to one of the exceptional presentations in [5] (Exception E2). We additionally prove that the group defined by this presentation has interesting torsion, and hence that the presentation is not aspherical.

Theorem H. *Let* $G = \langle g \mid g^6 \rangle$. *Then the element* xg^{-1} *has order* 12 *in the group generated by the relative presentation* $\mathcal{P} = \langle G, x \mid x^3 g^2 x^{-1} g \rangle$. *In particular,* $\mathcal{P}$ *is not aspherical.*

1.3 Organization of this Dissertation

Chapter 2 contains background material that is necessary to understand the theorems given in Section 1.2, as well as their proofs. In Section 2.1 we describe the basic notation for group presentations and relative presentation. We define asphericity and relative asphericity, the main subject of our theorems, in Section 2.2. Our proofs rely heavily on the theory of pictures, which is discussed at length in Section 2.3. We consider a

connection between relative asphericity and ordinary asphericity in Section 2.4. This also includes explanations of Corollaries A.1 and B.2. Finally, we include some basic results in the theory of 3-manifold groups in Section 2.5.

Chapter 3 is devoted to discussion of our picture-building method. Our method is described in detail in Section 3.1, and outlined in a flow chart in Figure 3.2. We provide basic examples in Sections 3.2 and 3.3 to give a sense of how our method works. We give details of our specific implementation in Section 3.4, and we discuss limitations of our method in general in Section 3.5.

Chapter 4 contains results obtained from our program. This includes both direct output (Section 4.1) and explicit constructions of spherical pictures (Section 4.2). These results are used in Chapter 5 to prove the theorems listed in Section 1.2.

Spherical pictures generated by our program for some presentations known to be nonaspherical are given in Appendix A.

2 PRELIMINARIES

2.1 Notation and Conventions

Here we define notation that will be used throughout the subsequent chapters. The usage of symbols in this section will be consistent with later sections (so G always represents a coefficient group, $\mathbf{x}$ always represents a set of generators, etc.) Unless otherwise stated, we adopt definitions and notation from [10].

A **relative group presentation** (or **relative presentation**) $\mathcal{P}$ is a triple

$$\mathcal{P} = \langle G, \mathbf{x} \mid \mathbf{r} \rangle$$

where G is a group (called the **coefficient group** of $\mathcal{P}$), $\mathbf{x}$ is a set (called the **generators** of $\mathcal{P}$), and $\mathbf{r}$ is a subset of $G * F(\mathbf{x})$ (called the **relators** of $\mathcal{P}$) where $F(\mathbf{x})$ denotes the free group on $\mathbf{x}$.

The relative presentation $\mathcal{P} = \langle G, \mathbf{x} \mid \mathbf{r} \rangle$ defines a group

$$G(\mathcal{P}) = (G * F(\mathbf{x}))/\langle\!\langle \mathbf{r} \rangle\!\rangle$$

where $\langle\!\langle \mathbf{r} \rangle\!\rangle$ is the normal closure of $\mathbf{r}$ in $G * F(\mathbf{x})$. If $\mathbf{s}$ is a subset of $\mathbf{r}$, we denote by $\mathbf{s}^*$ the set of all cyclic permutations of the set $\mathbf{s} \cup \mathbf{s}^{-1}$ that start with a member of $\mathbf{x} \cap \mathbf{x}^{-1}$. If G is the trivial group, the relative presentation $\langle G, \mathbf{x} \mid \mathbf{r} \rangle$ reduces to the ordinary group presentation $\langle \mathbf{x} \mid \mathbf{r} \rangle$.

Let $\mathcal{P} = \langle G, \mathbf{x} \mid \mathbf{r} \rangle$ be a relative presentation. To build some constructions explicitly, we need an ordinary presentation $\widetilde{\mathcal{P}}$ that generates the same group as $\mathcal{P}$. The construction is as follows:

Let $\mathcal{Q} = \langle \mathbf{a} \mid \mathbf{s} \rangle$ be an ordinary presentation for G. Then there is a homomorphism $\phi \colon F(\mathbf{a}) \to G$ with $\ker(\phi) = \langle\!\langle \mathbf{s} \rangle\!\rangle$. For each $g \in G$ choose a representative word from $\phi^{-1}(g) \subseteq F(\mathbf{a})$, and for each $r \in \mathbf{r} \subseteq G * F(\mathbf{x})$ use the representatives of G to form a

lifted word $\widetilde{r} \in F(\mathbf{a} \cup \mathbf{x})$. Define the **lifted presentation** $\widetilde{\mathcal{P}}$ for $\mathcal{P}$ to be the ordinary presentation

$$\widetilde{\mathcal{P}} = \langle \mathbf{a} \cup \mathbf{x} \mid \mathbf{s} \cup \widetilde{\mathbf{r}} \rangle$$

where $\widetilde{\mathbf{r}} = \{\widetilde{r} \mid r \in \mathbf{r}\}$.

2.2 The Cellular Model and Asphericity

A path connected topological space X is called **aspherical** if $\pi_n(X)$ is trivial for all $n \geq 2$. This restriction on higher homotopy groups does not by itself imply a restriction on the fundamental group. Indeed, for any group G we can form an aspherical space K with fundamental group $\pi_1(K) \cong G$. Such a space is called an **Eilenberg-MacLane space of type $K(G, 1)$.**

We can in fact construct a $K(G, 1)$ as a CW-complex, and thus take advantage of the rich theory such complexes provide. If X is a connected CW-complex and Y is aspherical, then any homomorphism $\pi_1(X) \to \pi_1(Y)$ is induced by a map $X \to Y$ [30, Proposition 1B.9]. It follows immediately from the Whitehead Theorem [58, 59] that any two aspherical CW-complexes with isomorphic fundamental group are homotopy equivalent. Since covering projections induce isomorphisms on the higher homotopy groups, we have a useful equivalence: a CW-complex is aspherical if and only if its universal cover is contractible.

Our interest is in the application of asphericity to the study of groups. While we can construct a $K(G, 1)$ complex for any group G, further restrictions on the shape of this complex impose strong group-theoretic consequences on G. A useful example is captured in the following theorem.

Theorem 2.2.1 ([30, Proposition 2.45])**.** *Every finite-dimensional aspherical CW-complex has torsion-free fundamental group.* $\qquad\square$

Fix a relative presentation $\mathcal{P} = \langle G, \mathbf{x} \mid \mathbf{r} \rangle$. The **relative cellular model** for $\mathcal{P}$ is a particular relative CW-complex (L, K), where K is taken to be a $K(G, 1)$-complex. The process for building L from K is as follows:

1. For each $x \in \mathbf{x}$ attach a 1-cell to K at a single point, forming the 1-point union

$$K \vee \bigvee_{\mathbf{x}} S_x^1.$$

2. For each $r \in \mathbf{r}$ take $\dot{\varphi}_r \colon S^1 \to K \vee \bigvee_{\mathbf{x}} S_x^1$ to be a cellular representative of the homotpy class $[\dot{\varphi}] \in \pi_1(K \vee \bigvee_{\mathbf{x}} S_x^1) \cong G * F(\mathbf{x})$ corresponding to the element $r \in G * F(\mathbf{x})$. Form L by attaching a 2-cell c_r^2 for each $r \in \mathbf{r}$ via a characteristic map φ_r that restricts to $\dot{\varphi}_r$ on the boundary of c_r^2:

$$L = K \vee \bigvee_{\mathbf{x}} S_x^1 \cup \bigcup_{\mathbf{r}} c_r^2.$$

Since any two $K(G, 1)$-complexes are homotopy equivalent, the homotopy type of L and the pair (L, K) is uniquely determined by the relative presentation $\mathcal{P}$. The relative cellular model of $\mathcal{P}$ is denoted $L(\mathcal{P})$, although for convenience we will often write L when the presentation is unambiguous.

If G is trivial, then K can be taken to be a point, and the relative model reduces to a 2-complex called the **ordinary cellular model** for the ordinary presentation $\langle \mathbf{x} \mid \mathbf{r} \rangle$. We typically write "cellular model" when referring to both ordinary and relative cellular models, with the appropriate definition being assumed based on the presentation being discussed.

The notion of asphericity, which is central to our work, is defined in terms of the cellular model for both ordinary and relative presentations.

Definition 2.2.2. *An ordinary presentation $\mathcal{P}$ is said to be **aspherical** if the (ordinary) cellular model for $\mathcal{P}$ is an aspherical space (i.e., $\pi_2(L(\mathcal{P}))$ is trivial).*

Definition 2.2.3 ([9], [10]). *A relative presentation $\mathcal{P}$ is said to be **aspherical in the relative sense** if the relative homotopy group $\pi_2(L(\mathcal{P}), K)$ is trivial.*

The following reformulation of relative asphericity gives some preliminary indication of its group-theoretic importance.

Lemma 2.2.4 ([10, Lemma 2.3]). *A relative presentation $\mathcal{P} = \langle G, \mathbf{x} \mid \mathbf{r} \rangle$ is aspherical if and only if the natural homomorphism $G \to G(\mathcal{P})$ is injective and $\pi_2(L(\mathcal{P})) = 0$.* $\square$

Proof. This follows from direct inspection of the long exact homotopy sequence of the pair $(L(\mathcal{P}), K)$:

$$0 = \pi_2(K) \to \pi_2(L(\mathcal{P})) \to \pi_2(L(\mathcal{P}), K) \to \pi_1(K) \to \pi_1(L(\mathcal{P})),$$

noting that the inclusion-induced homomorphism $\pi_1(K) \to \pi_1(L(\mathcal{P}))$ corresponds to the natural homomorphism $G \to G(\mathcal{P})$. $\square$

If $\mathcal{P} = \langle G, \mathbf{x} \mid \mathbf{r} \rangle$ is aspherical, we can view G as a subgroup of $G(\mathcal{P})$, and this subgroup has substantial influence over the structure of $G(\mathcal{P})$. The restrictions on torsion elements and finite subgroups of $G(\mathcal{P})$ are particularly rigid.

Theorem 2.2.5 ([10, Theorem 2.4(c)]). *Let $\mathcal{P} = \langle G, \mathbf{x} \mid \mathbf{r} \rangle$ be an aspherical relative presentation. Then*

(a) *every finite subgroup of $G(\mathcal{P})$ is conjugate to a subgroup of G,*

(b) *if $w \in G(\mathcal{P})$ and $G \cap wGw^{-1}$ contains a nontrivial element of finite order, then $w \in G$.* $\square$

If $\mathcal{P}$ is a relative presentation such that $G \to G(\mathcal{P})$ is injective, then Theorem 2.2.5 represents potential obstructions to the asphericity of $\mathcal{P}$. This is the cornerstone of our proofs that the relative presentations $\mathcal{P}$ in Theorems A, B and H are not aspherical. The presentations considered in Theorems A to E and H fall into a class of 1-generator, 1-relator relative presentations for which $G \to G(\mathcal{P})$ is known to be injective.

Theorem 2.2.6 ([38, Theorem 2]). *Let $\mathcal{P} = \langle G, x \mid xaxbx^{-1}c \rangle$ where $a, b, c \in G$. Then the natural map $G \to G(\mathcal{P})$ is injective.* $\square$

Theorem 2.2.7 ([20]). *Let $\mathcal{P} = \langle G, x \mid x^n g x^{-m} h \rangle$ where $n, m \in \mathbb{Z}$ with $n \neq m$ and $g, h \in G$ with $\{|g|, |h|\} \neq \{2, 3\}$. Then the natural map $G \to G(\mathcal{P})$ is injective.* $\square$

Perhaps not surprisingly, relative asphericity relies only on those coefficients present in the relators of $G(\mathcal{P})$.

Lemma 2.2.8 ([10, Lemma 2.14]). *Given a relative presentation $\mathcal{P} = \langle G, \mathbf{x} \mid \mathbf{r} \rangle$, if H is any subgroup of G for which the set of relators $\mathbf{r} \subseteq G * F$ is contained in the free product $H * F$, then $\mathcal{P}$ is aspherical if and only if $\langle H, \mathbf{x} \mid \mathbf{r} \rangle$ is aspherical.* $\square$

We may then assume without loss of generality that G is generated by the coefficients present in the elements of $\mathbf{r}$. For example, given the presentation $\langle G, x \mid x^2 g x^{-1} h \rangle$ we assume that $G = \langle g, h \rangle$. This assumption is useful in conjunction with Theorem 2.2.5, as it becomes easier to identify subgroups that prove non-asphericity.

2.3   Relative Pictures

2.3.1   Basic Definitions

In order to build elements of the relative homotopy group $\pi_2(L, K)$ of the cellular model L of $\mathcal{P}$, it is helpful to approach the problem from a combinatorial perspective. We start with the definition of relative pictures and related terminology given in [10].

Definition 2.3.1. *A **picture** $\mathbb{P}$ is a finite collection of pairwise disjoint discs $\{D_1, \ldots, D_m\}$ in the interior of an ambient disc D^2, together with a finite collection $\{\alpha_1, \ldots, \alpha_n\}$ of pairwise disjoint simple arcs properly embedded in the closure of $D^2 \setminus \bigcup \{D_1, \ldots, D_m\}$ such that each endpoint of an arc meets the boundary of a disc or the boundary of the ambient disc.*

The **boundary** of $\mathbb{P}$, denoted $\partial\mathbb{P}$, is the boundary of the ambient disc D^2. A **region** of $\mathbb{P}$ is the closure of a connected component of $D^2 \setminus (\bigcup\{D_1, \ldots, D_m\} \cup \bigcup\{\alpha_1, \ldots, \alpha_n\})$. An **inner region** of $\mathbb{P}$ is a simply connected region that does not intersect the boundary of $\mathbb{P}$.

By a **disc** of $\mathbb{P}$ we mean one of the discs D_i and not the ambient disc D^2. A **corner** of the disc D_i is a connected component of $\partial D_i \setminus \bigcup\{\alpha_1, \ldots, \alpha_n\}$ where ∂D_i denotes the boundary of D_i.

Definition 2.3.2. *A picture $\mathbb{P}$ is **connected** if $\bigcup\{D_1, \ldots, D_m\} \cup \bigcup\{\alpha_1, \ldots, \alpha_n\}$ is connected, is **nontrivial** if $m \geq 1$, and is **spherical** if it is nontrivial and none of its arcs meet the boundary of $\mathbb{P}$.*

Let $\mathcal{P} = \langle G, \mathbf{x} \mid \mathbf{r} \rangle$ be a relative presentation. Apply the following labeling to a picture $\mathbb{P}$:

- Each arc of $\mathbb{P}$ is given a transverse orientation, denoted by an arrow intersecting the arc, and is labeled by an element of $\mathbf{x} \cup \mathbf{x}^{-1}$.

- Each corner of $\mathbb{P}$ is given a counterclockwise orientation and is labeled by an element of G.

Let κ be a corner of a disc D_i of the picture $\mathbb{P}$. Denote by $W(\kappa)$ the word obtained by reading the labels of each corner and arc meeting D_i while traversing counterclockwise around the boundary of D_i ending at κ (we read the label of κ last). When we cross an arc labeled x in the direction of its transverse orientation, we read x, and we read x^{-1} when we cross in the direction opposite its orientation.

Definition 2.3.3. *Fix a relative presentation $\mathcal{P} = \langle G, \mathbf{x} \mid \mathbf{r} \rangle$. A **relative picture over $\mathcal{P}$** is a picture $\mathbb{P}$ with a labeling as above such that the following two conditions are satisfied:*

(1) $W(\kappa)$ is an element of $\mathbf{r}^*$ for any corner κ of $\mathbb{P}$,

(2) If $g_1, \ldots, g_k$ are the labels of the corners read in a clockwise order about the boundary of an inner region of $\mathbb{P}$, then $g_1 \cdots g_k = 1$ in G.

A spherical picture is called **strictly spherical** if it is connected and the product of the corner labels in the outer annular region read in a counterclockwise order gives the identity in G.

Connected spherical pictures are visualized as plane-embedded graphs, with each **vertex** representing a disc, each **edge** representing an arc, and each face representing a region. Figure 2.1 gives an example of a strictly spherical picture over the presentation $\langle G, x \mid x^2 g x^{-1} g^{-2} \rangle$ where G is the cyclic group of order 8 generated by g. Arc labels and orientation arrows are often omitted from our visual depictions, but can typically be deduced from the corner labels. From here on, graph-theoretic terms will be used interchangeably with the corresponding picture-based terminology.

FIGURE 2.1: A strictly spherical picture over the presentation $\langle G, x \mid x^2 g x^{-1} g^{-2} \rangle$ where $G = \langle g \mid g^8 \rangle$

2.3.2   The Pictorial van Kampen Lemma

If the group G is trivial, then the relative presentation $\langle G, \mathbf{x} \mid \mathbf{r} \rangle$ becomes the ordinary presentation $\mathcal{P} = \langle \mathbf{x} \mid \mathbf{r} \rangle$. A corresponding definition for a picture over $\mathcal{P}$ is obtained by ignoring corner labels.

Definition 2.3.4. *Fix an ordinary presentation $\mathcal{P} = \langle \mathbf{x} \mid \mathbf{r} \rangle$. A **picture over $\mathcal{P}$** is a picture $\mathbb{P}$ satisfying the following two conditions:*

1. *Each arc is given a transverse orientation and is labeled by an element of $\mathbf{x} \cup \mathbf{x}^{-1}$.*

2. *For each disc D_i in $\mathbb{P}$, the word in $\mathbf{x} \cup \mathbf{x}^{-1}$ obtained by reading the labels of the arcs intersecting ∂D_i in counterclockwise order (accounting for transverse orientation) from any starting point is an element of $\mathbf{r}^*$.*

Define the **boundary label** of a picture $\mathbb{P}$ over the ordinary presentation $\langle \mathbf{x} \mid \mathbf{r} \rangle$ to be the word in $\mathbf{x} \cup \mathbf{x}^{-1}$ obtained by reading the labels (accounting for transverse orientations) of each arc meeting the boundary of $\mathbb{P}$ in a counterclockwise traversal of $\partial \mathbb{P}$. Over ordinary presentations, pictures are dual (as graphs) to van Kampen diagrams, and in analogy, there is a pictorial version of the van Kampen Lemma:

Theorem 2.3.5 ([8, Theorem 1.4])**.** *Let $\mathcal{P} = \langle \mathbf{x} \mid \mathbf{r} \rangle$ be an ordinary presentation. A word u in $\mathbf{x} \cup \mathbf{x}^{-1}$ represents the identity in $G(\mathcal{P})$ if and only if there is a picture over $\mathcal{P}$ with boundary label u.* $\qquad\qquad\square$

Let $\mathbb{P}$ be a picture over an ordinary presentation $\mathcal{P}$. If β is the image of any simple closed curve in $\mathbb{P}$ that does not intersect any discs and only intersects arcs transversely, then β bounds a subpicture $\mathbb{P}_0$ of $\mathbb{P}$. As we traverse β in a counterclockwise direction, the arcs that intersect β define the boundary label u of $\mathbb{P}_0$. By Theorem 2.3.5 u represents the identity in $G(\mathcal{P})$. Thus, we can find representatives of the identity in $G(\mathcal{P})$ by drawing simple closed curves in the picture $\mathbb{P}$.

We can likewise find representatives of the identity in $G(\mathcal{P})$ when $\mathcal{P}$ is a relative presentation. Let $\mathbb{P}$ be a relative picture over $\mathcal{P} = \langle G, \mathbf{x} \mid \mathbf{r} \rangle$ and consider a lifted presentation $\widetilde{\mathcal{P}} = \langle \mathbf{a} \cup \mathbf{x} \mid \mathbf{s} \cup \widetilde{\mathbf{r}} \rangle$ for $\mathcal{P}$, where $\mathcal{Q} = \langle \mathbf{a} \mid \mathbf{s} \rangle$ is a presentation for G. We can build a **lifted picture** $\widetilde{\mathbb{P}}$ over $\widetilde{\mathcal{P}}$ from $\mathbb{P}$ by the following process:

Identify all corner labels of $\mathbb{P}$ with their corresponding representative words in $\mathbf{a} \cup \mathbf{a}^{-1}$. The corner labels read clockwise about an inner region Δ of $\mathbb{P}$ give a word $u \in F(\mathbf{a})$ that is trivial in $G(\mathcal{Q}) \cong G$. Reading the corner labels instead in a counterclockwise order gives the word u^{-1}. By Theorem 2.3.5 there is a picture $\mathbb{P}_\Delta$ over $\mathcal{Q}$ with boundary label u^{-1}. Place $\mathbb{P}_\Delta$ in the inner region Δ and extend the arcs meeting $\partial\mathbb{P}_\Delta$ so that they connect with their corresponding corner (do not allow the arcs to cross). Note that a single corner may connect to any number of extended arcs. For regions Δ' that meet the boundary of $\mathbb{P}$, add arcs from the corners of Δ' corresponding to that corner's label (where the corner label is considered as an element of $F(\mathbf{a})$) and extend these arcs until the meet the boundary of $\mathbb{P}$. Give these arcs the appropriate transverse orientation and label in $\mathbf{a}$. Finally removing the now redundant corner labels from $\mathbb{P}$ gives the lifted picture $\widetilde{\mathbb{P}}$.

While the lifted picture lets us apply Theorem 2.3.5 to relative spherical pictures, we do not usually explicitly construct these lifted pictures. Instead, we rely on our imagination to fill in the missing discs and arcs. As an example, consider the 1-relator relative presentation $\mathcal{P} = \langle G, x \mid x^2 g x^{-1} g^{-2} \rangle$. A spherical picture $\mathbb{P}$ for $\mathcal{P}$ was given in Figure 2.1. In order to find an identity in $G(\mathcal{P})$, we draw a loop β on $\mathbb{P}$ as in Figure 2.2. In the regions through which β passes, we imagine that all extra discs are added outside the area bounded by β. If we travel around β counterclockwise, the extra arcs that intersect β inside a region Δ of $\mathbb{P}$ correspond to those corner labels (read clockwise about Δ) that are within the area bounded by β. These are the corner labels to the left of β as we travel along it counterclockwise.
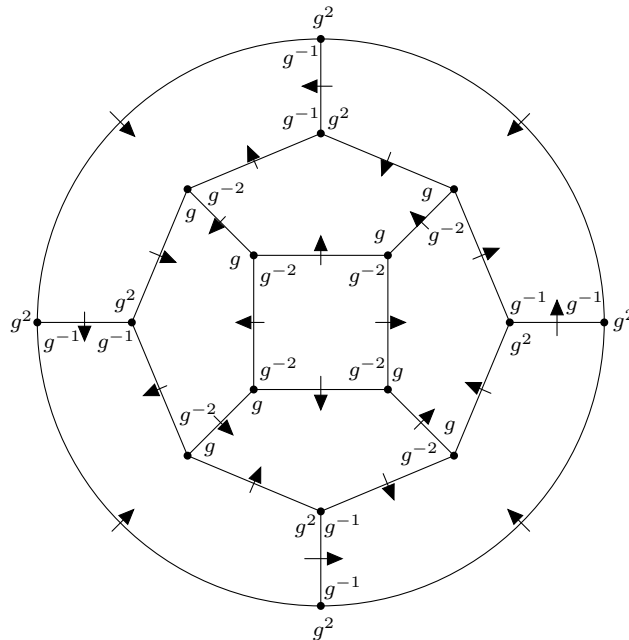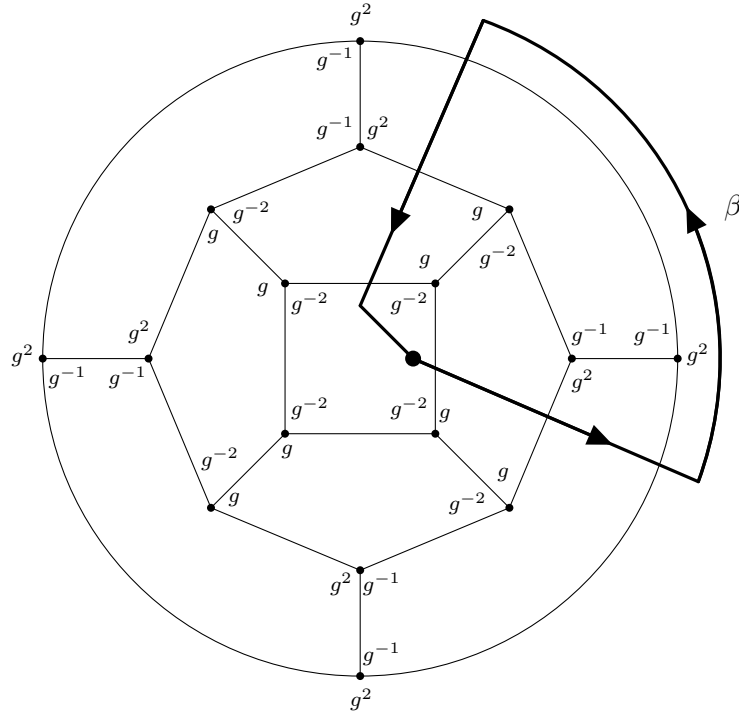
FIGURE 2.2: A loop in a spherical picture over the presentation $\langle G, x \mid x^2 g x^{-1} g^{-2} \rangle$ where $G = \langle g \mid g^8 \rangle$

Consider the closed curve β in the picture $\mathbb{P}$ given in Figure 2.2. Start at the distinguished point given in the central region and begin to travel counterclockwise around β. When we cross the first arc of $\mathbb{P}$ we read x (transverse orientations for the arcs of $\mathbb{P}$ are given in Figure 2.1). As we travel through the next region, we read the corner labels that are within the area bounded by β in clockwise order around the region, giving $(1)(g^{-2})(1) = g^{-2}$. we next cross an arc reading x^{-1}, then read g^2 in the following region, and then x^{-1} as we cross the outermost arc. On the path from the central region to the outer region, we have so far read the word

$$y = xg^{-2}x^{-1}g^2x^{-1}.$$

We now continue counterclockwise through the outer region, passing by a single corner and reading g^2. The path we take from the outer region back to the central region is essentially the same (due to symmetry) as the path we took going out, but traversed in

the opposite direction. We therefore read the word y^{-1}. Finally, to reach our starting point we travel past a single corner in the central region, reading g^{-2}. The identity in $G(\mathcal{P})$ given by β is

$$yg^2y^{-1}g^{-2}$$

where y is as above. We conclude that y and g^2 commute in $G(\mathcal{P})$. The word y is related to the polar words of [47]. We use a similar path in the proof of Theorem A.

2.3.3   Spherical Pictures as Elements of $\pi_2(L, K)$

Fix a relative presentation $\mathcal{P} = \langle G, \mathbf{x} \mid \mathbf{r} \rangle$ with cellular model L. Given a connected spherical picture $\mathbb{P}$ over $\mathcal{P}$ we can construct an element $[f] \in \pi_2(L, K)$ by following a process analogous to that outlined in [41]. The map $f \colon (D^2, S^1) \to (L, K)$ is defined as follows:

- Fix a lifted presentation $\widetilde{\mathcal{P}} = \langle \mathbf{a} \cup \mathbf{x} \mid \mathbf{s} \cup \widetilde{\mathbf{r}} \rangle$ of $\mathcal{P}$, where $\mathcal{Q} = \langle \mathbf{a} \mid \mathbf{s} \rangle$ is a presentation for G. Choose K to be a $K(G, 1)$-complex whose 2-skeleton is the cellular model for $\mathcal{Q}$.

- Build a lifted picture $\widetilde{\mathbb{P}}$ over $\widetilde{\mathcal{P}}$ and identify (D^2, S^1) with $(\widetilde{\mathbb{P}}, \partial\widetilde{\mathbb{P}})$. Expand each arc α_j of $\widetilde{\mathbb{P}}$ to a collared neighborhood of α_j as in Figure 2.3. Expand all discs so that these neighborhoods are flush with the disc boundaries as in Figure 2.4(iii).

- Along each expanded arc, let f map each collar line onto L characteristically with respect to the arc label and transverse orientation. Some curving of collar lines must be done near the boundary of a disc to ensure f is continuous.
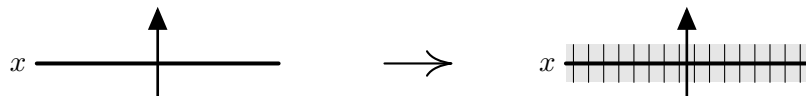
FIGURE 2.3: An arc expanded to a collared neighborhood
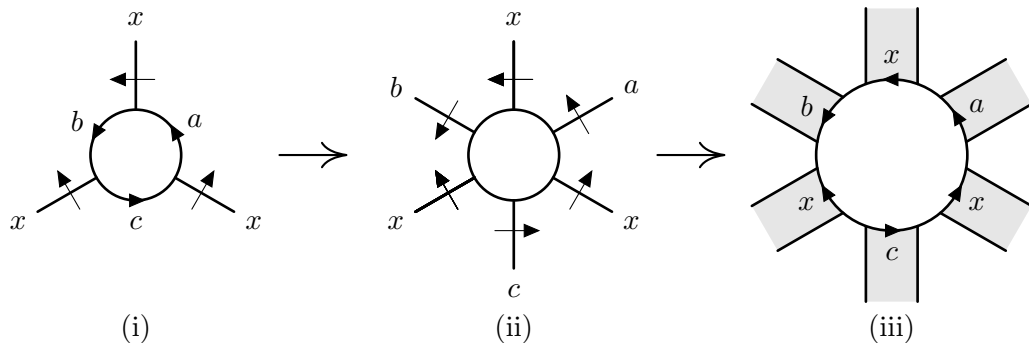
FIGURE 2.4: (i) a relative disc, (ii) a lifted disc, and (iii) an expanded disc in the case $\mathcal{P} = \langle G, x \mid xaxbx^{-1}c \rangle$

- For each disc D_i there is an associated boundary word r^ε where $r \in \widetilde{\mathbf{r}}$ and $\varepsilon = \pm 1$. Let f map D_i characterstically (i.e., by φ_r) onto L precomposed by an orientation-reversing map in the case $\varepsilon = -1$.

Conversely, any continuous map $(D^2, S^1) \to (L, K)$ can be represented by a (not necessarily connected) spherical picture over $\mathcal{P}$ (see the proof of theorem 4.1 in [7]). In this way, the process of finding elements of $\pi_2(L, K)$ becomes the combinatorial exercise of building spherical pictures.

2.3.4 Dipoles

Our main results involve the construction of reduced spherical pictures, that is, spherical pictures that do not contain a certain degenerate subpicture called a dipole. This is analogous to reduced words in a free group.

Definition 2.3.6 ([7]). *A **dipole** in a spherical picture $\mathbb{P}$ over $\mathcal{P} = \langle G, \mathbf{x} \mid \mathbf{r} \rangle$ is a pair of corners κ and κ' together with an arc meeting the closure of each corner such that the following two conditions are satisfied:*

(1) κ and κ' are contained in the same region of $\mathbb{P}$.

(2) If $W(\kappa) = Sg$ where $g \in G$ and S begins and ends with an element of $\mathbf{x} \cup \mathbf{x}^{-1}$, then $W(\kappa') = S^{-1}g^{-1}$.

Intuitively, a dipole is a mirrored pair of discs, with one disc representing a relator r, and the other disc representing r^{-1}. Figure 2.5 gives an example of the construction of a dipole in the case $\mathcal{P} = \langle G, x \mid r \rangle$ where $r = xaxbx^{-1}c$.

$r = xaxbx^{-1}c$ $\qquad\qquad$ $r^{-1} = c^{-1}xb^{-1}x^{-1}a^{-1}x^{-1}$

(i) $\qquad\qquad\qquad\qquad$ (ii) $\qquad\qquad\qquad\qquad$ (iii)
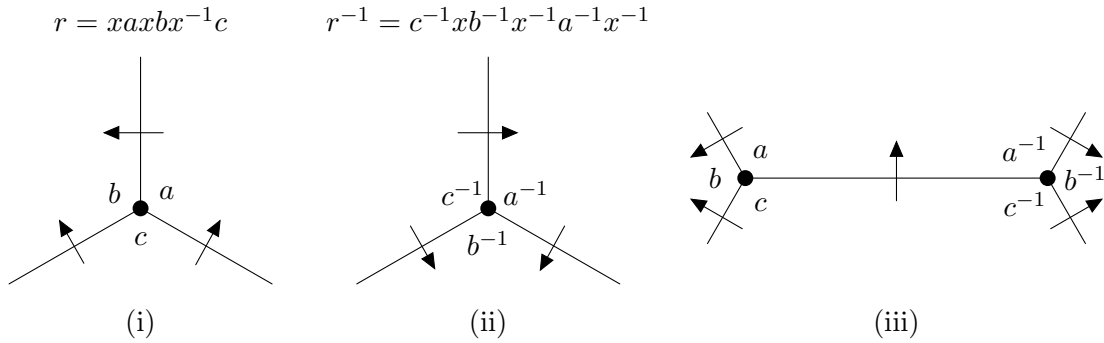
FIGURE 2.5: (i) and (ii) vertices (discs) representing r and r^{-1}. (iii) A dipole is formed when these discs are connected by an arc with a mirrored orientation.

It is easy to construct spherical pictures with dipoles. Indeed, joining the right top arc with the left top arc and the right bottom arc with the left bottom arc in Figure 2.5(iii) gives a strictly spherical picture over $\langle G, x \mid xaxbx^{-1}c \rangle$.

Definition 2.3.7. *A relative presentation $\mathcal{P}$ is **orientable** no relator of $\mathcal{P}$ is a cyclic permutation of its inverse.*

In the case that $\mathcal{P}$ is orientable, the picture formed by a single diplole is homotopically trivial (via a homotopy that folds the two discs together), and hence does not represent an obstruction to asphericity. This need not be the case for non-orientable presentations. Consider the non-orientable relative presentation $\mathcal{P} = \langle C_2, x \mid [x, a]^2 \rangle$ where C_2 is the cyclic group of order 2 generated by a. [7, Figure 1] gives a lifted picture for a single relative dipole over $\mathcal{P}$ that is not homotopically trivial. Another example of a non-orientable presentation is given in [6, Example 3.5]. The presentations in Theorems A, B and H are easily checked to be orientable.

The "folding" homotopy can be used to remove any dipole from a spherical picture over an orientable relative presentation without changing its homotopy class (see [7, theo-

rem 4.1]). In terms of pictures, removing a dipole means removing the two mirrored discs and connecting the corresponding arcs. An example is given in Figure 2.6.
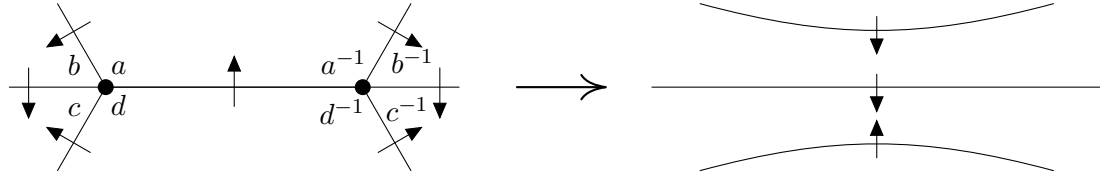
FIGURE 2.6: Removal of a dipole in the case $\langle G, x \mid xaxbxcx^{-1}d \rangle$

Definition 2.3.8. *A picture over a relative presentation is called **reduced** if it contains no dipoles.*

Definition 2.3.9. *A relative presentation $\mathcal{P}$ is **diagrammatically reducible** if every connected spherical picture over $\mathcal{P}$ contains a dipole.*

If an orientable relative presentation is diagrammatically reducible, then every strictly spherical picture represents the identity in $\pi_2(L, K)$, and hence the presentation is aspherical. Notice that the strictly spherical picture given in Figure 2.1 is reduced, so $\mathcal{P} = \langle G, x \mid x^2gx^{-1}g^{-2} \rangle$ is not diagrammatically reducible.

2.3.5 The Star Graph

Let $\mathcal{P} = \langle G, \mathbf{x} \mid \mathbf{r} \rangle$ be a relative presentation. The **star graph** $\mathcal{P}^{\text{st}}$ of $\mathcal{P}$ is a directed graph with vertex set $\mathbf{x} \cup \mathbf{x}^{-1}$ and edge set $\mathbf{r}^*$, together with an edge labeling function $\lambda \colon \mathbf{r}^* \to G$. Fix $R \in \mathbf{r}^*$ and write $R = Sg$ where $g \in G$ and S begins and ends with an element of $\mathbf{x} \cup \mathbf{x}^{-1}$. We say that R is an edge from $y \in \mathbf{x} \cup \mathbf{x}^{-1}$ to $z \in \mathbf{x} \cup \mathbf{x}^{-1}$ if y is the first symbol of S and z^{-1} is the last symbol of S. We assign the label $\lambda(R) = g^{-1}$ to the edge R and extend this labeling scheme to directed walks in $\mathcal{P}^{\text{st}}$ by right multiplication in G. That is, if a walk w consists of the sequence $R_1, R_2, \ldots, R_n$ of edges in $\mathcal{P}^{\text{st}}$, then $\lambda(w) = \lambda(R_1)\lambda(R_2) \cdots \lambda(R_n)$.

For $R = Sg \in \mathbf{r}^*$ as above, there is a corresponding edge $\bar{R} = S^{-1}g^{-1} \in \mathbf{r}^*$ which is a cyclic permutation of R^{-1}. If R is an edge from y to z with label $\lambda(R) = g^{-1}$, then $\bar{R}$ is an edge from z to y with label $\lambda(\bar{R}) = g$. When drawing the star graph, we typically only draw one of these two edges for each corresponding pair, as in Figure 2.7. The traversal of $\bar{R}$ in $\mathcal{P}^{\text{st}}$ can then be understood as a traversal of R in the direction opposite its orientation. Thus, when we travel backwards along an edge R, we read the label $\lambda(R)^{-1}$. The two-edge walk consisting of edges R and $\bar{R}$ is called a **backtracking.**

(i)   (ii)
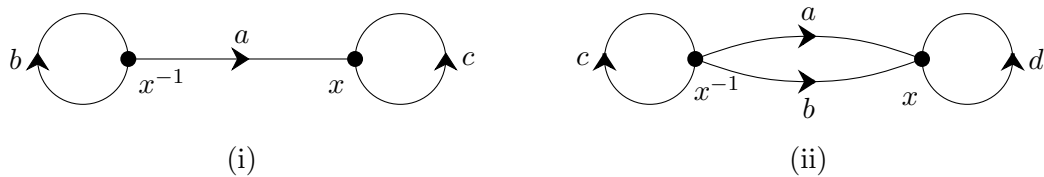
FIGURE 2.7: The star graphs for the presentations (i) $\langle G, x \mid xaxbx^{-1}c \rangle$ and (ii) $\langle G, x \mid xaxbxcx^{-1}d \rangle$

The star graph is useful, because it gives insight into the construction of a reduced spherical picture $\mathbb{P}$ over $\mathcal{P}$. If $\kappa_1, \ldots, \kappa_n$ is the sequence of corners read counterclockwise about an inner region of $\mathbb{P}$, then $W(\kappa_1), \ldots, W(\kappa_n)$ gives a closed walk in $\mathcal{P}^{\text{st}}$ [7, Lemma 2.1(i)]. Likewise, a closed walk w satisfying $\lambda(w) = 1$ in G gives rise to a picture with a single inner region whose corner labels are the inverses of the labels of each edge in w. A backtracking in the star graph then corresponds to a dipole in the picture [7, Lemma 2.1(ii)].

The results in the preceding paragraph are obtained rather intuitively. Consider the discs of a picture over $\mathcal{P}$ given in Figure 2.8 where κ_1, κ_2 are corners, and $z \in \mathbf{x} \cup \mathbf{x}^{-1}$ is an arc label. As the arcs labeled z have matching transverse orientations, they can be joined so that κ_1 and κ_2 are adjacent corners in the same region. Now write $W(\kappa_2) = Sg$ and $W(\kappa_1) = Th$ where S, T start and end with symbols in $\mathbf{x} \cup \mathbf{x}^{-1}$ and $g, h \in G$. If S ends with z^{-1}, as in Figure 2.8, then $W(\kappa_1)$ is an edge in $\mathcal{P}^{\text{st}}$ ending at z. If T starts with z, then $W(\kappa_1)$ is an edge in $\mathcal{P}^{\text{st}}$ ending at z. Hence, connecting the arc labeled z in

the picture corresponds to the walk $W(\kappa_1), W(\kappa_2)$ in $\mathcal{P}^{\text{st}}$. The correspondence between backtracking and dipoles follows directly.

FIGURE 2.8: Two discs in a picture over $\mathcal{P}$. The star graph determines whether the discs can be joined along an arc.

A sequence of corners $\kappa_1, \ldots, \kappa_n$ defines an **admissible region** (or **admissible face**) if $\overline{W(\kappa_n)}, \ldots, \overline{W(\kappa_1)}$ defines a closed walk w in $\mathcal{P}^{\text{st}}$ with $\lambda(w) = 1$ in G. We form this region by placing the corners in a clockwise order about the region. An **admissible word** is a sequence of corner labels read clockwise about an admissible region.

2.4 Retraction Kernels

Given a group presentation $\mathcal{P}$, the **Reidemeister-Schreier method** allows us to construct presentations for subgroups of $G(\mathcal{P})$ (see [46, Section 2.3]). Consider the one-generator, one-relator relative presentation $\mathcal{P} = \langle G, x \mid r \rangle$, and suppose $G \to G(\mathcal{P})$ is split by a retraction $\nu\colon G(\mathcal{P}) \to G$. We can then write $G(\mathcal{P})$ as a semidirect product $G(\mathcal{P}) \cong \ker(\nu) \rtimes G$. We adapt the Reidemeister-Schreier rewriting process outlined in [6, Section 2] to build a presentation for $\ker(\nu)$ as follows.

The presentation for $\ker(\nu)$ has generators $\{x_d\}_{d \in G}$ which are elements of $G(\mathcal{P})$. Define $x_e = x\nu(x)^{-1}$ where e is the identity in G. For any element u in $G(\mathcal{P})$ we can write

$$u = g_1 x_e^{\varepsilon_1} g_2 x_e^{\varepsilon_2} \cdots g_n x_e^{\varepsilon_n} g_{n+1}.$$

where $\varepsilon_i = \pm 1$. Then $u \in \ker(\nu)$ if and only if $g_1 g_2 \cdots g_{n+1} = e$ in G. We can thus write

any $u \in \ker(\nu)$ as a product of G-conjugates of powers of x_e:

$$u = \prod_{i=1}^{n} {}^{\Pi_{k=1}^{i} g_k} x_e^{\varepsilon_i}$$

where ${}^{h}g = hgh^{-1}$. There is a Reidemeister-Schreier rewriting process ρ defined by

$$\rho(u) = \prod_{i=1}^{n} x_{\Pi_{k=1}^{i} g_k}^{\varepsilon_i}.$$

In particular, $\rho(dx\nu(x)^{-1}d^{-1}) = x_d$ for $d \in G$. [46, Theorem 2.9] gives the presentation

$$\langle x_d \ (d \in G) \mid \rho(drd^{-1}) \ (d \in G) \rangle$$

for $\ker(\nu)$.

Example 2.4.1. Consider the relative presentation $\mathcal{P} = \langle G, x \mid x^2 g x^{-1} h \rangle$ where $|g| = n$, $|h| = 2$, and $|g^{-1}h| = 2$. Then $G = \langle g, h \rangle$ is isomorphic to the dihedral group D_{2n}. There is a retraction $\nu \colon G(\mathcal{P}) \to G$ given by $\nu(x) = hg$, and we define $x_e = xg^{-1}h$. The relator $r = x^2 g x^{-1} h$ can be written as

$$r = (xg^{-1}h)hg(xg^{-1}h)hggg^{-1}h(hgx^{-1})h$$
$$= x_e(hg)x_e(hg)^{-1}(h)x_e^{-1}(h)^{-1}$$

The Reidemeister-Schreier rewriting process gives

$$\rho(r) = x_e x_{hg} x_h^{-1}.$$

Applying ρ to drd^{-1} has the effect of left-multiplication by d on each subscript. That is,

$$\rho(drd^{-1}) = x_d x_{dhg} x_{dh}^{-1}.$$

A presentation for $\ker(\nu)$ is given by

$$\langle x_d \ (d \in G) \mid x_d x_{dhg} x_{dh}^{-1} \ (d \in G) \rangle.$$

Suppose now that G is the cyclic group of order n generated by g, and let $\nu^f : G(\mathcal{P}) \to$ G be the retraction defined by $\nu_f(x) = g^f$. The Reidemeister-Schreier rewriting process ρ^f from [6] produces a cyclic presentation for the kernel of ν_f. Specifically, letting $\rho^f(xg^{-f}) = x_0$ and $\rho^f(g^i x_0 g^{-i}) = x_i$ $(0 \leq i \leq n-1)$ allows us to write elements of $\ker(\nu_f)$ in terms of the cyclic generators $x_0, \ldots, x_{n-1}$. The presentation for $\ker(\nu_f)$ under this rewriting process is $\mathcal{G}_n(\rho^f(r))$. A connection between relative asphericity of $\mathcal{P}$ and ordinary asphericity of $\mathcal{G}_n(\rho^f(r))$ is captured in the following theorem.

Theorem 2.4.2 ([6, Theorem 4.1(b)])**.** *Let L be the cellular model of a relative presentation $\mathcal{P} = \langle G, x \mid r \rangle$ where G is the cyclic group of order n generated by g. Suppose that $\nu_f : G(\mathcal{P}) \to G$ is a retraction given by $\nu_f(g) = g$ and $\nu_f(x) = g^f$. Let $w = \rho^f(r)$. If $\mathcal{G}_n(w)$ is orientable and combinatorially aspherical, then $\pi_2 L = 0$.* $\hfill\square$

Here the concept of an "orientable" cyclic presentation differs from the relative case given in Definition 2.3.7.

Definition 2.4.3. *A cyclic presentation $\mathcal{G}_n(w)$ is **orientable** if w is not a cyclic permutation of the inverse of any of its shifts.*

For our purposes, it is enough to note that if $\mathcal{G}_n(w)$ is nonorientable, then n is even [6, Lemma 3.6]. In particular, $\mathcal{H}(9,4)$ and $\mathcal{H}(9,7)$ are orientable. A definition of combinatorial asphericity can be found in [16]. Combinatorial asphericity is a weaker condition than ordinary asphericity ([16, proposition 1.3]), so if a presentation is not combinatorially aspherical, then it is not aspherical.

Using Theorem 2.4.2, we can relate the relative asphericity of the presentation $\mathcal{P}$ in Theorem A with the ordinary asphericity of the presentation $\mathcal{H}(9,4)$. This will establish Corollary A.1.

- Consider the relative presentation $\mathcal{P} = \langle G, x \mid x^2 g x^{-1} g^3 \rangle$ where G is the cyclic group of order 9 generated by g. We apply the following Tietze transformations to $\mathcal{P}$:

(1) Invert the relator:

$$g^{-3}xg^{-1}x^{-2}$$

(2) Apply a cyclic permutation (conjugate by x^2):

$$x^{-2}g^{-3}xg^{-1}$$

(3) Apply the change of variables $z = x^{-1}$:

$$z^2g^{-3}z^{-1}g^{-1}$$

This produces a series of relative presentations with homotopy equivalent cellular models. Since $G \to G(\mathcal{P})$ is injective, $\mathcal{P}$ is aspherical if and only if $\mathcal{V} = \langle G, z \mid z^2g^{-3}z^{-1}g^{-1} \rangle$ is aspherical.

There is a retraction $\nu_4 \colon G(\mathcal{V}) \to G$ given by $\nu_4(z) = g^4$. The Reidemeister-Schreier process gives the presentation $\mathcal{G}_n(w)$ for $\ker(\nu_4)$ where

$$w = \rho^4\left(z^2g^{-3}z^{-1}g^{-1}\right) = \rho^4\left((zg^5)g^4(zg^5)g^{-4}g(zg^5)^{-1}g^{-1}\right) = x_0x_4x_1^{-1}.$$

This is precisely the presentation $\mathcal{H}(9, 4)$. Now, if $\mathcal{P}$ is not relatively aspherical, then neither is $\mathcal{V}$, and hence the presentation $\mathcal{G}_n(w) = \mathcal{H}(9, 4)$ is not aspherical by Theorem 2.4.2. This establishes Corollary A.1.

It is helpful to recognize that the groups $H(9, 4)$ and $H(9, 7)$ are isomorphic to retraction kernels without the need for a series of preliminary Tietze transformations.

Lemma 2.4.4 ([3, Lemma 1.1(3)]). $G_n(m, k) \cong G_n(n - m, n - m + k)$. □

Let $\mathcal{P} = \langle G, x \mid x^2gx^{-1}g^3 \rangle$ where $G = \langle g \mid g^9 \rangle$ as in Theorem A. Then there is a retraction $\nu_5 \colon G(\mathcal{P}) \to G$ defined by $\nu_5(x) = g^5$. The Reidemeister-Schreier rewriting process ρ^5 gives the presentation $\mathcal{G}_9(5, 6) = \mathcal{G}_9(x_0x_5x_6^{-1})$ for $\ker(\nu_5)$, and by Lemma 2.4.4 we have

$$\ker(\nu_5) \cong G_9(5, 6) \cong G_9(4, 1) = H(9, 4).$$

Now let $\mathcal{P} = \langle G, x \mid x^2 g x^{-1} g^{-3} \rangle$ where $G = \langle g \mid g^9 \rangle$ as in Theorem B. Then there is a retraction $\nu_2 \colon G(\mathcal{P}) \to G$ defined by $\nu_2(x) = g^2$. From a Reidemeister-Schreier rewriting process and Lemma 2.4.4 we get

$$\ker(\nu) \cong G_9(2, 3) \cong G_9(7, 1) = H(9, 7).$$

If J is a finite subgroup of $\mathcal{P}$ not isomorphic to a subgroup of G, then $\nu_2|_J$ is not injective, so $J \cap \ker(\nu_2)$ is a nontrivial finite subgroup of $H(9, 7)$. By Theorem 2.2.1 $\mathcal{H}(9, 7)$ cannot be aspherical. This establishes Corollaries B.1 and B.2.

2.5   3-Manifold Groups

A **3-manifold** is a Hausdorff space in which every point has a neighborhood that is homeomorphic to the 3-ball. We consider only connected 3-manifolds, so that their fundamental group is well defined irrespective of chosen base point. We make no further assumptions about the structure of 3-manifolds (e.g., whether they are closed or orientable). A **3-manifold group** is a group that is isomorphic to the fundamental group of a 3-manifold.

Let $\mathcal{P}$ be an aspherical relative presentation. Theorem 2.2.5 shows that asphericity of $\mathcal{P}$ imposes restrictions on the structure of finite subgroups of $G(\mathcal{P})$. There are similarly strong restrictions on the 3-manifold status of finite-index subgroups of $G(\mathcal{P})$.

Theorem 2.5.1 ([10, Theorem 2.19]). *Let $\mathcal{P} = \langle G, \mathbf{x} \mid \mathbf{r} \rangle$ be a relative presentation with $G, \mathbf{x}, \mathbf{r}$ finite and suppose the natural map $G \to G(\mathcal{P})$ is split by a retraction $\nu \colon G(\mathcal{P}) \to G$. Assume that $G(\mathcal{P})$ is a virtual 3-manifold group.*

(a) If $\mathcal{P}$ is a aspherical, then $|\mathbf{r}| \leq |\mathbf{x}|$.

*(b) If $|\mathbf{r}| = |\mathbf{x}|$ (i.e., $\mathcal{P}$ is **balanced**), then $\mathcal{P}$ is aspherical if and only if $G \to G(\mathcal{P})$ is an isomorphism.* $\square$

The presentations in Theorems A and B are balanced, and the retraction kernels $H(9,4)$ and $H(9,7)$ calculated in Section 2.4 are finite-index subgroups. Since these presentations are not aspherical, it is natural to ask if these kernels are 3-manifold groups. We find that $H(9,4)$ is not (this is Theorem F). It may still be possible that the presentation in Theorem A defines a virtual 3-manifold group. We partially address this situation in Theorem E. We do not eliminate the possibility that $H(9,7)$ is a 3-manifold group, but we restrict it to the case $H(9,7) \cong C_{37}$ (this is Theorem G).

As in groups with aspherical presentations, 3-manifold groups have restrictions on the ways in which torsion can occur.

Theorem 2.5.2 ([23, Theorem 8.2] see also [33, Theorem 9.8])**.** *If M is a 3-manifold and J is a finite subgroup of $\pi_1(M)$, then either*

(i) *$J \cong C_2$, and the nontrivial element of J is conjugate in $\pi_1(M)$ to a loop on a two-sided projective plane submanifold of M.*

(ii) *$M = M_1 \# Q$ where Q is closed and orientable, $\pi_1(Q)$ is finite, and J is conjugate to a subgroup of $\pi_1(Q)$.* $\qquad\square$

Here, a compact codimension-1 submanifold P of M is said to be **2-sided** if there is an embedding

$$h \colon P \times [-1,1] \to M$$

such that $h(z,0) = z$ for each $z \in P$ and

$$h(P \times [-1,1]) \cap \partial M = h(\partial P \times [-1,1]).$$

If M contains a 2-sided projective plane, then $P \times [-1,1] \subseteq M$ is a non-orientable submanifold of codimension 0, so M is necessarily non-orientable.

Since C_2 is the fundamental group of the orientable 3-manifold $\mathbb{R}P^3$, we can conclude immediately from Theorem 2.5.2 that any finite 3-manifold group is the fundamental

group of a closed, orientable 3-manifold. We may then apply the Elliptization Theorem
(a consequence of the Geometrization Theorem, see [53]).

Theorem 2.5.3 (Elliptization Theorem [2, Theorem 1.7.3]). *Every closed 3-manifold with finite fundamental group is spherical.* □

A **spherical 3-manifold** is one that is obtained as the quotient S^3/Γ where Γ is a finite subgroup of group of rotations $SO(4)$ in $\mathbb{R}^4$. The fundamental groups of spherical 3-manifolds are well known, and were classified by Hopf [37]. We use the classification presented in [2, Section 1.7].

Theorem 2.5.4 ([2]). *The fundamental group of a spherical manifold is precisely one of the following types of groups:*

(1) *the trivial group,*

(2) $Q_{4n} = \langle x, y \mid x^2 = (xy)^2 = y^n \rangle$ *where $n \geq 2$,*

(3) $P_{48} = \langle x, y \mid x^2 = (xy)^3 = y^4, x^4 = 1 \rangle$,

(4) $P_{120} = \langle x, y \mid x^2 = (xy)^3 = y^5, x^4 = 1 \rangle$,

(5) *the dihedral group*

$$D_{2^m(2n+1)} = \langle x, y \mid x^{2^m} = 1, y^{2n+1} = 1, xyx^{-1} = y^{-1} \rangle,$$

where $m \geq 2$ and $n \geq 1$,

(6) *the group*

$$P'_{8 \cdot 3^m} = \langle x, y, z \mid x^2 = (xy)^2 = y^2, zxz^{-1} = y, zyz^{-1} = xy, z^{3^m} = 1 \rangle,$$

where $m \geq 1$,

(7) *the direct product of any of the above groups with a cyclic group of relatively prime order.* □

We also consider structural requirements of some infinite 3-manifold groups.

Proposition 2.5.5. *If H is an infinite 2-generator 3-manifold group with a nontrivial finite subgroup not satisfying condition (i) of Theorem 2.5.2, then H is the free product of two cyclic groups.*

Proof. Let M be a 3-manifold with fundamental group H, and let J be a nontrivial finite subgroup of H not satisfying condition (i) of Theorem 2.5.2. Then $M = M_1 \# Q$ and

$$H = \pi_1(M) = \pi_1(M_1) * \pi_1(Q)$$

with $\pi_1(Q)$ finite and nontrivial. Since H is assumed to be infinite, this free product must be proper, and by Grushko's theorem [26] (see also [50]) the factors must be cyclic. □

The abelianization of any group H satisfying the conditions of Proposition 2.5.5 is a direct product of two nontrivial cyclic groups. The order of the abelianization for many cyclically-presented groups can be calculated as a particular resultant involving a representer polynomial (see [42, Section 9]). It was reported in [61] that $H(9,4)^{\mathrm{ab}} \cong C_{19}$ and $H(9,7)^{\mathrm{ab}} \cong C_{37}$. Since the order of each is odd, they cannot have a subgroup of index 2, and hence cannot be the fundamental group of a non-orientable 3-manifold. Notice that both abelianizations are indecomposable, which is inconsistent with the conclusion of Proposition 2.5.5.

Given elements x, y of a group H, a **Baumslag-Solitar relation** has the form $y x^a y^{-1} = x^b$. In the proof of Theorem E we find that a surprising Baumslag-Solitar relation occurs in the group defined by $\langle G, x \mid x^2 g x^{-1} g^3 \rangle$ where $G = \langle g \mid g^9 \rangle$. Such relations are restricted in 3-manifold groups.

Proposition 2.5.6 ([44, Proposition 1]). *If x is an element of infinite order in a 3-manifold group such that x^m and x^n are conjugate ($m, n \in \mathbb{Z}$), then $m = \pm n$.* □

3   COMPUTATIONAL METHODS

3.1   A Method for Finding Spherical Pictures

In this section we describe a method for building connected, reduced spherical pictures. Briefly, we build up a picture face-by-face, starting with a single face and progressively adding faces in a spiral order. It is sometimes necessary to add new faces outside of this spiral order (which we call "hop" faces). This process is continued until the picture becomes spherical. We implemented our method in the C programming language and used it to find pictures over the presentations given in Theorems A, B and H. Program output is given in Section 4.1 and the completed pictures are given in Section 4.2.

There is potential for further development of picture-searching methods. Our method is limited to adding faces in a particular order, and this may cause us to miss pictures even when they exist. A breadth-first method could likely overcome this limitation, although care would need to be taken to address reconvergence of the breadth-first graph and computer memory limitations. Our method was chosen for ease of implementation and proved sufficient for some outstanding cases.

3.1.1   Notation

Our current implementation is designed only to handle 1-generator, 1-relator relative presentations. That is, presentations of the form $\mathcal{P} = \langle G, x \mid r \rangle$ where

$$r = x^{\varepsilon_1} g_1 x^{\varepsilon_2} g_2 \cdots x^{\varepsilon_n} g_n$$

with $\varepsilon_i = \pm 1$ and $g_i \in G$. Elements of G that occur in r are represented by the first n lower case letters of the alphabet (a, b, c, ...), and G is assumed to be generated by these elements. The inverse of a generator of G is represented by the corresponding uppercase letter (e.g., $a^{-1} = A$).

The presentations in Theorems A, B and H have cyclic coefficient groups, so we will also assume that $G = \langle g \mid g^n \rangle$. We experimented with a few non-cyclic coefficient groups, but no new pictures were found.

As an example, consider the relative presentation $\langle G, x \mid x^2 g x^{-1} g^{-2} \rangle$ where G is the cyclic group of order 8 generated by g. A spherical picture over this presentation was given in Figure 2.1. When written using the notation of this section, the presentation becomes $\langle G, x \mid xaxbx^{-1}c \rangle$ where $a = 1$, $|b| = 8$, and $c = b^{-2}$. Figure 3.1 gives the picture for this presentation using the labeling specified in this section and with transverse arc arrows omitted (compare with Figure 2.1).
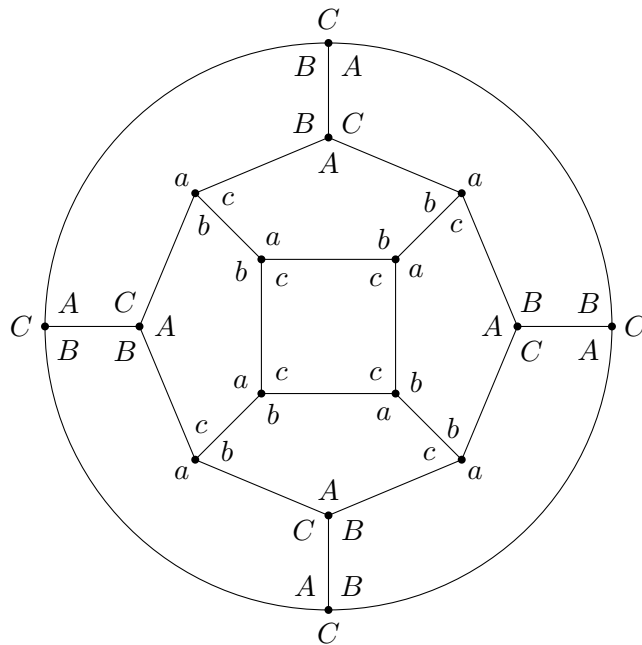
FIGURE 3.1: A spherical picture over the presentation $\langle G, x \mid xaxbx^{-1}c \rangle$ where $a = 1$, $|b| = 8$, and $c = b^{-2}$

When describing connected spherical pictures in this chapter, we avoid the picture theoretic terms **disc**, **arc**, and **region** in favor of the respective graph-theoretic terms **vertex**, **edge**, and **face** as in the discussion at the end of Section 2.3.1. To extend this to a non-spherical connected picture $\mathbb{P}$, we define a **half edge** to be an arc of $\mathbb{P}$ that meets

the boundary of $\mathbb{P}$. Since our depictions of pictures do not typically include the boundary, a half edge appears as an edge with an initial vertex, but no terminal vertex. Each edge can be thought of as two connected half edges (after disconnecting these half edges from $\partial\mathbb{P}$).

We define the **depth** of a connected picture $\mathbb{P}$ to be the number of inner faces of $\mathbb{P}$.

3.1.2 Input and Output

Let $\mathcal{P} = \langle G, x \mid r \rangle$ be a 1-generator, 1-relator relative presentation where G is cyclic generated by g and

$$r = x^{\varepsilon_1} g^{\sigma_1} x^{\varepsilon_2} g^{\sigma_2} \cdots x^{\varepsilon_n} g^{\sigma_n}$$

with $\varepsilon_i = \pm 1$ and $\sigma_i \in \mathbb{Z}$. Our method searches for spherical pictures over $\mathcal{P}$ and takes the following values as input:

- `relatorLength`: A positive integer representing the number of occurrences n of the letter x in the relator r.

- `relatorShape`: A string representing the exponents ε_i in the relator r. 'x' represents an exponent of 1, while 'X' represents -1. For example, the word $r = xaxbx^{-1}c$ is represented by `xxX`.

- `groupOrder`: A positive integer representing the order of the finite cyclic coefficient group G.

- `coefficientExponents`: A list of integers representing the exponents σ_i in the relator r.

- `symmetry`: A positive integer representing the order of rotational symmetry. Any picture detected will have `symmetry`-fold rotational symmetry about the starting face.

- `startWord`: A cyclically reduced word in the generators of G such that `startWord` repeated `symmetry` times represents the corner labeling of an admissible face.

- `maxVertices`: A positive integer representing the maximum number of vertices allowed in a single segment of the complete spherical picture. `symmetry` gives the number of segments in the picture. A segment represents a fundamental domain of the rotation action on the symmetric picture. The maximum number of vertices for the entire picture is then `symmetry * maxVerts`.

- `maxFaces`: A positive integer representing the maximum number of regions allowed in a single segment of the complete spherical picture.

- `maxHalfEdges`: A positive integer representing the maximum number of half edges allowed in a single segment of current picture.

- `maxNewVertices`: A positive integer representing the maximum number of new vertices added with each new face.

Upon successfully finding a reduced spherical picture $\mathbb{P}$, the method prints a list of words representing the corner labels of the faces of $\mathbb{P}$ in the order that they were added (with indications for "hop" faces). Since faces are added in a prescribed order, this gives an unambiguous description of $\mathbb{P}$. Details about the output for our specific implementation are given in Section 4.1. We do not present a method for efficiently drawing the resulting pictures. We labored carefully to construct usable depictions of the pictures given in this work.

3.1.3 Method Overview

Here we give a description of our method to search for spherical pictures over a relative presentation $\mathcal{P}$. Information about our specific implementation is given in Section 3.4.

As we follow our method, the state of the search always represents a reduced connected picture over $\mathcal{P}$, which we call the **current picture**. The method attempts to find a spherical picture by adding admissible faces to the current picture. If `symmetry` ≥ 1 then "adding a face" implicitly means adding that face at all equivalent positions as dictated by the symmetry.

Assume we are given input as in Section 3.1.2. Let d be a variable representing the current depth. We present a procedural description of our method. A flowchart outlining the method is given in Figure 3.2. Our method is as follows:

1. Place the initial face with corner labels specified by `startWord` and `symmetry`. Vertices are added in a clockwise order about the initial face.

2. Define β_d to be the first half edge immediately clockwise to the clockwise-most edge of the newly added face. When determining β_1, this is the counterclockwise-most half edge of the first added vertex.

3. Add and record a "hop" face if possible:

   (a) If there are fewer than 3 remaining half edges, go to step 4.

   (b) Let α_d be the half edge immediately clockwise to β_d when traveling around the picture. Read the subword in G from α_d to β_d.

   (c) If the subword is not admissible, go to step 4.

   (d) The subword is admissible, so add a new face by connecting α_d and β_d into a single edge

   (e) Record that the face added at depth d is a hop face.

   (f) Go to step 2.

4. Generate an ordered list L_d of the possible next faces:

    (a) Let γ_d be the half edge immediately counterclockwise to β_d when traveling around the picture.

    (b) Read the subword in G from β_d to γ_d.

    (c) Use the star graph to build a list L_d of admissible words beginning with that subword (there are only finitely many choices satisfying the restriction `maxNewVertices`). If the subword itself is admissible, we stipulate that this be the first element of L_d.

5. If L_d is nonempty, go to step 9.

6. L_d is empty, so remove the most recently added face from the picture. Removing a face means removing all vertices and half edge connections that were added when the face was added.

7. If $d = 0$, then the picture is empty, so terminate with failure.

8. If the removed face was a hop face, go to step 4. Otherwise, go to step 5.

9. Add the face between β_d and γ_d corresponding to the first element in the list L_d and remove this element from L_d.

10. If no half edges remain, the picture is spherical, so print a description of this picture and terminate.

11. If any of `maxVertices`, `maxFaces`, or `maxHalfEdges` is not satisfied, remove the most recently added face and go to step 5. Otherwise, go to step 2.
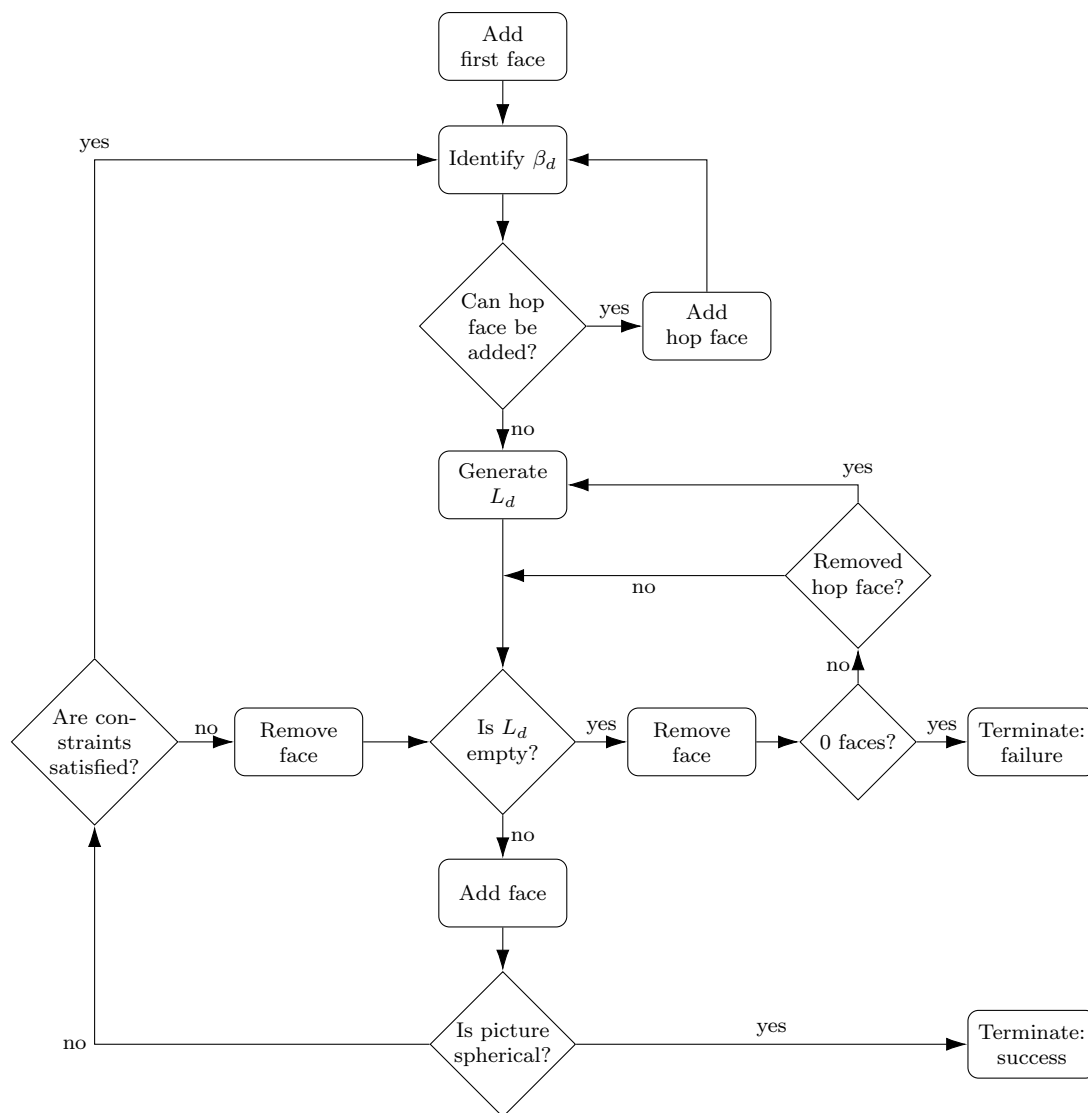
FIGURE 3.2: A flowchart outlining our method

3.2 Example 1

Let $\mathcal{P} = \langle G, x \mid xaxbx^{-1}c \rangle$ where $a = 1$, $|b| = 8$, and $c = b^{-2}$. The star graph for this presentation is given in Figure 2.7(i). We specify the following input for our method:

- `symmetry = 1`
- `maxVertices = 10000`
- `maxHalfEdges = 5`

- `startWord = cccc`
- `maxFaces = 10000`
- `maxNewVerts = 3`

The other input parameters are set by the definition of $\mathcal{P}$. It is helpful to construct a list of short admissible words using the star graph. We give the list of admissible words of length at most 8 in Table 3.1. This list is complete up to cyclic permutation. There are a large number of length-8 words; however, since `maxNewVerts = 3`, we would only add a face with a word of length 8 if we already had a subword of length 5. Notice that for any valid subword of length 5 there are at most two admissible words of length 8 containing that subword. While this limits the possible pictures that can be found, such constraints are often necessary to reduce branching and ensure the search completes in a reasonable amount of time.

Length 4	Length 5	Length 6	Length 7	Length 8	
cccc	acAbb		acccABB	acAbaCAB	aCCABBBB
CCCC	aCABB		aCCCAbb	acABaCAb	bbbbbbbb
				accAbbbb	BBBBBBBB
				accABBBB	cccccccc
				aCCAbbbb	CCCCCCCC

TABLE 3.1: Admissible words of length up to 8 for the presentation $\langle G, x \mid xaxbx^{-1}c \rangle$ where $a = 1$, $|b| = 8$, and $c = b^{-2}$

Figure 3.3 shows the first few iterations of our method. We also give a brief description of these steps:
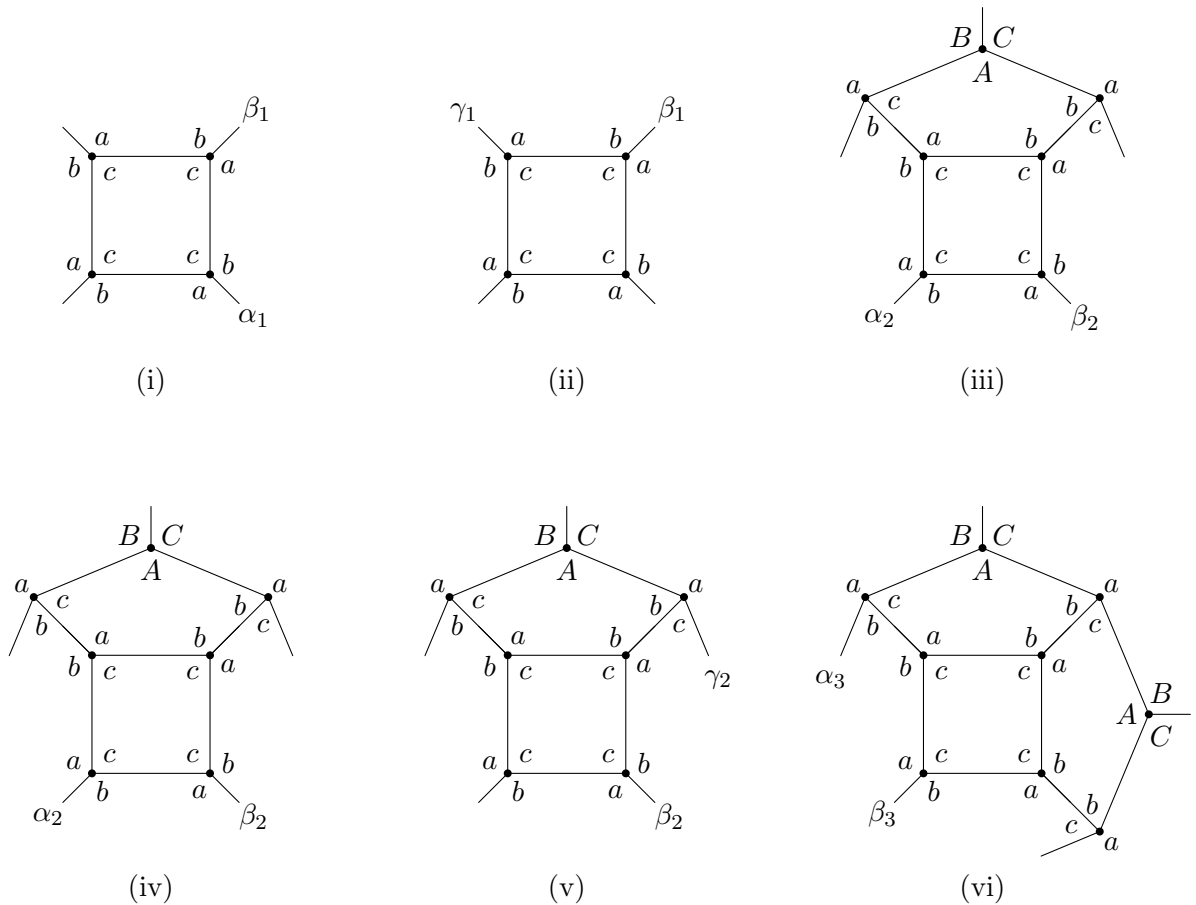
FIGURE 3.3: Our method applied to the presentation $\langle G, x \mid xaxbx^{-1}c \rangle$ where $a = 1$, $|b| = 8$, and $c = b^{-2}$

1. We start by placing a face with corner labels *cccc* as in Figure 3.3(i). When placing this face, we place the rightmost edge first, and then place the subsequent edges in a clockwise order.

2. We define β_1 to be the counterclockwise-most half edge of the first added vertex, as in Figure 3.3(i).

3. We let α_1 be the half edge immediately clockwise to β_1, as in Figure 3.3(i). The subword in G from α_1 to β_1 reads *ba*. Since this is not an admissible path, no hop faces can be added.

4. We let γ_1 be the half edge immediately counterclockwise to β_1, as in Figure 3.3(ii). The subword in G from β_1 to γ_1 reads ba. Since `maxNewVertices = 3` and ba has length 2, the elements of L_1 must have length at most 5. There is only one such admissible word (up to cyclic permutation) containing ba, so $L_1 = \{bacAb\}$.

5. L_1 is not empty, so we go to step 9.

9. We add the face with corner labels $bacAb$ between β_1 and γ_1 as in Figure 3.3(iii). We remove the first (and only) element from L_1 to get $L_1 = \{\}$.

10. There are 5 remaining half edges, so we do not terminate at this step.

11. All of our constraints are satisfied, so we go to step 2.

2. We define β_2 to be the first half edge immediately clockwise to the clockwise-most edge of the newly added face, as in Figure 3.3(iii)

3. As indicated by Figure 3.3(iv), no hop faces are possible.

4. As indicated by Figure 3.3(v), the subword between β_2 and γ_2 is bac. There is only one admissible word up to length 6 starting with bac, so we define $L_2 = \{bacAb\}$.

5. L_2 is not empty, so we go to step 9.

9. We add the face $bacAb$ between β_2 and γ_2 as in Figure 3.3(vi).

Continuing this process eventually yields the picture shown in Figure 3.4 with faces numbered in the order that they were added. At this point, the word from α_d to β_d is $CCCC$, which is admissible. The spherical picture could be completed with a hop face that encloses the C corners. Completing a picture with a hop face generally gives less symmetric pictures than completion with an ordinary face. We therefore insist that a picture be completed with a non-hop face. This is the reason for the restriction on the

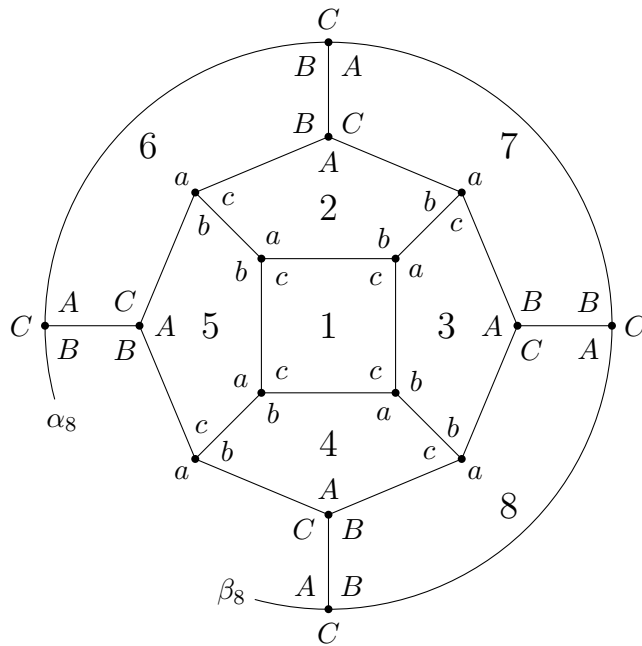FIGURE 3.4: A nearly spherical picture over the presentation $\langle G, x \mid xaxbx^{-1}c \rangle$ where $a = 1$, $|b| = 8$, and $c = b^{-2}$. Numbers indicate the order in which faces were added.

number of half edges in step 3(a) of our method. The process terminates after finding the spherical picture shown in Figure 3.1.

Our implementation gives the following output:

```
0001  cccc (x1)      0005  bbac A        0009  BBaCA

0002  ba cAb         0006  BaC AB        0010  CCCC (x1)

0003  bac Ab         0007  BaCA B

0004  bac Ab         0008  BaCA B
```

Each line gives the number of a face and the admissible word (sometimes separated into two pieces) representing the corner labels of that face. If a word is separated into two pieces by a space, the subword before the space represents the subword already present in the picture before that face was added, and the subword after the space represents the subword that was added to make the complete word admissible. The final line gives the

corner labeling of the outer annular face. The (x1) in the first and last lines indicates 1-fold symmetry (asymmetry).

The picture over this presentation is clearly symmetric of degree 4. If we run our program with symmetry = 4 and startWord = c, we get the following output.

```
0001   c (x4)

0002   ba cAb

0003   BaC AB

0004   C (x4)
```

3.3   Example 2

Consider the presentation $\mathcal{P} = \langle G, x \mid xaxbx^{-1}c \rangle$ where $a = 1$, $|b| = 8$, and $c = b^2$. This presentation was shown to be non-aspherical by a calculation in [3, table 4]. A reduced spherical picture for $\mathcal{P}$ with labels omitted is given in Figure 3.5. The picture can be labeled by specifying that the central face is labeled with B^9. All other corner labels can be deduced from the fact that the picture is reduced.

We use this picture to illustrate the usefulness of hop faces. Suppose that we specify the following input for our method:

- symmetry = 4
- startWord = BB
- maxVertices = 10000
- maxFaces = 10000
- maxHalfEdges = 10
- maxNewVerts = 6

After many iterations, we arrive at the picture given in Figure 3.6, with numbers indicating the order in which faces were added. At this point, no hop faces have been used. The half edges α_{13}, β_{13}, and γ_{13} are indicated in the upper left part of the picture. If hop faces are not allowed, then we must make a face between β_{13} and γ_{13}, preventing β_{13}
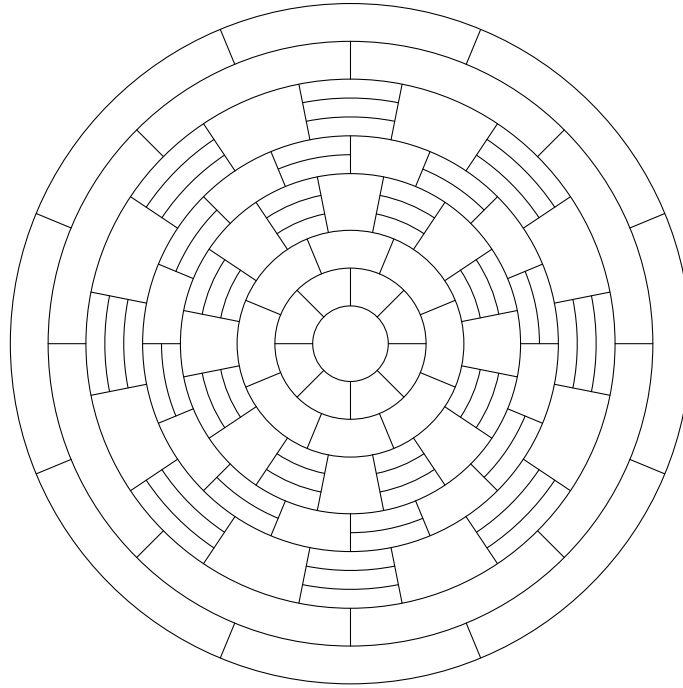
FIGURE 3.5: An unlabeled spherical picture over the presentation $\langle G, x \mid xaxbx^{-1}c \rangle$ where $a = 1$, $|b| = 8$, and $c = b^2$

from connecting with α_{13}. Thus, under the given inputs, we cannot build the picture in

Figure 3.5 without hop faces.

Our implementation gives the following output:

0001	BB (x4)		0010	CCCC		0019	CAb ba
0002	CA bba		0011	cABB a		0020	cAb acAbac
0003	aCAb b		0012	Abb aC		0021	CAbba
0004	acc cAbb		0013	ABB BBacc		0022	CAbb a
0005	baccc Ab		0014	CCCC (hop)		0023	accAb acAb
0006	Bac AB		0015	cABBa		0024	cccc
0007	aCA BaCCAB		0016	Abba C		0025	bbaC A
0008	BacA B		0017	ccABB BBa		0026	BaC CCAB
0009	BaCA BaCCA		0018	CAbb a		0027	cccc (hop)
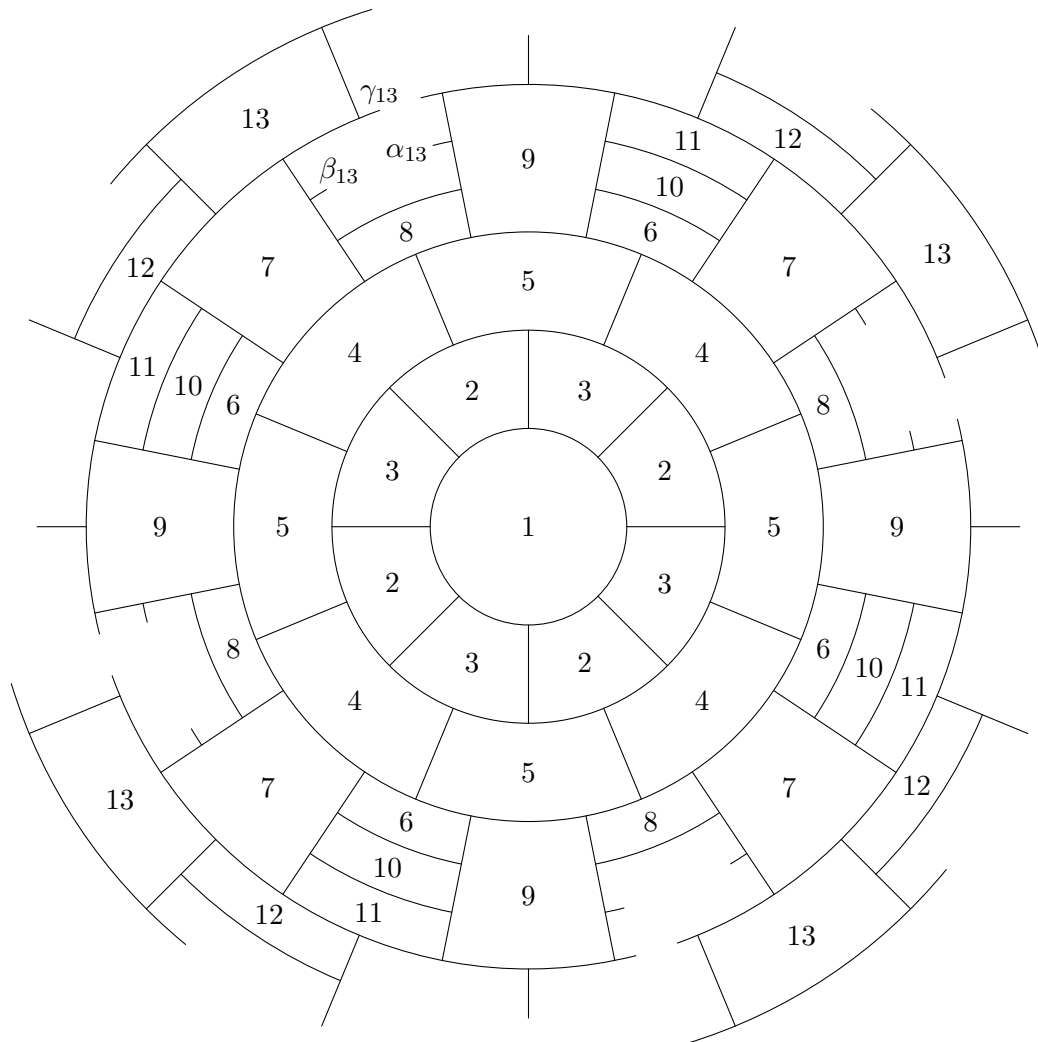
FIGURE 3.6: A hop face between α_{13} and β_{13} is necessary to complete the picture.

```
0028  bbaCA          0030  ABB ac        0032  bb (x4)
0029  ABBaCC C       0031  cABBa
```

Lines that end in (hop) indicate a hop face. We can also find this picture with an 8-fold symmetric search. This gives the following output.

```
0001  B (x8)         0003  acc cAbb      0005  BaCA BaCCA
0002  CA bba         0004  Bac AB        0006  CCCC
```

0007	cABB a	0011	CAb ba	0015	BBaC CCA
0008	Abb aC	0012	accAb acAb	0016	ABB ac
0009	ccABB BBa	0013	cccc	0017	b (x8)
0010	CAbb a	0014	bbaC A		

Notice that the 8-fold symmetric search did not require a hop face.

3.4 Implementation Details

We implemented our method for finding pictures over $\mathcal{P}$ using the C programming language. Our code [49] can be found at the following address.

https://ir.library.oregonstate.edu/concern/datasets/6395wf63g

We now give a brief description of the details of our implementation.

Let $\mathcal{P} = \langle G, x \mid r \rangle$ where G is a finite cyclic group generated by g and

$$r = x^{\varepsilon_1} g^{\sigma_1} x^{\varepsilon_2} g^{\sigma_2} \cdots x^{\varepsilon_n} g^{\sigma_n}$$

with $\varepsilon_i = \pm 1$ and $\sigma_i \in \mathbb{Z}$. We start by constructing a representation of the star graph $\mathcal{P}^{\mathrm{st}}$. The edges of $\mathcal{P}^{\mathrm{st}}$ are ordered, so that each path in $\mathcal{P}^{\mathrm{st}}$ can be represented by a list of integers. All paths in $\mathcal{P}^{\mathrm{st}}$ of length up to `maxNewVertices` without backtracking are stored in a cache.

To represent the current picture, we maintain three stacks, S_V, S_C, and S_E, containing respectively the vertices, corners, and half edges. Here we expand the definition of half edge given in Section 3.1.1. We now allow a half edge to be part of a complete edge (and so disconnected from the boundary of the current picture). As faces are added to the picture, corners and half edges eventually become part of a complete face. Each corner and half edge is therefore given an integer **depth flag** indicating at what depth that corner or half edge became part of a complete face. The corners and half edges that

are not yet part of a complete face are given a depth flag value of 0, and will be called **outer** corners or half edges.

When a new face is added to the picture, we push new vertices to S_V in the order matching a clockwise path around the new face. As an example, consider the face added in Figure 3.3(iii) of Section 3.2. We would push the three new vertices to S_V in the order indicated in Figure 3.7.
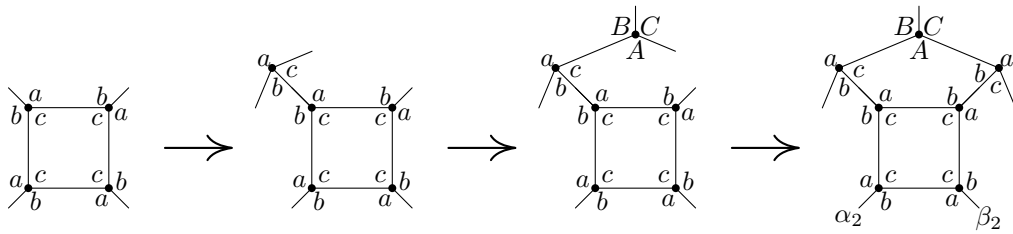

FIGURE 3.7: Adding vertices in a clockwise order about a new face

Since each vertex has the same number of corners and half edges, S_E and S_C should always have the same length. For any half edge ℓ in S_E, the corner at the same relative position in S_C is the corner immediately counterclockwise to ℓ.

When a vertex is pushed to S_V, we also push its corners and half edges to S_C and S_E respectively. These corners and half edges are pushed in a clockwise order about the newly added vertex starting from the corner inside the newly added face. In Figure 3.7 , the new corner labels are pushed to S_C in the order $c, b, a, A, B, C, b, a, c$.

Our construction of the corner and half edge stacks gives the following invariants:

- the first outer half edge from the bottom of the stack S_E represents β_d as defined in step 2 of the method.

- reading the outer corners or half edges in S_C or S_E respectively from bottom to top represents reading clockwise around the boundary of the picture.

As a result, γ_d is always the last outer half edge from the bottom of S_E. We can thus add vertices (and corners and half edges) between γ_d and β_d by pushing them onto the

top of the stack. Notice that α_d (as defined in step 3 of the method) is always the second outer half edge from the bottom of S_E. Since hop faces are only added by connecting two existing half edges, we never add vertices (or corners or half edges) between β_d and α_d.

We can read the subword between the outer half edges β_d and γ_d by starting at the corner whose position in S_C is the same as the position of β_d in S_E. We continue reading each outer edge as we move towards the bottom of the stack. When we reach the bottom of the stack, we loop back to the top and continue reading outer corners until we reach the corner whose position in S_C is immediately above the equivalent position of γ_d in S_E.

Rather than calculating the list L_d every time we reach step 4 of the method, we instead construct the lists for all possible starting subwords that we could read in step 4(b) and store these lists in a lookup table. Any starting subword w can be represented by a triple (u, v, h) where u is the first corner label of w, v is the last corner label of w, and words and h is the element of G corresponding to w. This is visualized in Figure 3.8. To find an admissible word that starts with w, we need to find a word w' that can follow v and be followed by u in $\mathcal{P}^{\text{st}}$ such that w' defines h^{-1} in G. When `maxNewVertices` is small, it is possible to test all paths w' in $\mathcal{P}^{\text{st}}$ from v to u.
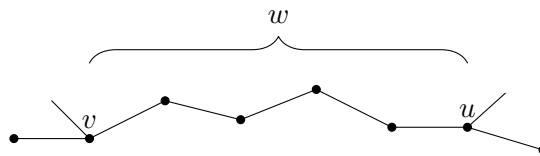

FIGURE 3.8: Corner labels from u to v give the starting word w.

3.5 Discussion of Limitations

Section 3.3 gave a situation in which hop faces were needed to complete a picture. In that case, sufficiently complicated structure in a picture prevented the naive search order (i.e., with no hops) from finding the picture. Hop faces solved this problem and allowed us

to find pictures in previously unsolved cases, but there is no reason to think that hop faces are sufficient to deal with all possible picture structures. Indeed, the primary motivation for our definition of hop faces was ease of implementation.

We noted at the end of Section 3.3 that an 8-fold symmetric search could find a picture without using hop faces. In that case, the increased level of symmetry allowed a more limited method to succeed. This is not always the case. The picture given in Section 4.1.3 has 6-fold symmetry, but cannot be found by applying our method with 6-fold symmetry. We instead used 3-fold symmetry to find this picture.

Experimentally, the method seems to be less effective when the relator r in $\langle G, x \mid r \rangle$ has more x symbols. It appears likely that this is at least partly the result of our restrictive prescribed order for adding new faces. Allowing for a more general face placement would require different data structures than those presented in Section 3.4. For example, using linked lists, rather than stacks, for storing corners and half edges and vertices would allow faces to be added between any two outer half edges in the current picture.

There are two chief difficulties with allowing new faces to be added anywhere on the picture:

1. The average branching factor of the search graph (the number of choices we can make at each search state) is much larger. Although we can explore more of the search graph, poor choices may take us down time-wasting paths that are unlikely to result in a complete picture.

2. There is significant reconvergence of the search graph. That is, we often reach the same search state from different paths, causing us to repeat work that has already been completed.

We expect that a breadth-first search with periodic pruning can likely address these issues. Unlike our depth-first search, which only stores a single picture at a time, a breadth-first search would simultaneously store every picture up to the current depth. A hash function

could then be used to identify different paths in the search graph that result in the same picture. This addresses the high level of reconvergence.

To address the large average branching factor, we could periodically prune the breadth-first graph by removing branches that have some undesirable quality (e.g., a large number of outer half edges). Although this limits the search area, a reasonable choice of pruning criteria would likely give us a better chance of finding a picture in a reasonable amount of time than a search without pruning.

The biggest limitation of a breadth-first search is the high memory usage from storing every branch of the search graph. We are hopeful that the current availability of high capacity memory storage will be sufficient for a usable implementation.

4   COMPUTATIONAL RESULTS

4.1   Program Output

In this section we give the direct output from our program for the presentations in Theorems A, B and H. We follow the conventions given in Section 3.1.1. Output looks like a list of words in G which represent the corner labels of the faces in a reduced spherical picture. Since our pictures are built by placing adding faces in the prescribed order defined in Section 3.1, this list is enough to construct the spherical picture. We build these pictures explicitly in Section 4.2.

When searching for spherical pictures, we generally began with a starting word with some degree of symmetry. We set `maxNewVertices` to a value in the range 3 to 7, and set `maxVertices` and `maxFaces` to be large enough that they would not influence the search. We then ran the search multiple times, incrementally increasing `maxHalfEdges`.

Each line of our output gives an admissible word that represents the corner labeling of a face in the picture. When a word is split into two subwords by a space, the first subword represents the corner labels that were in the picture before the face was added, and the subword after the space represents the corner labels that were added to complete the face. Hop faces are indicated by `(hop)`. Faces are added in a clockwise spiral pattern. as can be seen in Figure 3.4.

The first and last lines contain a (not necessarily admissible) subword and a multiplier denoted `(xn)`, where `n` is the order of symmetry for the picture. The words for the first and last faces are formed by repeating the respective subwords `n` times. When `n > 1`, the output only represents a single section of the picture, with `n` sections forming the complete spherical picture. See Figure 3.6 for an example of constructing a spherical picture when `n = 4`.

Program output for some other presentations is given in Appendix A. In each of those cases, the presentations were known to be non-aspherical, but no explicit pictures had been constructed.

4.1.1 $\mathcal{P} = \langle G, x \mid x^2 g x^{-1} g^3 \rangle$ with $G = \langle g \mid g^9 \rangle$

Let $\mathcal{P} = \langle G, x \mid x^2 g x^{-1} g^3 \rangle$ where G is the cyclic group of order 9 generated by g. This matches the presentation in Theorem A. Rewriting $\mathcal{P}$ using the notation of Section 3.1.1 gives

$$\mathcal{V} = \langle G, x \mid xaxbx^{-1}c \rangle$$

where $a = 1$, $b = g$, and $c = g^3$. We feed our program the following input (see Section 3.1.2):

- relatorLength = 3
- relatorShape = xxX
- groupOrder = 9
- coefficientExponents = $\{0,1,3\}$
- symmetry = 3

- startWord = BBB
- maxVertices = 10000
- maxFaces = 10000
- maxHalfEdges = 27
- maxNewVertices = 6

This gives the following output:

0001 BBB (x3)	0007 accA BaCABB	0013 ccc
0002 CA bbba	0008 ccc (hop)	0014 Abac ABaC
0003 CAb bba	0009 bbacA bacA	0015 CCC (hop)
0004 aCAb acAB	0010 CCC (hop)	0016 cABBB a
0005 acA BBB	0011 CABaC ABBa	0017 Abb baC
0006 acA baCAB	0012 aCAb bb	0018 BBB acA

0019 CCC	0046 acA baCAB	0073 AbbbaC
0020 aCABa cAb	0047 acA BBB	0074 BBBBB BBBB
0021 ccc	0048 CCC (hop)	0075 ccc (hop)
0022 bbaC Ab	0049 CABacA ba	0076 bbaCA b
0023 BBac AB	0050 acAb accAB	0077 Bac ABB
0024 CCA BBBa	0051 ccc (hop)	0078 ccc (hop)
0025 CAb bba	0052 AbacA BaC	0079 bbaCA b
0026 BacAb aCA	0053 CCC (hop)	0080 Bac AbaCA
0027 CCC	0054 acABBB	0081 CCC
0028 cABB Ba	0055 ccc (hop)	0082 BacABB
0029 acAbb acAb	0056 AbacAb bac	0083 aCAb acAB
0030 ccc	0057 BBBa cA	0084 acA BBB
0031 cAbaC ABa	0058 CCC	0085 ccA bbba
0032 bbbb bbbbb	0059 cABa CAba	0086 Abbb aC
0033 BBac AB	0060 CCAbb acAba	0087 CCC (hop)
0034 CCC (hop)	0061 CAb acABa	0088 cABBB a
0035 CABaCA BBa	0062 aCAb bb	0089 CAbb ba
0036 CAb bba	0063 ccc	0090 CAb acABa
0037 acAb aCAB	0064 Abac Abbac	0091 CAb bba
0038 ccc (hop)	0065 CCC (hop)	0092 BaCAb acA
0039 CAbacA Ba	0066 CABBa CABa	0093 CCC
0040 ccAb bba	0067 ccc (hop)	0094 BaCABa CAB
0041 bbb aCA	0068 bbaCAb	0095 ccc (hop)
0042 BBaC ABaCA	0069 bacA BaCA	0096 bbaCA b
0043 CCC	0070 CCC (hop)	0097 CCC (hop)
0044 acABB B	0071 acABaC Ab	0098 CABac Aba
0045 acA BBB	0072 ccc	0099 aCAb acAB

0100 acA BBB	0109 BBa cAB	0118 ccc
0101 ccc (hop)	0110 BaCCA BB	0119 bbbaC A
0102 ccc (hop)	0111 ccc (hop)	0120 CCC (hop)
0103 bbacAbacA	0112 bbaCA b	0121 BBaCABaC A
0104 BaCA baCCA	0113 CCC (hop)	0122 CCC
0105 CCC	0114 aCABac Ab	0123 cABBBa
0106 acABB B	0115 ccc	0124 bbb (x3)
0107 ccc (hop)	0116 AbaC ABac	
0108 AbbacA bac	0117 aCABa cAb	

This defines a reduced spherical picture over $\mathcal{V}$ with $2 + 3(122) = 368$ faces. An explicit construction of this picture is given in Section 4.2.1.

4.1.2 $\mathcal{P} = \langle G, x \mid x^2 g x^{-1} g^{-3} \rangle$ with $G = \langle g \mid g^9 \rangle$

Let $\mathcal{P} = \langle G, x \mid x^2 g x^{-1} g^{-3} \rangle$ where G is the cyclic group of order 9 generated by g. This matches the presentation in Theorem B. Rewriting $\mathcal{P}$ using the notation of Section 3.1.1 gives

$$\mathcal{V} = \langle G, x \mid xaxbx^{-1}c \rangle$$

where $a = 1$, $b = g$, and $c = g^{-3}$. We feed our program the following input (see Section 3.1.2):

- relatorLength = 3
- relatorShape = xxX
- groupOrder = 9
- coefficientExponents = {0,1,-3}
- symmetry = 9

- startWord = B
- maxVertices = 10000
- maxFaces = 10000
- maxHalfEdges = 15
- maxNewVertices = 7

This gives the following output:

0001 B (x9)	0026 ccc	0051 ccc (hop)
0002 CA bacABa	0027 bbbac A	0052 bbaCAb accA
0003 ccA BacAba	0028 BBaC AB	0053 CCC (hop)
0004 bbb acA	0029 CCA BacABBa	0054 cABBaC Abba
0005 CCC (hop)	0030 ccc (hop)	0055 bbb acA
0006 cABaC Aba	0031 bbacAb	0056 BBaC AB
0007 bbb acA	0032 CCC (hop)	0057 aCA BBB
0008 BaC ABB	0033 CABBacA bba	0058 ccc (hop)
0009 ccc (hop)	0034 aCAb acAB	0059 bbacA b
0010 bbaCA baCA	0035 CCC (hop)	0060 bac ABaCA
0011 BBaC AB	0036 cABBacA Ba	0061 BBaC AB
0012 ccc (hop)	0037 bbb acA	0062 aCA BBB
0013 bbaCA BBacA	0038 BaC AbaCCA	0063 ccc (hop)
0014 BBaC AbbacA	0039 CCC	0064 bbacA b
0015 CCC	0040 aCABB B	0065 CCC (hop)
0016 aCABa cAb	0041 ccc (hop)	0066 CABBac Abba
0017 ccc	0042 bbacA b	0067 BaCAb acA
0018 AbaC ABac	0043 CCC (hop)	0068 CCC
0019 CCC (hop)	0044 ccABac Aba	0069 cABa cABBa
0020 CABBBa	0045 bbb acA	0070 Abb bac
0021 cAbb ba	0046 BBaC AB	0071 CCC (hop)
0022 bbb acA	0047 aCA BacAb	0072 CABBBa
0023 BBaC AB	0048 ccc	0073 BaCAbb acAB
0024 aCA BBB	0049 AbaC AbbaC	0074 aCA BBB
0025 acA bbb	0050 BaCABB	0075 ccc (hop)

0076	bbbacA	0080	ccc (hop)	0084	ccc
0077	BaCA baCCA	0081	bbacAb	0085	AbaCAB ac
0078	CCC	0082	CCC (hop)	0086	b (x9)
0079	CABB Ba	0083	aCABacA b		

This defines a reduced spherical picture over $\mathcal{V}$ with $2 + 9(84) = 758$ faces. An explicit construction of this picture is given in Section 4.2.2.

4.1.3 $\mathcal{P} = \langle G, x \mid x^3 g^2 x^{-1} g \rangle$ with $G = \langle g \mid g^6 \rangle$

Let $\mathcal{P} = \langle G, x \mid x^3 g^2 x^{-1} g \rangle$ where G is the cyclic group of order 6 generated by g. This matches the presentation in Theorem H. Rewriting $\mathcal{P}$ using the notation of Section 3.1.1 gives

$$\mathcal{V} = \langle G, x \mid xaxbxcx^{-1}d \rangle$$

where $a = b = 1$, $c = g^2$, and $d = g$. We feed our program the following input (see Section 3.1.2):

- relatorLength = 4
- relatorShape = xxxX
- groupOrder = 6
- coefficientExponents = $\{0,0,2,1\}$
- symmetry = 3

- startWord = DD
- maxVertices = 10000
- maxFaces = 10000
- maxHalfEdges = 10
- maxNewVertices = 3

This gives the following output:

0001	DD (x3)	0004	aB (hop)	0007	bd dAC
0002	AC bdd	0005	dACb dAb	0008	ccaB c
0003	Ba	0006	ccc	0009	Ba (hop)

0010	Cbd dA	0015	caDDB	0020	bA (hop)
0011	caDD B	0016	Ba (hop)	0021	aDDBc
0012	Ba (hop)	0017	CCbA C	0022	dd (x3)
0013	CbA CC	0018	DDB ca		
0014	bA (hop)	0019	Ab		

This defines a reduced spherical picture over $\mathcal{V}$ with $2 + 3(20) = 62$ faces. An explicit construction of this picture is given in Section 4.2.3.

4.2 Explicit Spherical Pictures

In this section we construct explicit descriptions of the spherical pictures found in Section 4.1. We utilized the R software environment [56] with the igraph [19] and rgl [1] packages for some basic visualizations. We then observed further symmetry (in addition to the inherent rotational symmetry), allowing us to simplify our descriptions. Notation matches the conventions in Section 3.1.1.

4.2.1 $\mathcal{P} = \langle G, x \mid x^2 g x^{-1} g^3 \rangle$ with $G = \langle g \mid g^9 \rangle$

Let $\mathcal{P} = \langle G, x \mid xaxbx^{-1}c \rangle$ where $a = 1$, $|b| = 9$, and $c = b^3$. This matches the presentation in Theorem A where $g = b$. The program output in Section 4.1.1 defines a segment comprising one third of a complete spherical picture. In fact, this segment can be broken down into two related pieces, which we draw as truncated squares. The first square is given in Figure 4.1. The second square is given in Figure 4.2 and is obtained by flipping the first square over a horizontal axis and replacing each corner label with its inverse (i.e., replace a with A, etc.). Notice that the edges of these squares have the same basic structure up to rotation and reflection and inverting of corner labels. We can thus attach these squares together by allowing their edges to overlap in certain ways.
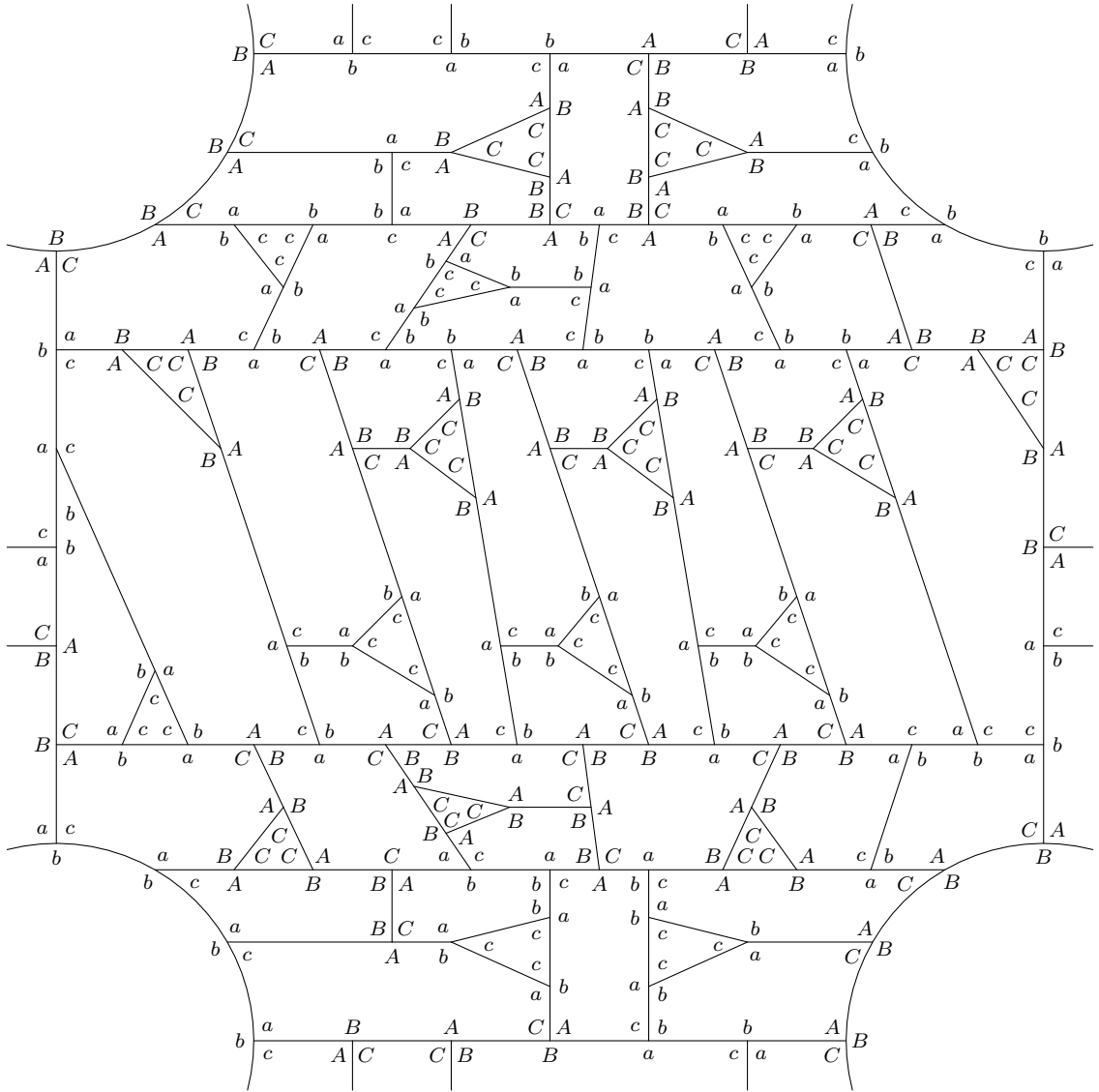
FIGURE 4.1: A truncated square representing one sixth of a complete spherical picture
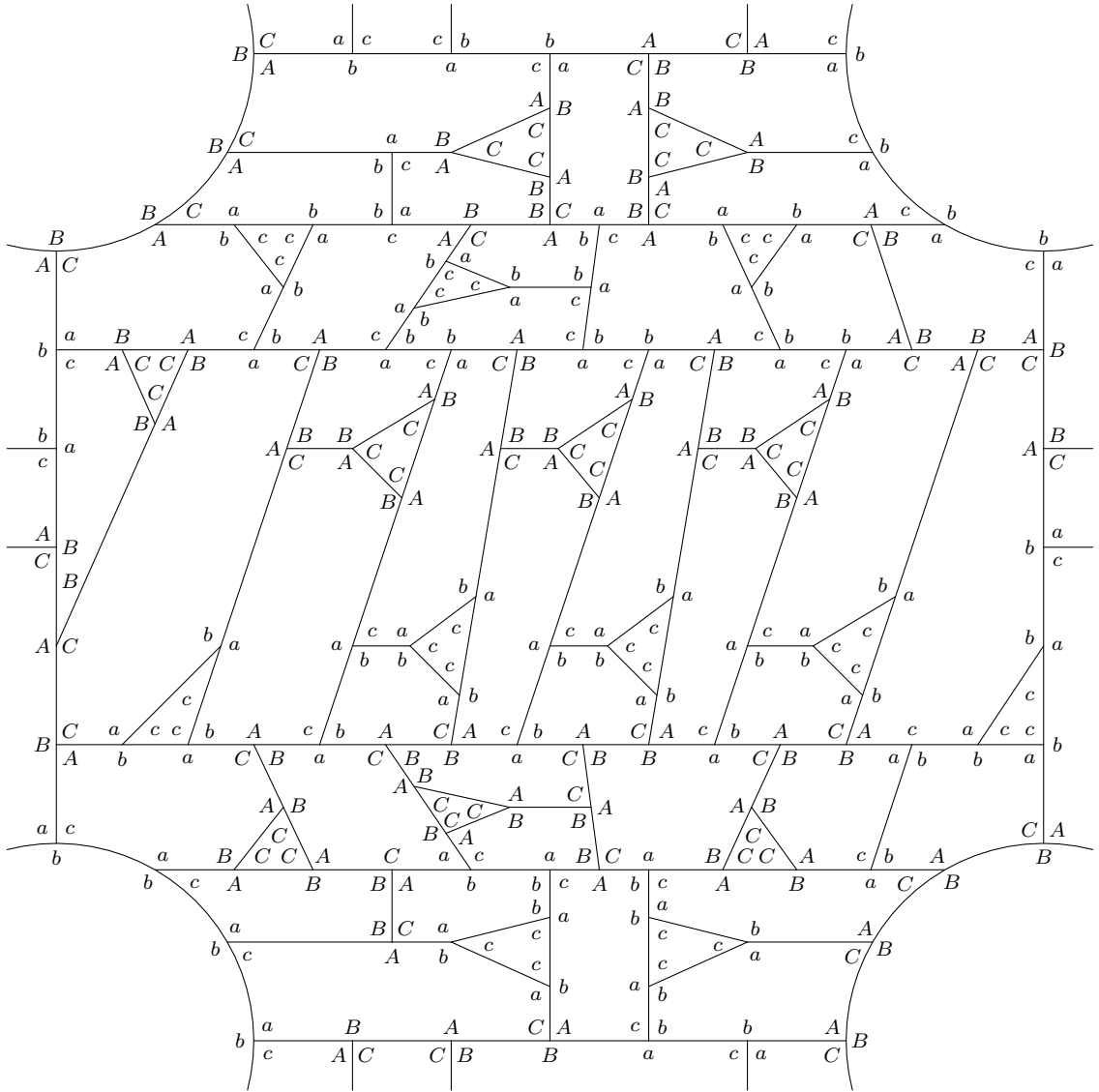
FIGURE 4.2: A flipped square with inverted corner labels

Denote Figures 4.1 and 4.2 by truncated squares containing the letter "F" to indicate orientation. Specifically, ⬚F represents Figure 4.1, and ⬚Ⅎ represents Figure 4.2. We visualize the picture as a truncated cube obtained by folding the net given in Figure 4.3.
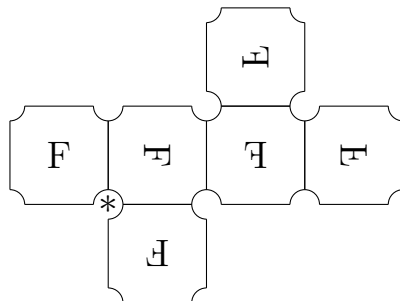

FIGURE 4.3: The picture is constructed by folding this net into a truncated cube.

We also visualize the picture as a rotationally symmetric plane-embedded graph. Consider the truncated cube formed from Figure 4.3. We visualize this cube using an isometric projection centered on the point marked $*$ in Figure 4.3, resulting in three non-visible facets. We send the point opposite $*$ to the point at infinity in the plane and stretch to non-visible facets accordingly. This is represented in Figure 4.4. Note that each of the small circles in Figure 4.4 are faces of the spherical picture with corner labels b^9 or B^9. The face containing $*$ has corner label B^9. Note from Figure 4.3 that there is only a single axis of 3-fold rotational symmetry, which passes through the point $*$ to the opposite corner of the truncated cube.
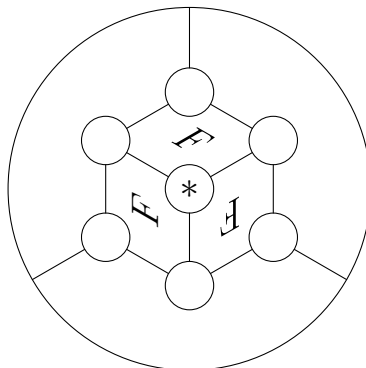

FIGURE 4.4: A symmetric visualization of the picture

4.2.2 $\mathcal{P} = \langle G, x \mid x^2 g x^{-1} g^{-3} \rangle$ with $G = \langle g \mid g^9 \rangle$

Let $\mathcal{P} = \langle G, x \mid xaxbx^{-1}c \rangle$ where $a = 1$, $|b| = 9$, and $c = b^{-3}$. This matches the presentation in Theorem B where $g = b$. The program output in Section 4.1.2 defines a segment comprising one ninth of a complete spherical picture. Each segment is composed of two annular sectors. The first sector is given in Figure 4.5.
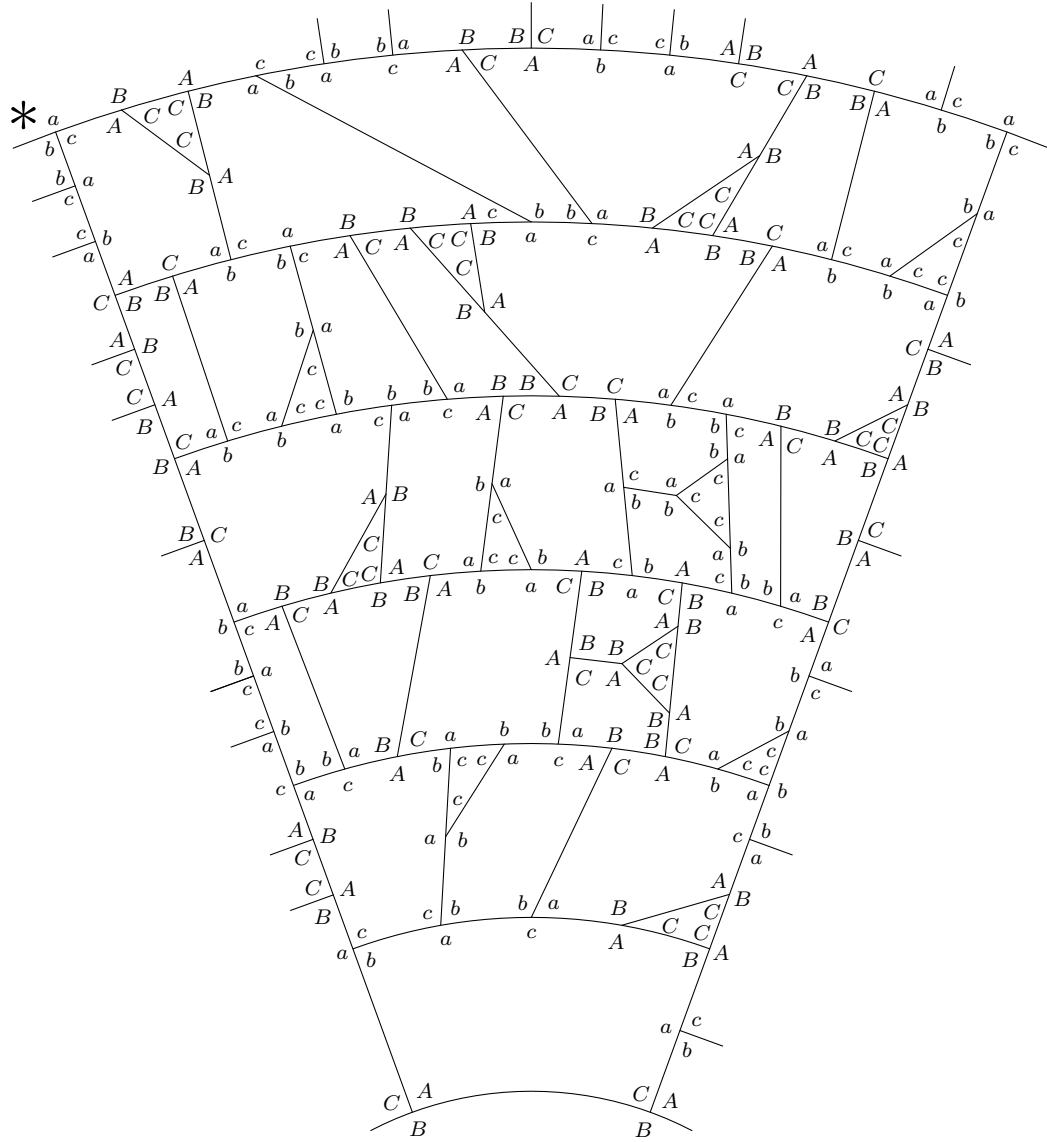

FIGURE 4.5: An annular sector representing one eighteenth of a spherical picture

The second sector is given in Figure 4.6 and is obtained by reflecting the first sector over a horizontal axis and replacing each corner label with its inverse (i.e., replace a with A, etc.).
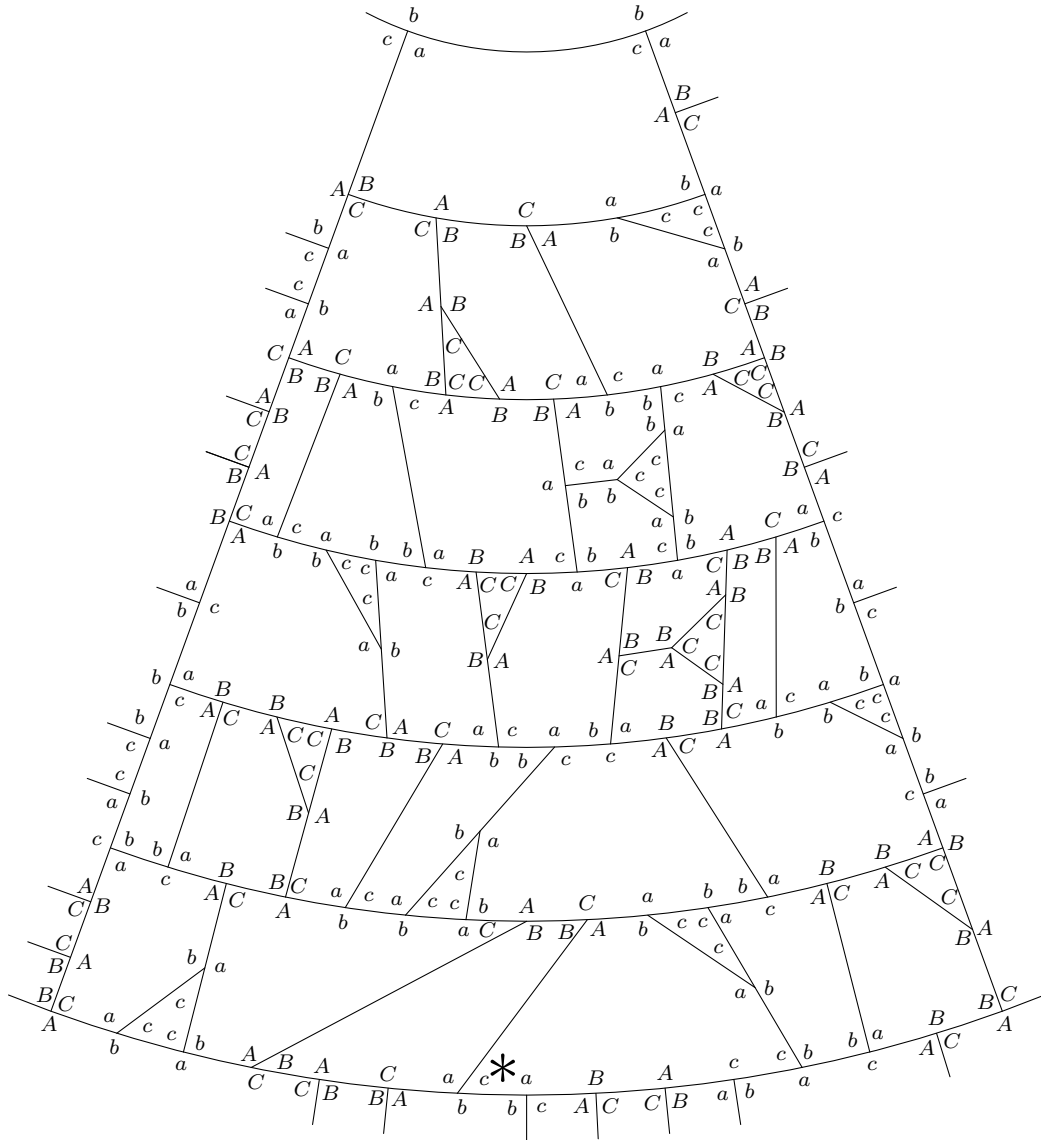

FIGURE 4.6: A flipped annular sector with inverted corner labels

Denote Figures 4.5 and 4.6 by annular sectors containing the letter "F" to indicate orientation. Specifically, ⟨F⟩ represents Figure 4.5, and ⟨E⟩ represents Figure 4.6. Notice that the left and right sides of the sector in Figure 4.5 have the same basic structure. Reading the labels on the outward side from top to bottom along the left side of the sector is the same as reading the labels on the inward side of the right side. After some squashing and stretching, we can attach sectors together along overlapping sides to form a circle. 9 sectors are required to make the central face admissible. We can likewise form a circle from 9 copies of the flipped sector. These circles are visualized in Figure 4.7.

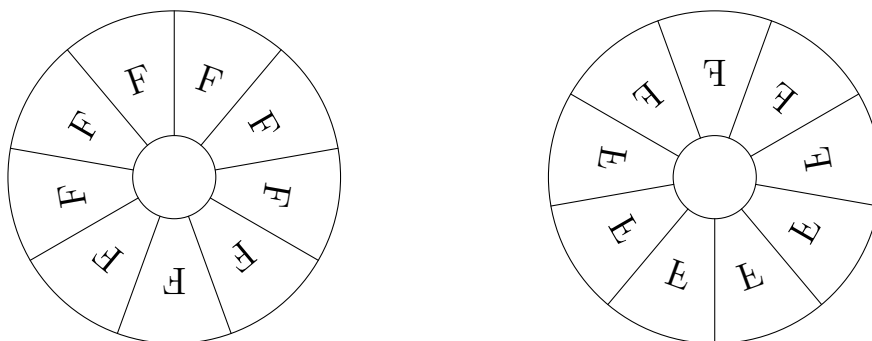

FIGURE 4.7: Circles formed from 9 copies of the the annular sectors

Each circle in Figure 4.7 represents a single hemisphere. These hemispheres can be attached along their circumference as follows:

Consider the points marked by ∗ in Figures 4.5 and 4.6. In each case, reading the corner labels to the right of the marked point in order along the arc gives the same sequence. Notice then that we can attach the two sectors by overlapping their long arc as indicated in Figure 4.8(i). We can likewise attach another flipped sector as in Figure 4.8(ii). Repeating this with 9 copies of each sector indicates the attachment of the two hemispheres.

Attaching these hemispheres gives a reduced spherical picture over $\mathcal{P}$. To visualize the picture in the plane, we orient the sphere so that only one hemisphere is visible. We then send the center of the opposite hemisphere to the point at infinity in the plane
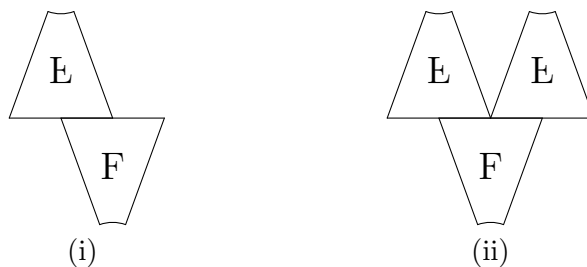
FIGURE 4.8: Oppositely oriented sectors can be attached along their long arcs

and stretch the annular sectors of that hemisphere accordingly. This is represented in Figure 4.9.
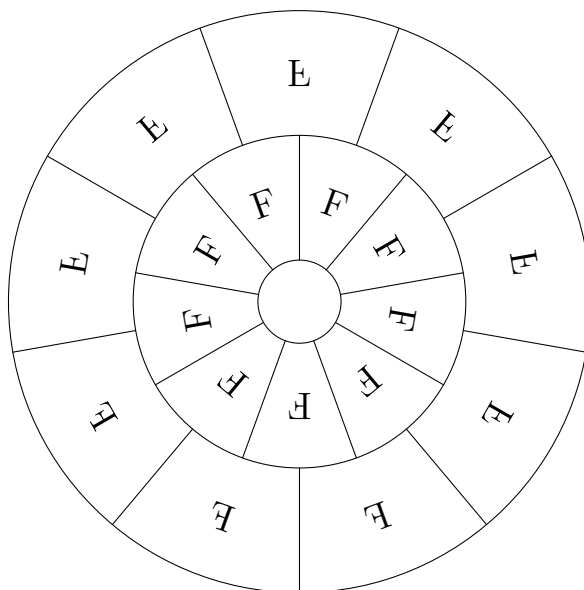

FIGURE 4.9: A symmetric visualization of the picture

4.2.3 $\mathcal{P} = \langle G, x \mid x^3 g^2 x^{-1} g \rangle$ with $G = \langle g \mid g^6 \rangle$

Let $\mathcal{P} = \langle G, x \mid xaxbx^{-1}c \rangle$ where $a = b = 1$, $c = d^2$, and $|d| = 6$. This matches the presentation in Theorem H where $g = d$. The program output in Section 4.1.3 defines a segment comprising one third of a complete spherical picture. We note that the picture actually has 6-fold symmetry, but a limitation of our method did not allow us to find this picture with a 6-fold symmetric search. Words of length 2 in the program output are

represented by double edges in the picture with corner labels omitted.

We form the spherical picture over $\mathcal{P}$ by attaching two grooved hemispheres. The first hemisphere is given in Figure 4.10. The other hemisphere is given in Figure 4.11 and is obtained by reflecting the first hemisphere over a horizontal axis and replacing each corner label with its inverse (i.e., replace a with A, etc.). A complete picture is formed by fitting the two hemispheres together along their boundaries like gears.
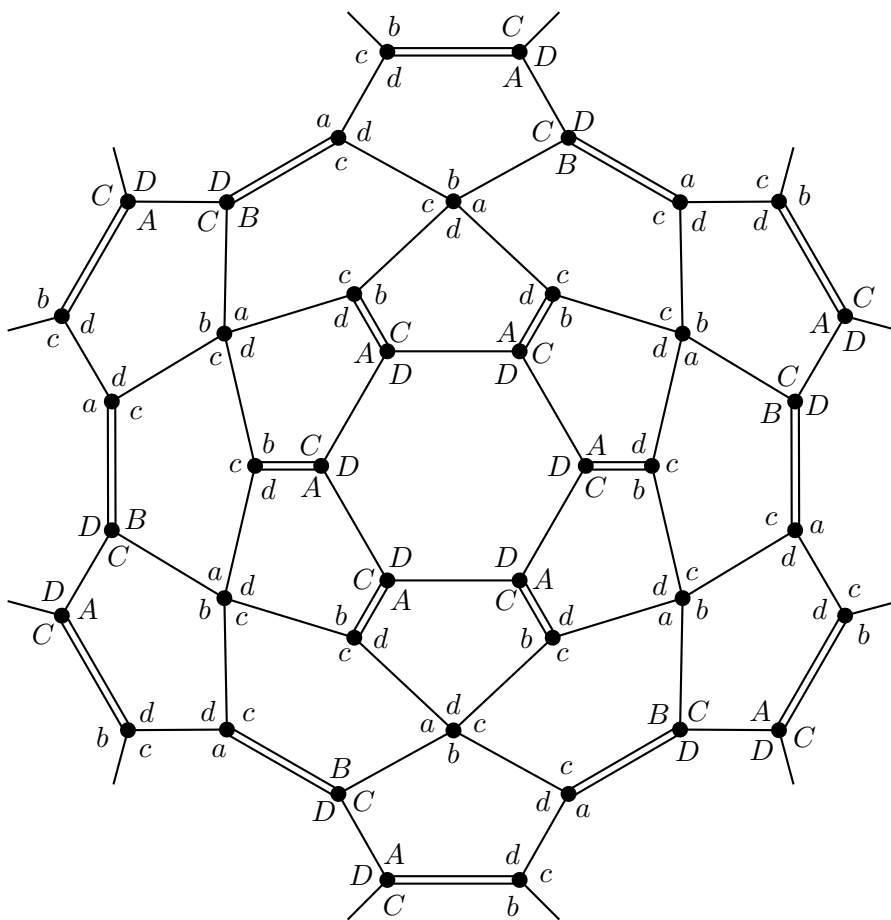

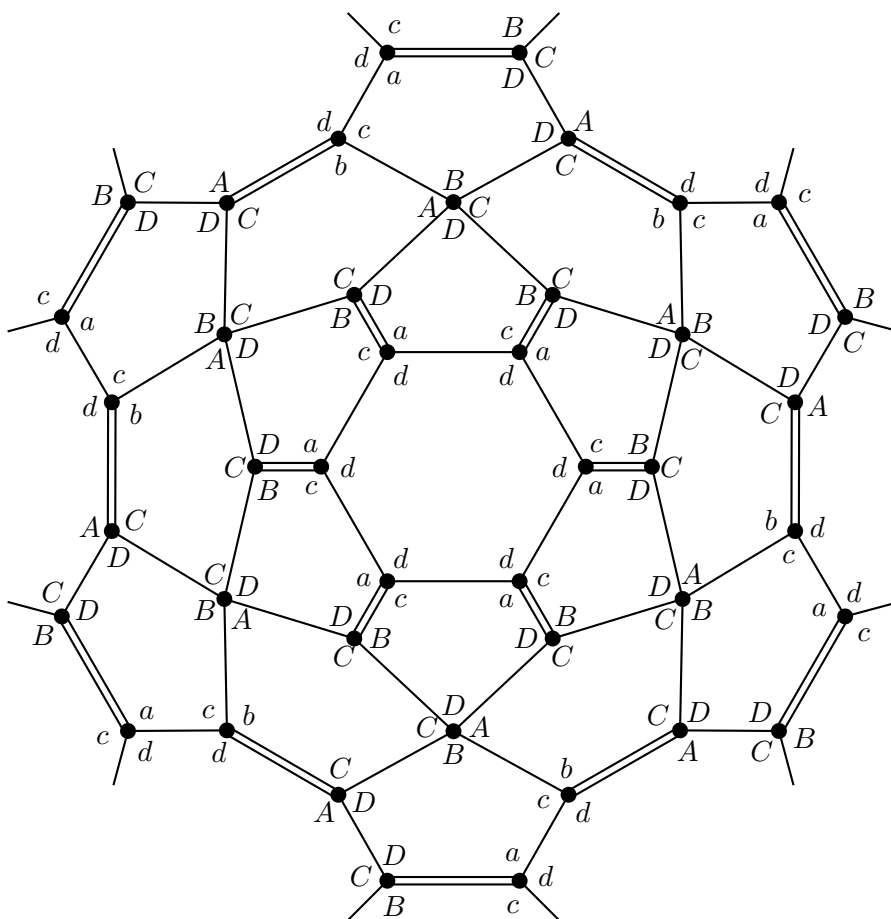FIGURE 4.10: A hemisphere representing one half of complete picture

FIGURE 4.11: A flipped hemisphere with inverted corner labels

5 PROOFS OF MAIN THEOREMS

In this chapter we give proofs of the theorems in Section 1.2. We make repeated use of the GAP computer algebra system [24].

In proving that the presentations of Theorems A, B and H are not aspherical, we do not attempt to show that the pictures given in Chapter 4 are nontrivial elements of the second relative homotopy group $\pi_2(L, K)$. Instead, we draw paths in the pictures and use the process of Section 2.3.2 to find representations of the identity in $G(\mathcal{P})$ that reveal violations of Theorem 2.2.5.

Recall that as our path passes through a face of the picture, we read the corner labels of that face that are to the left of the path. Arc orientation arrows are omitted, but for the presentations in Theorems A and B we can use the rule of thumb that orientation arrows point towards b and B, and point away from c and C (see Figures 2.5(i) and 2.5(ii)). That is, if we cross an arc α into a face κ, and one of the corners of κ meeting α has a label b or B, then we read x, and otherwise we read x^{-1}.

5.1 Proof of Theorem A

Let $\mathcal{P} = \langle G, x \mid x^2 g x^{-1} g^3 \rangle$ where G is cyclic of order 9 generated by g, and recall the reduced spherical picture depicted in Figures 4.3 and 4.4. Figure 5.1 depicts a loop drawn over our symmetric picture (compare with Figure 4.4). We also depict this loop in Figure 5.2 drawn over our folding net (compare with Figure 4.3).

The labels in Figure 5.1 represent the words read as the path passes along the labeled segments. Paths reading u and u^{-1} are shown explicitly in Figure 5.3, drawn on top of Figure 4.1. Here the corner labels represent the elements of G by the correspondence $a = A = 1$, $b = g$, $B = g^{-1}$, $c = g^3$, and $C = g^{-3}$.
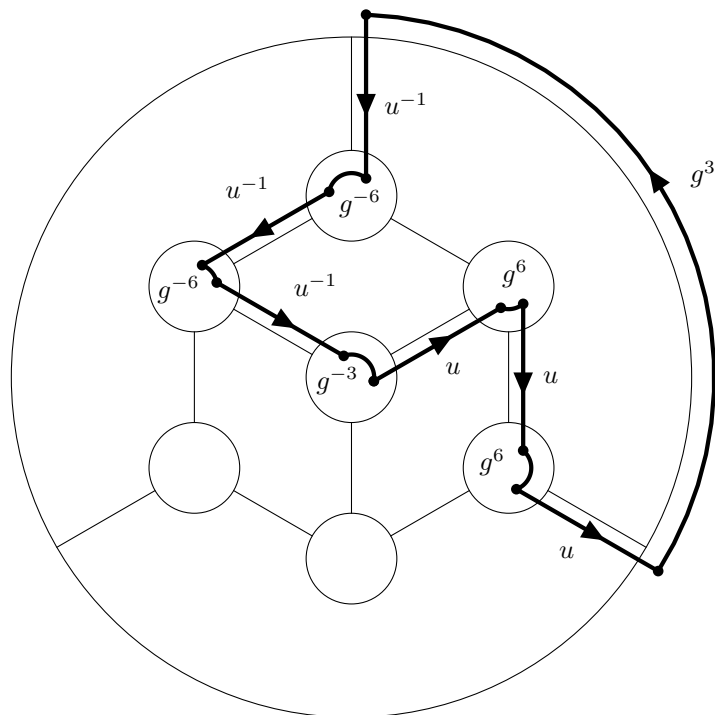
FIGURE 5.1: A loop in the picture over $\langle G, x \mid x^2 g x^{-1} g^3 \rangle$ where $|g| = 9$ (compare with Figure 4.4)
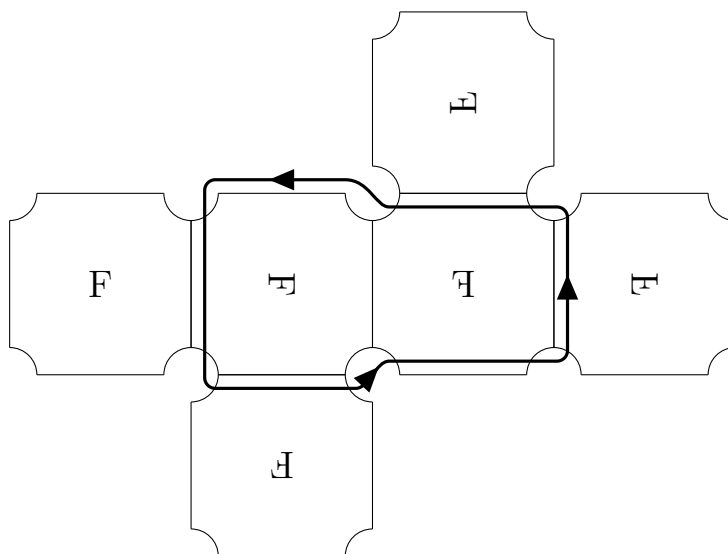

FIGURE 5.2: A loop in the picture over $\langle G, x \mid x^2 g x^{-1} g^3 \rangle$ where $|g| = 9$ (compare with Figure 4.3)

Figure 5.3 omits corner labels that are not read. We read u from the path traveling bottom-to-top on the right side of Figure 5.3:

$$u = x^{-1}g^2x^{-1}g^3x^{-1}g^5x.$$

Notice that reading along the path from left to right on the bottom of Figure 5.3 gives u^{-1}.

We now assume that $\mathcal{P}$ is aspherical in order to reach a contradiction. Starting from the central circle, the loop in Figure 5.1 gives the identity

$$ug^6ug^6ug^3u^{-1}g^{-6}u^{-1}g^{-6}u^{-1}g^{-3} = 1.$$

Grouping reveals the commutator relation

$$(ug^6ug^6u)g^3(ug^6ug^6u)^{-1}g^{-3} = 1.$$

Thus g^3 commutes with $w = ug^6ug^6u$, so $g^3 \in wGw^{-1} \cap G$. Since $\mathcal{P}$ is assumed to be aspherical, we have $w \in G$ by Theorem 2.2.5(b). There is a retraction $\nu_5 \colon G(\mathcal{P}) \to G$ given by $\nu_5(x) = g^5$, and we can easily calculate $\nu_5(u) = 1$. Therefore $\nu(w) = g^{12} = g^3$, so $w = g^3$. A calculation in GAP shows that $[w] \neq [g^3]$ in the finite quotient $G/\langle\!\langle x^6 \rangle\!\rangle$ (this quotient has order 1512). The GAP commands are as follows.

```
gap> F := FreeGroup("g", "x");;
gap> AssignGeneratorVariables(F);
#I  Assigned the global variables [ g, x ]
gap> Q := F / [g^9, x^2 * g * x^-1 * g^3, x^6];;
gap> AssignGeneratorVariables(Q);
#I  Global variable 'g' is already defined and will be overwritten
#I  Global variable 'x' is already defined and will be overwritten
#I  Assigned the global variables [ g, x ]
gap> u := x^-1 * g^2 * x^-1 * g^3 * x^-1 * g^5 * x;;
```

```
gap> w := u * g^6 * u * g^6 * u;;

gap> w = g^3;

false
```
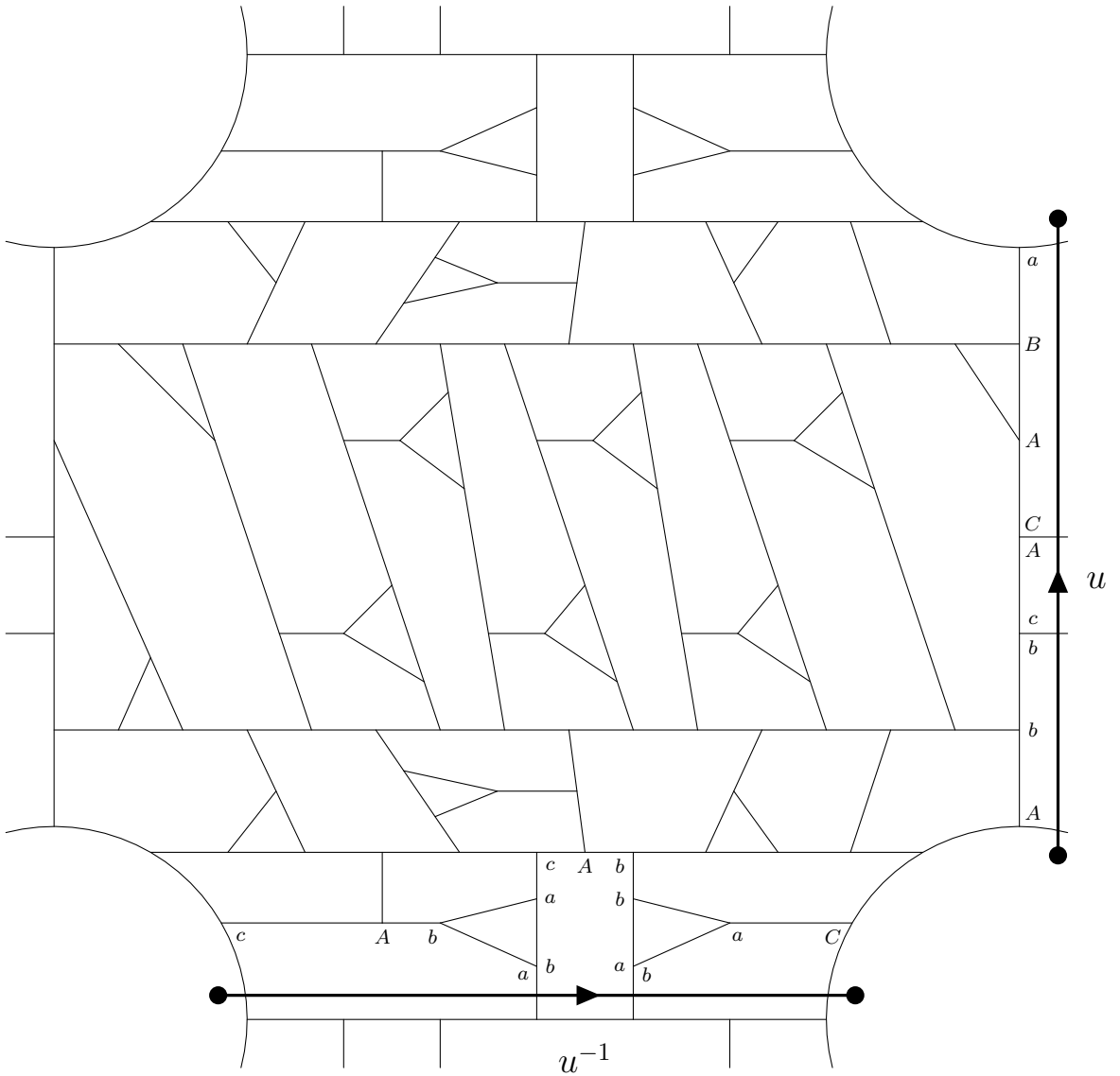

FIGURE 5.3: Explicit paths for $u = x^{-1}g^2x^{-1}g^3x^{-1}g^5x$ in the case $\langle G, x \mid x^2gx^{-1}g^3 \rangle$ where $|g| = 9$ (compare with Figure 4.3)

5.2 Proof of Theorem B

Let $\mathcal{P} = \langle G, x \mid x^2 g x^{-1} g^{-3} \rangle$ where G is cyclic of order 9 generated by g, and recall the reduced spherical picture depicted in Figure 4.9. Figure 5.4 depicts a loop drawn over this picture, where labels represent the words read as the path passes along the labeled segments. Here the corner labels represent the elements of G by the correspondence $a = A = 1$, $b = g$, $B = g^{-1}$, $c = g^{-3}$, and $C = g^3$. As in the proof of Theorem A, we follow the rule that arc arrows point towards b and B and point away from c and C (see Figures 2.5(i) and 2.5(ii)).

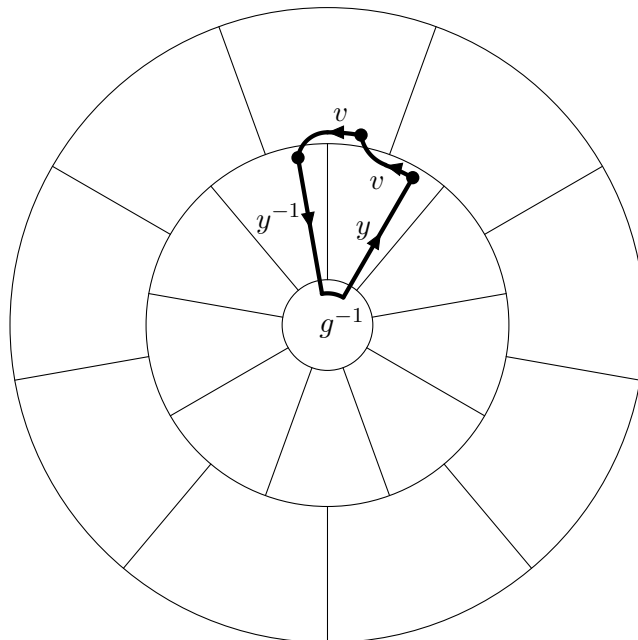
FIGURE 5.4: A loop in the picture over $\langle G, x \mid x^2 g x^{-1} g^{-3} \rangle$ where $|g| = 9$ (compare with Figure 4.9)

Explicit paths for y and v are given in Figure 5.5. We need to be careful when reading the words y and v where their respective paths meet. It is probably easiest to read v starting from the point labeled $*$ in Figure 5.5. As we travel along this path, we

cross into the identical adjacent sector. We read the word

$$v = cABacxaCAx^{-1}$$

which simplifies to

$$v = g^{-7}xg^3x^{-1}$$

We want the path ending at $*$ to read v as well, so we must choose y accordingly. Note that reading yv gives

$$yv = x^{-1}gxg^2xg^5xg^4x^{-1}g^{-1}xxg^3x^{-1}.$$

Solving for y gives

$$y = x^{-1}gxg^2xg^5xg^4x^{-1}g^{-1}xg^7.$$

The loop in Figure 5.4 reveals the conjugate relation

$$yv^2y^{-1}g^{-1} = 1.$$

Letting $w = yvy^{-1}$ we see that $w^2 = g$. Since g has order 9 in $G(\mathcal{P})$, w has order 9 or 18. If w has order 18, then we have a finite subgroup not isomorphic (and hence not conjugate) to a subgroup of G. Suppose then that w has order 9, so that $G(\mathcal{P}) \cong G(\mathcal{P})/\langle\!\langle w^9 \rangle\!\rangle$. A calculation in GAP shows that $G(\mathcal{P})/\langle\!\langle w^9 \rangle\!\rangle$ is finite of order 333, so we again have a finite subgroup not isomorphic (and hence not conjugate) to a subgroup of G. In either case, $\mathcal{P}$ is not aspherical by Theorem 2.2.5(a). The GAP calculations are faster if we use the fact that $w^9 = w(w^2)^4 = wg^4$. The commands are as follows.

```
gap> F := FreeGroup("g", "x");;
gap> AssignGeneratorVariables(F);
#I  Assigned the global variables [ g, x ]
gap> v := g^-7 * x * g^3 * x^-1;;
gap> y := x^-1 * g * x * g^2 * x * g^5 * x * g^4 * x^-1 * g^-1 * x * g^7;;
gap> w := y * v * y^-1;;
```
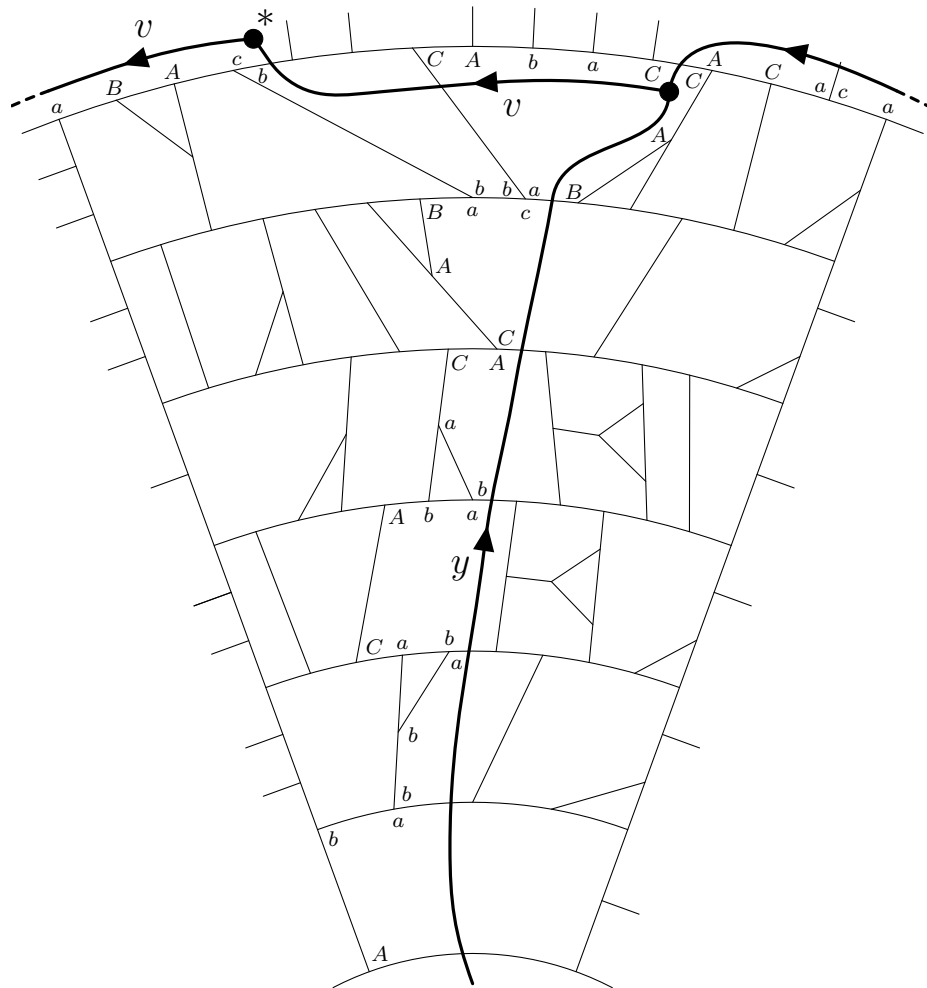
FIGURE 5.5: Explicit paths for u and y in the case $\langle G, x \mid x^2 g x^{-1} g^{-3} \rangle$ where $|g| = 9$ (compare with Figure 4.5)

```
gap> Q := F / [g^9, x^2 * g * x^-1 * g^-3, w * g^4];;

gap> Order(Q);

333
```

5.3 Proof of Theorems C and D

We offer a sketch of a proof of Theorem C. Edjvet proved in [21] that $\mathcal{P}$ is aspherical when $|g| = \infty$ or when none of (a)–(l) of Theorem C hold. He additionally gave explicit reduced spherical pictures over $\mathcal{P}$ in cases (a)–(h) and (j). A proof of non-asphericity in case (i) was reported by Bardakov and Vesnin in [3]. Cases (k) and (l) represent Theorems A and B respectively.

For each case (a)–(l), we show that at least one of the conditions (ii)–(iv) given in Theorem D holds. By Theorems 2.2.5(a) and 2.5.1(b) and Theorem B, these presentations are not aspherical. This has the effect of simultaneously proving Theorem D.

With the exception of cases (k) and (l), the proofs given here were previously known, and were developed by William Bogley. We thank Bogley for his personal communications on this topic. Let $n = |g|$. Proofs of the non-asphericity of $\mathcal{P}$ in cases (a)–(l) are as follows.

(a) $\dfrac{1}{|g|} + \dfrac{1}{|h|} + \dfrac{1}{|gh^{-1}|} > 1$: We break this case into a number of subcases.

- $h = g$: Inverting the relator of $\mathcal{P}$, applying the change of variables $x \mapsto t^{-1}$ and cyclicly permuting the resulting relator gives the presentation

$$\mathcal{V} = \langle G, t \mid t^2 g^{-1} t^{-1} g^{-1} \rangle.$$

  Using the retraction $\nu_2 \colon G(\mathcal{V}) \to G$ defined by $\nu_2(x) = g^2$ we find by a Reidemeister-Schreier rewriting process that $\ker(\nu_2) \cong S(2, n)$, so $G(\mathcal{P}) \cong S(2, n) \rtimes C_n$. For each $n \geq 2$, $S(2, n)$ is a 3-manifold group (reported in [40, Theorem 2], see [57, 12] for details).

- $|g| = |h| = 2$ and $|gh^{-1}| = q$: it is easy to check that $\langle\!\langle x \rangle\!\rangle$ has index 2 in $G(\mathcal{P})$. By applying the general Reidemeister-Schreier method, one can prove that $\langle\!\langle x \rangle\!\rangle$ is cyclic of order $3q$, so $|G(\mathcal{P})| = 6q$. The calculations are routine in this case, and we omit the details. Note that this does not follow the method

presented in Section 2.4, as here we do not use a retraction $G(\mathcal{P}) \to G$.

- **$|h| = 2$ and $|gh^{-1}| = 2$:** There is a retraction $\nu : G(\mathcal{P}) \to G$ defined by $\nu(x) = hg$. In Example 2.4.1 we found a presentation

$$\langle x_z \ (z \in G) \mid x_z x_{zhg} x_{zh}^{-1} \ (d \in G) \rangle.$$

for $\ker(\nu)$. Letting $z = e$ and $z = h$ gives the respective relators $x_e x_{hg} x_h^{-1}$ and $x_h x_g x_e^{-1}$. The product of these relators gives the relation

$$x_e x_{hg} x_g x_e^{-1} = 1.$$

We conclude that $x_{hg} = x_g^{-1}$ and hence $x_{zhg} = x_{zg}^{-1}$ for all $z \in G$. Letting $z = g^{1-i}$ and using the fact that $hg = g^{-1}h$ we have

$$x_{hg^i} = x_{g^{2-i}}^{-1},$$

so $\ker(\nu)$ is generated by $\{x_{g^i}\}_{0 \leq i < n}$. $\ker(\nu)$ then has a presentation

$$\langle x_{g^i} \ (0 \leq i < n) \mid x_{g^i} x_{g^{i+1}}^{-1} x_{g^{i+2}} \ (0 \leq i < n) \rangle.$$

Replacing each relator with a cyclic permutation of its inverse gives

$$\langle x_{g^i} \ (0 \leq i < n) \mid x_{g^i}^{-1} x_{g^{i+2}}^{-1} x_{g^{i+1}} \ (0 \leq i < n) \rangle.$$

A change of variables $t_i = x_{g^i}^{-1}$ reveals the presentation

$$\langle t_i \ (0 \leq i < n) \mid t_i t_{i+2} t_{i+1}^{-1} \ (0 \leq i < n) \rangle = \mathcal{S}(2, n).$$

Then $G(\mathcal{P}) \cong \mathcal{S}(2, n) \rtimes D_{2n}$, and $\mathcal{S}(2, n)$ is a 3-manifold group as in the previous case.

- **Spherical von Dyck groups:** there are 8 cases, each corresponding to one of the non-dihedral spherical von Dyck groups A_4, S_4, and A_5. Each case is

approached similarly. Let $p = |h|$ and $q = |gh^{-1}|$. A cyclic permutation of the relator $x^2gx^{-1}h$ shows that

$$xgx^{-1} \cdot hx = 1,$$

so $|xh| = |hx| = |g| = n$. We similarly find $x^{-1}hx \cdot xg = 1$ and deduce that $|xg| = |h| = p$. The element

$$(xg)(xh)^{-1} = xgh^{-1}x^{-1}$$

has order $|gh^{-1}| = q$. The group $J = \langle xg, xh \rangle$ is then a finite von Dyck group of the same type as G, so $J \cong G$. If $G(\mathcal{P})$ were aspherical, then J must also be conjugate to G. However, calculations in GAP show that the images of J and G are not conjugate in some finite quotient of $G(\mathcal{P})$. The results of these calculations are given in Table 5.1.

(n, p, q)	m	$|G(\mathcal{P})/\langle\!\langle x^m \rangle\!\rangle|$	$J \sim G?$
$(3, 3, 2)$	4	168	No
$(4, 3, 2)$	4	1440	No
$(5, 3, 2)$	4	14880	No
$(3, 2, 3)$	0	1440	No
$(3, 2, 4)$	7	168	No
$(3, 2, 5)$	8	14800	No
$(4, 2, 3)$	7	336	No
$(5, 2, 3)$	5	660	No

TABLE 5.1: GAP calculations show that in each case the finite subgroup $\langle xg, xh \rangle \cong G$ of $G(\mathcal{P})$ is not conjugate to G.

(b) $\boldsymbol{h = g^{-1}}$: The relation $x^2gx^{-1}g^{-1} = 1$ is equivalent to $gxg^{-1} = x^2$. We conclude that $x^{2^n-1} = 1$ and $G(\mathcal{P}) \cong \langle g, x \mid g^n, x^{2^n-1}, gxg^{-1} = x^2 \rangle \cong C_{2^n-1} \rtimes C_n$.

(c) $\mathbf{h = g^{-2}}$ **or** $\mathbf{g = h^{-2}}$: We can assume without loss of generality that $h = g^2$ (otherwise invert the relator of $\mathcal{P}$ and apply the change of variables $x \mapsto t^{-1}$). Note that $n \geq 3$, since otherwise $h = 1$. Using the retraction $\nu_1 \colon G(\mathcal{P}) \to G$ defined by $\nu_1(x) = g$ we find by a Reidemeister-Schreier rewriting process that $\ker(\nu_1) \cong F(2, n)$, so $G(\mathcal{P}) \cong F(2, n) \rtimes C_n$. If $n \geq 9$ is odd, then $F(2, n)$ has an element of order 2 [3, Proposition 3.1]. If $n \geq 4$ is even, then $F(2, n)$ is a 3-manifold group (reported in [40, Theorem 1], see [32, 34, 35, 14] for details). If $n = 3$, 5, or 7, then $F(2, n)$ is a nontrivial finite group [18, 31].

(d) $\mathbf{|h| = 2}$ **and** $\mathbf{[g, h] = 1}$: Note that $G = \langle h, g \rangle \cong C_2 \times C_n$. Using the retraction $\nu \colon G(\mathcal{P}) \to G$ defined by $\nu(x) = g^{-1}h$ we find by a Reidemeister-Schreier rewriting process that $\ker(\nu)$ has a presentation

$$\ker(\nu) \cong \langle x_z \ (z \in G) \mid x_{zg} x_{zh} x_{zgh}^{-1} \ (z \in G) \rangle.$$

Letting $z = 1$ and $z = h$ we get the respective relators $x_g x_h x_{gh}^{-1}$ and $x_{gh} x_1 x_g^{-1}$. The product of these relators gives the relation

$$x_g x_h x_1 x_g^{-1} = 1$$

We conclude that $x_h = x_1^{-1}$ and hence $x_{zh} = x_z^{-1}$ for all $z \in G$. Applying this identity to the relator $x_{zg} x_{zh} x_{zgh}^{-1}$ yields

$$x_{zg} x_z^{-1} x_{zg} = 1.$$

Solving for x_z gives $x_z = x_{zg}^2$ for all $z \in G$. We deduce that

$$\ker(\nu) \cong \langle x_1 \rangle \cong C_{2^n - 1},$$

so $G(\mathcal{P}) \cong C_{2^n - 1} \rtimes (C_2 \times C_n)$.

(e) $\mathbf{|g| = 3}$, $\mathbf{|h| = 2}$, **and** $\mathbf{(gh)^2 = (hg)^2}$: A calculation in GAP shows that $|G| = 18$ and $|G(\mathcal{P})| = 27216$.

(f) $|g| = |h| = 3$ and $[g, h] = 1$: A calculation in GAP shows that $|G(\mathcal{P})| = 13608$.

(g) $|g| = 6$ and $h = g^2$: A calculation in GAP shows that $|G(\mathcal{P})| = 336$.

(h) $|g| = 7$, and $h = g^2$ or $g = h^2$: Briefly, $G(\mathcal{P}) \cong H(7,3) \rtimes C_7$, and $H(7,3)$ has an element of order 2 (see [10, Example 4.3(c)] for details).

(i) $|g| = 8$, and $h = g^2$: Using the retraction $\nu_5 \colon G(\mathcal{P}) \to G$ defined by $\nu_5(x) = g^5$ we find that $G(\mathcal{P}) \cong \ker(\nu_5) \rtimes G$. A Reidemeister-Schreier rewriting process gives the presentation

$$\mathcal{G}_8(5, 6) = \mathcal{G}_8(x_0 x_5 x_6^{-1})$$

for $\ker(\nu_5)$. In [3, Table 4] this group was found to have order 295245. Alternatively, the order of $G(\mathcal{P})$ can be calculated easily with GAP by adding the relation $x^{24} = 1$. This relation can be deduced from the picture in Figure 3.5.

(j) $|g| = 9$, and $h = g^2$ or $g = h^2$: Briefly, $G(\mathcal{P}) \cong H(9,3) \rtimes C_7$, and $H(9,3)$ has an element of order 2 (see [10, Example 4.3(b)] for details).

(k) $|g| = 9$ and $h = g^3$: This is Theorem A.

(l) $|g| = 9$ and $h = g^{-3}$: This is Theorem B.

5.4 Proof of Theorem E

Let $\mathcal{P} = \langle G, x \mid x^2 g x^{-1} g^3 \rangle$ where G is cyclic of order 9 generated by g. Recall the picture over $\mathcal{P}$ given in Figure 4.1 and the word

$$u = x^{-1} g^2 x^{-1} g^3 x^{-1} g^5 x$$

read from Figure 5.3. We note two interesting relations involving u. From the loop in Figure 5.6 we obtain the relation

$$u \left(g x^{-1} g^2 x^{-1} \right) g^4 x \left(g x^{-1} g^2 x^{-1} \right)^{-1} = 1,$$

so u is conjugate to $(g^4 x)^{-1}$. From the loop in Figure 5.7 we obtain the relation

$$u^{-1}\left(g^{-2}x^{-1}g^3 x^{-1}g^{-1}\right)(g^4 x)^8 \left(g^{-2}x^{-1}g^3 x^{-1}g^{-1}\right)^{-1} = 1,$$

so u is conjugate to $(g^4 x)^8$. Together, these conjugacy relations reveal the Baumslag-Solitar relation

$$w(g^4 x)w^{-1} = (g^4 x)^{-8}$$

where w is some element of $G(\mathcal{P})$.

We now proceed with the proof of Theorem E. Assume that every finite subgroup of $G(\mathcal{P})$ has order dividing 18. Let $\nu \colon G(\mathcal{P}) \to G$ be the retraction defined by $\nu(x) = g^4$. Then $g^4 x = g^4(xg^4)g^{-4}$ corresponds to the generator $x_4 \in \ker(\nu) \cong H(9,4)$ via the Reidemeister-Schreier rewriting process ρ^4. Any generator x_i of $H(9,4)$ cannot be contained in the commutator subgroup, for if it were, then so too would be all of its shifts, and hence all of $H(9,4)$. Therefore, the image of x_4, and hence of x_4^{18}, is nontrivial in $H(9,4)^{\mathrm{ab}} \cong C_{19}$. In particular, $(g^4 x)^{18} = x_4^{18}$ is nontrivial in $G(\mathcal{P})$. By our assumption, $g^4 x$ must then have infinite order. We can also conclude that w has infinite order, since otherwise repeated conjugation would give $(g^4 x)^{(-8)^{18}} = g^4 x$.

Let H be any finite-index subgroup of $G(\mathcal{P})$. Since $g^4 x$ and w have infinite order, H must contain some nontrivial power of each, say $(g^4 x)^k$ and w^ℓ. We then have the relation

$$w^\ell (g^4 x)^k w^{-\ell} = (g^4 x)^{k(-8)^\ell}$$

in H. Since $(g^4 x)^k \in H$ has infinite order, we conclude from Proposition 2.5.6 that H is not a 3-manifold group.
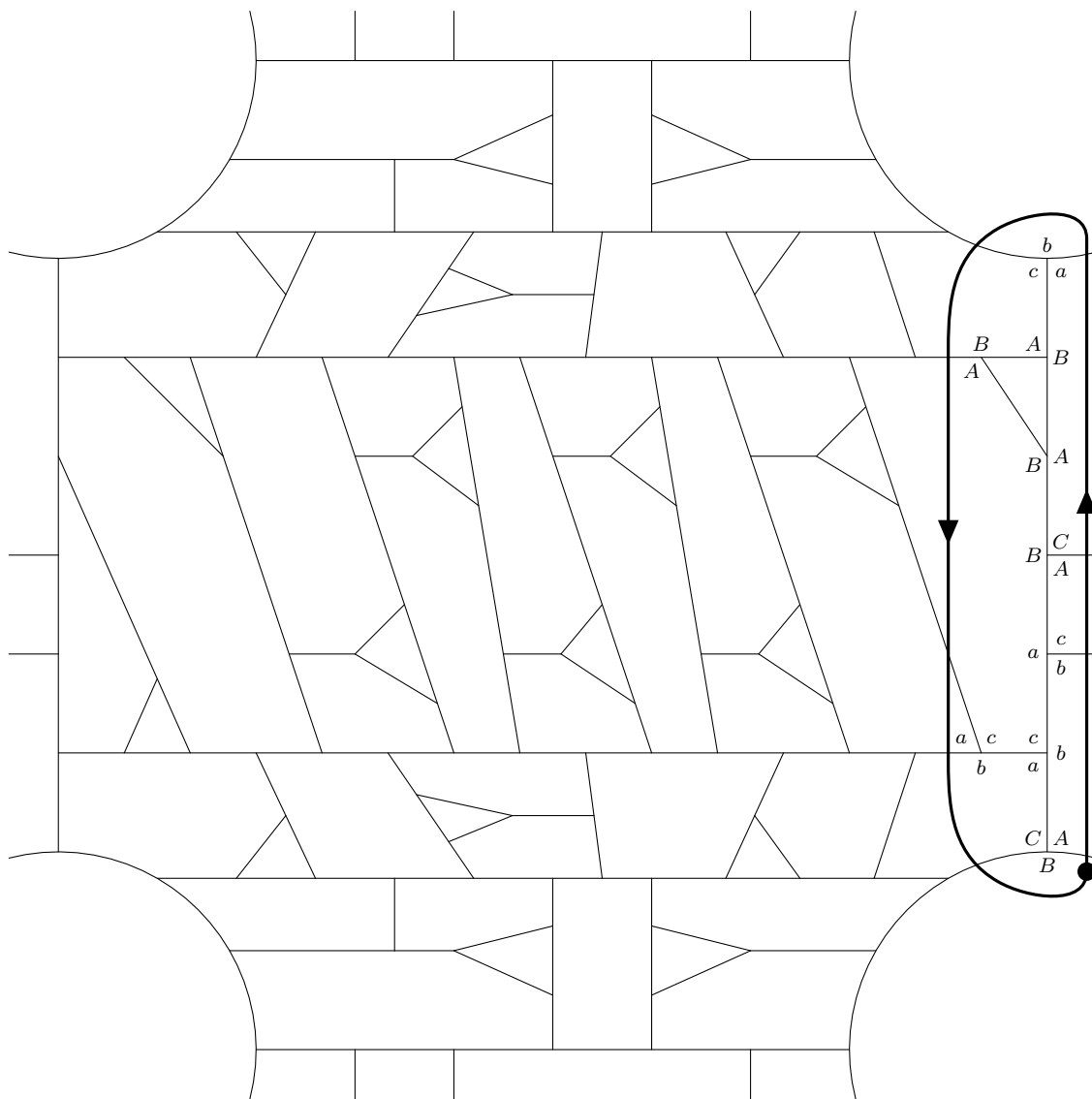
FIGURE 5.6: A path in a picture over $\mathcal{P}$ reveals that u is conjugate to $(g^4x)^{-1}$.
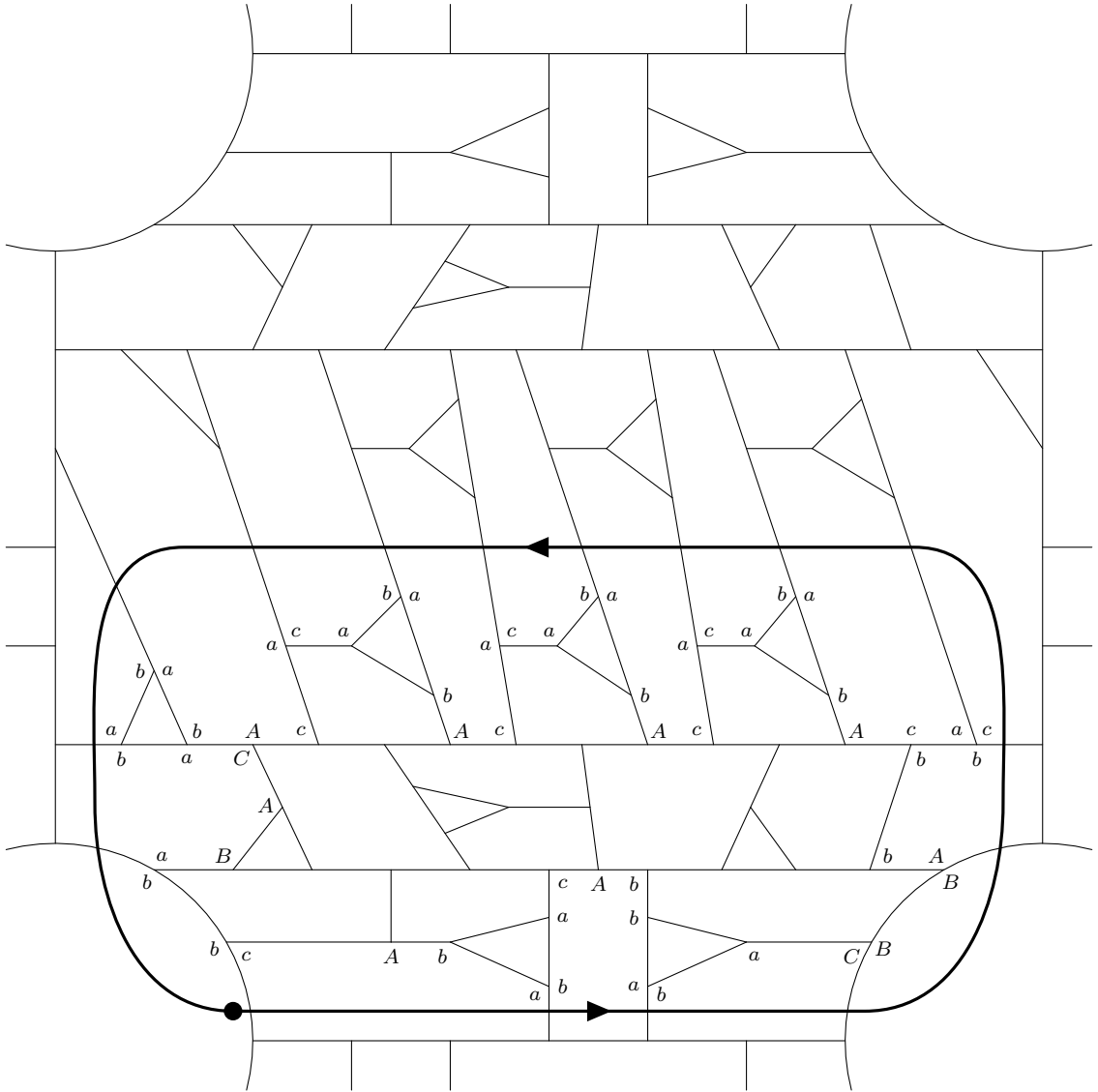
FIGURE 5.7: A path in a picture over $\mathcal{P}$ reveals that u is conjugate to $(g^4x)^8$.

5.5 Proofs of Theorems F and G

We collect these two proofs into a single section due to their similarity. We begin with a simple lemma.

Lemma 5.5.1. $H(9,4)$ *and* $H(9,7)$ *are 2-generated.*

Proof. We prove this fact for $H(9,7)$. A similar argument can be used to prove that $H(9,4)$ is 2-generated. A 2-generator presentation for $H(9,4)$ was found by Eamonn O'Brien and reported in [61].

To see that $H(9,7)$ is 2-generated, consider the presentation

$$\mathcal{H}(9,7) = \langle x_0, \ldots, x_8 \mid \theta^i(x_0 x_7 x_1^{-1}) \ (0 \leq i \leq 8) \rangle.$$

From the relators

$$x_2 x_0 x_3^{-1} \qquad x_5 x_3 x_6^{-1}$$
$$x_3 x_1 x_4^{-1} \qquad x_6 x_4 x_7^{-1}$$
$$x_4 x_2 x_5^{-1} \qquad x_7 x_5 x_8^{-1}$$

we can see that $x_2, x_4, x_5, x_6, x_7, x_8 \in \langle x_0, x_1, x_3 \rangle$. Using the above relations to rewrite x_7 gives

$$x_7 = x_6 x_4$$
$$= x_5 x_3 x_4$$
$$= x_4 x_2 x_3 x_4$$
$$= x_3 x_1 x_2 x_3^2 x_1$$
$$= x_3 x_1 x_3 x_0^{-1} x_3^2 x_1$$

The relation $x_0 x_7 x_1^{-1} = 1$ becomes

$$x_0 x_3 x_1 x_3 x_0^{-1} x_3^2 = 1,$$

so $x_1 = x_3^{-1} x_0^{-1} x_3^{-2} x_0 x_3^{-1} \in \langle x_0, x_3 \rangle$, and hence $H(9,7) = \langle x_0, x_3 \rangle$. □

5.5.1 Proof of Theorem F

Let $\mathcal{P} = \langle G, x \mid x^2 g x^{-1} g^3 \rangle$ where $G = \langle g \mid g^9 \rangle$. Then $H(9, 4)$ is isomorphic to the kernel of a retraction $\nu \colon G(\mathcal{P}) \to G$ as shown in Section 2.4, and hence $H(9, 4)$ has index 9 in $G(\mathcal{P})$. We noted in Section 2.5 that $H(9, 4)^{\mathrm{ab}} \cong C_{19}$ (see [61]). Consider first the infinite case.

Proposition 5.5.2. *If $H(9, 4)$ is infinite, then it is not a 3-manifold group.*

Proof. Assume that $H(9, 4)$ is infinite. If $H(9, 4)$ has a finite subgroup of order greater than 2, then it is not a 3-manifold group by Lemma 5.5.1 and Proposition 2.5.5, since $H(9, 4)^{\mathrm{ab}} \cong C_{19}$ is indecomposable.

Now assume that every finite subgroup of $H(9, 4)$ has order at most 2. If J is a finite subgroup of $G(\mathcal{P})$, then ν induces an isomorphism of $J/(J \cap \ker(\nu))$ onto a subgroup of G. Since $J \cap \ker(\nu)$ is either trivial or cyclic of order 2, we conclude that J has order dividing 18, so the conditions of Theorem E are satisfied. Since $H(9, 4)$ is a finite-index subgroup of $G(\mathcal{P})$, we conclude that $H(9, 4)$ is not a 3-manifold group. $\qquad\square$

With this proposition in hand, we now consider the possibility that $H(9, 4)$ is a finite 3-manifold group. Such groups are limited by the Elliptization Theorem to one of the types given in Theorem 2.5.4. Specifically, $H(9, 4) \cong C_m \times J$ where J is one of the groups (1)–(6) and $m \geq 1$ is relatively prime to the order of J. It is easy to check that J^{ab} has an element of order 2 or 3 unless $J = 1$ or $J = P_{120}$. Since $H(9, 4)^{\mathrm{ab}} \cong C_{19}$, we must have either $H(9, 4) \cong C_{19}$ or $H(9, 4) \cong C_{19} \times P_{120}$. However, neither of these cases is possible, as $H(9, 4)$ has the order-504 group $\mathrm{PSL}(2, 8)$ as a quotient (found by Eamonn O'Brien and reported in [61]).

5.5.2 Proof of Theorem G

Let $\mathcal{P} = \langle G, x \mid x^2 g x^{-1} g^{-3} \rangle$ where $G = \langle g \mid g^9 \rangle$. Then $H(9, 7)$ is isomorphic to the kernel of the retraction $\nu \colon G(\mathcal{P}) \to G$ defined by $\nu(x) = g^2$. We saw in the

proof of Theorem B that $v = g^{-7}xg^3x^{-1} \in G(\mathcal{P})$ has order either 9 or 18. Moreover, if v has order 9, then $G(\mathcal{P})$ is finite of order 333. We noted in Section 2.5 that $H(9,7)^{\mathrm{ab}} \cong C_{37}$ (see [61]).

Proposition 5.5.3. *If $H(9,7)$ is infinite, then it is not a 3-manifold group.*

Proof. Assume that $H(9,7)$ is infinite. Then v^9, considered as is an element of $H(9,7)$, must have order 2. Assume in order to reach a contradiction that $H(9,7)$ is isomorphic to the fundamental group of some 3-manifold M. Since $H(9,7)^{\mathrm{ab}}$ has odd order, $H(9,7)$ cannot have a quotient of order 2. In particular, M must be orientable, so condition (i) of Theorem 2.5.2 does not hold. Therefore $H(9,7)$ is the free product of two nontrivial cyclic groups by Lemma 5.5.1 and Proposition 2.5.5. However, $H(9,7)^{\mathrm{ab}} \cong C_{37}$ is indecomposable, a contradiction. $\qquad\square$

If $H(9,7)$ is assumed to be a finite 3-manifold group, the proof works similarly to the proof of Theorem F. We find that either $H(9,7) \cong C_{37}$ or $H(9,7) \cong C_{37} \times P_{120}$. Here P_{120} is the binary icosahedral group, which is a central extension of A_5 by C_2. Since every element of A_5 has order 1, 2, 3, or 5, every element of P_{120} has order dividing 4, 6, or 10.

Assume in order to reach a contradiction that $H(9,7) \cong C_{37} \times P_{120}$. If z is any element of order 37 in $H(9,7)$, then $H(9,7)/\langle\!\langle z \rangle\!\rangle \cong P_{120}$. Any generator x_i of $H(9,7)$ cannot be contained in the commutator subgroup, for if it were, then so too would be all of its shifts, and hence all of $H(9,7)$. In particular, the image of x_0 has order 37 in $H(9,7)^{\mathrm{ab}}$, so x_0 has order dividing 37. Then x_0^ℓ must have order exactly 37 for some $\ell \in \{4,6,10\}$, but calculations in GAP show that $H(9,7)/\langle\!\langle x_0^\ell \rangle\!\rangle \cong 1$ in each case. Therefore $H(9,7) \not\cong C_{37} \times P_{120}$. The only remaining case is $H(9,7) \cong C_{37}$.

5.6 Proof of Theorem H

Let $\mathcal{P} = \langle G, x \mid x^3 g^2 x^{-1} g \rangle$ where G is cyclic of order 6 generated by g, and recall the picture depicted in Figure 4.10. A circular loop in this picture is given in Figure 5.8. Using the identifications $a = A = b = B = 1$, $c = g^2$, $C = g^{-2}$, $d = g$, and $D = g^{-1}$ along with the rule that arc arrows point towards d and D, we can read the relation

$$(xg^{-1})^{12} = 1$$

in $G(\mathcal{P})$. Calculations in GAP show that $|G(\mathcal{P})/\langle\!\langle (xg^{-1})^4 \rangle\!\rangle| = 4$ and $|G(\mathcal{P})/\langle\!\langle (xg^{-1})^6 \rangle\!\rangle| = 78$. If is easy to check that $G(\mathcal{P})^{\mathrm{ab}} \cong C_{12}$, which is not a factor of 4 or 78. Therefore xg^{-1} has order 12 in $G(\mathcal{P})$. The GAP commands are as follows.

```
gap> F := FreeGroup("g", "x");;
gap> AssignGeneratorVariables(F);
#I  Assigned the global variables [ g, x ]
gap> P := F / [g^6, x^3 * g^2 * x^-1 * g, (x * g^-1)^4];;
gap> Order(P);
4
gap> Q := F / [g^6, x^3 * g^2 * x^-1 * g, (x * g^-1)^6];;
gap> Order(Q);
78
```
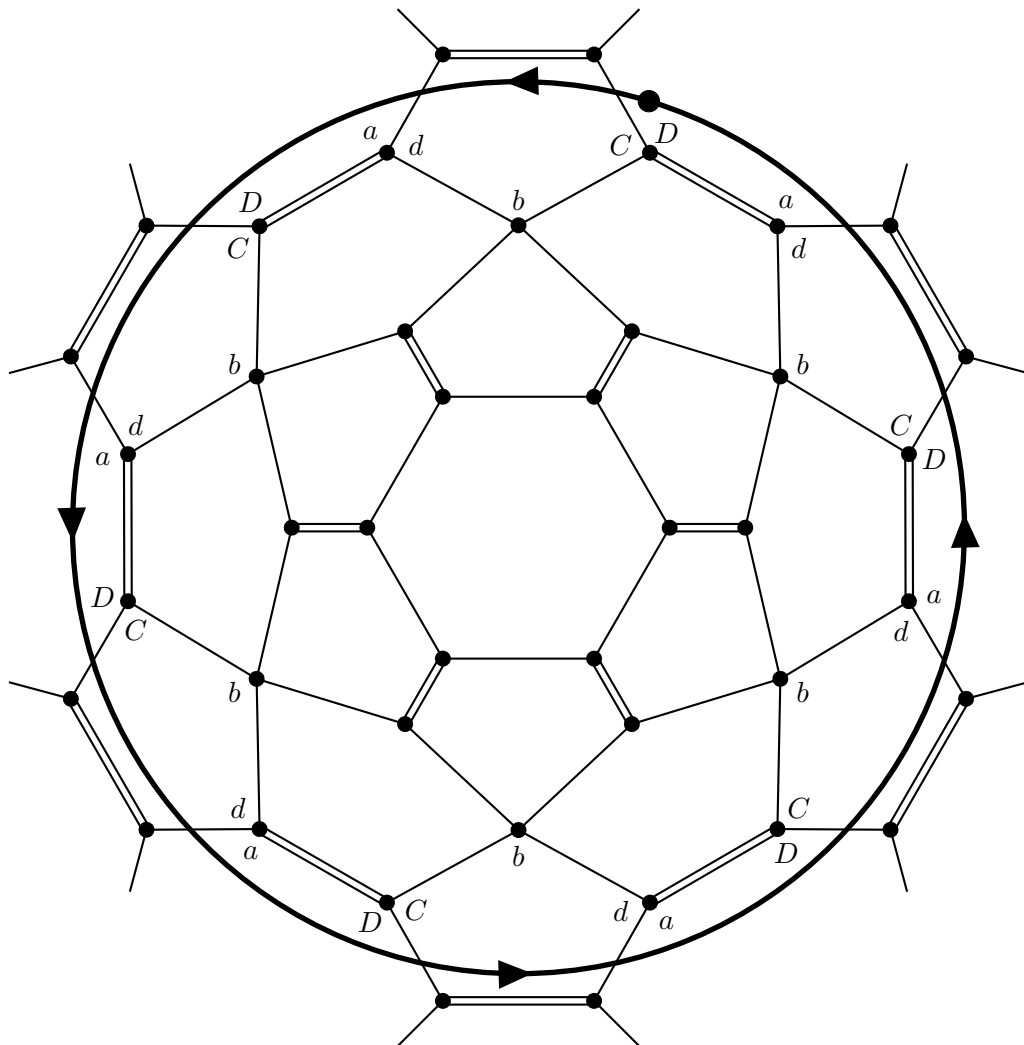
FIGURE 5.8: A path in a picture over $\mathcal{P}$ reveals the relation $(xg^{-1})^{12} = 1$.

6   CONCLUSIONS

We conclude this dissertation with a discussion of unresolved questions and future avenues of research. In Section 3.5 we discussed possible modifications to our picture searching method to overcome its limitations. Based on encouraging results with our limited search method, we believe that further development of automated tools for study pictures is warranted.

Our method is intended to prove that a presentation is not aspherical. A common technique for proving the opposite is to use curvature arguments to show that reduced spherical pictures over a presentation $\mathcal{P}$ cannot exist. One of the simplest formulations of this argument is the weight test, which specifies a curvature for each edge of the star graph $\mathcal{P}^{\mathrm{st}}$, and hence for each corner of a picture $\mathbb{P}$ over $\mathcal{P}$. It is then possible to define a curvature γ at each vertex v and face f of $\mathbb{P}$ so that these curvatures satisfy a Gauss-Bonnet formula

$$\sum_v \gamma(v) + \sum_f \gamma(f) = 2\pi\chi(S^2) = 4\pi.$$

Under certain conditions, it can be shown that this curvature is nonpositive at every vertex and face, so the picture $\mathbb{P}$ cannot exist (see [8, Section 1.1]).

While the weight test is easy to apply and is often effective, there are many presentations for which it is insufficient. In some of these cases, it is possible to define curvatures so that any region of positive curvature is sufficiently compensated by regions of negative curvature (see [10, Section 3.3]). Proofs of this type were pioneered by Edjvet in [21]. As further presentations have been considered, these proofs have become increasingly difficult, usually involving a complicated case analysis (e.g., see [22]) and often still leaving some unresolved cases (e.g., see [5]). Just as an automated approach to picture building produced pictures that likely could not have been constructed by hand, we wonder if an automated approach to curvature distribution might provide proofs that could not have

been found by hand. Understanding these difficult cases could give insight into the tension between the group theoretic and topological aspects of asphericity.

We now note some of the unresolved questions regarding the groups $H(9,4)$ and $H(9,7)$. The most notable problem is the finiteness question.

Question 1. Is $H(9,4)$ infinite?

Question 2. Is $H(9,7)$ infinite?

Many of the techniques used for other groups of Fibonacci type have been insufficient. Their presentations are not aspherical, and they do not satisfy the $C(3)$-$T(6)$ small cancellation condition [39]. Newman's criterion [51] requires the existence of large finite quotients, but so far the only known nontrivial proper quotients of $H(9,4)$ and $H(9,7)$ are $\mathrm{PSL}(2,8) \times C_{19}$ and its factors for $H(9,4)$ and C_{37} for $H(9,7)$. Holt [36] gave an alternate computer proof that $F(2,9)$ is infinite by showing that it is automatic and using the corresponding automatic structure to prove that its generators have infinite order. $H(9,4)$ and $H(9,7)$ have resisted all attempts to find an automatic structure.

A possibly promising idea is the non-computational proof that $F(2,9)$ is infinite given by Chalk [15]. This proof relies on reducing spherical pictures over $\mathcal{F}(2,9)$ with respect to a known spherical picture and using curvature arguments to show that certain elements have infinite order. However, the spherical picture over $\mathcal{F}(2,9)$ is much smaller than those that we can construct over $\mathcal{H}(9,4)$ and $\mathcal{H}(9,7)$. A proof of this type, if it exists, may require an infeasible case analysis. Still, we remain hopeful that the insights gained from our pictures may help to solve this problem.

Regarding Theorem D, we ponder the following questions.

Question 3. Is $H(9,4)$ torsion-free?

Question 4. Is $H(9,4)$ a virtual 3-manifold group?

We can conclude from Theorem E that if $H(9, 4)$ is torsion free, then it is not a virtual 3-manifold group. We showed that $H(9, 7)$ has nontrivial torsion, but we were not able to determine the exact nature of a torsion element. Either a particular element has order 2 or the group is cyclic of order 37. This leads to the following question.

Question 5. Is $H(9, 7)$ cyclic of order 37?

We believe it is not, although we present no particular evidence for this belief. Theorem G shows that this is equivalent to the 3-manifold question, so a resolution would complete the 3-manifold classification for groups of Fibonacci type.

BIBLIOGRAPHY

1. Daniel Adler, Duncan Murdoch, and others. *rgl: 3D Visualization Using OpenGL*, 2018. R package version 0.99.16.

2. Matthias Aschenbrenner, Stefan Friedl, and Henry Wilton. *3-Manifold Groups*. EMS Series of Lectures in Mathematics. European Mathematical Society, 2015.

3. V. G. Bardakov and A. Yu. Vesnin. A generalization of Fibonacci groups. *Algebra and Logic*, 42:73–91, 2003.

4. Abd Ghafur Bin Ahmad. *The application of pictures to decision problems and relative presentations*. PhD thesis, University of Glasgow, 1995.

5. Abd Ghafur Bin Ahmad, Muna A Al-Mulla, and Martin Edjvet. Asphericity of a length four relative group presentation. *Journal of Algebra and Its Applications*, page 1750076, 2016.

6. William Bogley. On shift dynamics for cyclically presented groups. *Journal of Algebra*, 418:154–173, 2014.

7. William Bogley and Stephen Pride. Aspherical relative presentations. *Proceedings of the Edinburgh Mathematical Society*, 35:1–39, 02 1992.

8. William Bogley and Stephen Pride. Calculating generators of Π_2. In Cynthia Hog-Angeloni, Wolfgang Metzler, and Allan J. Sieradski, editors, *Two-Dimensional Homotopy and Combinatorial Group Theory*, chapter 5, pages 157–188. Cambridge Univ. Press, Cambridge, 1993.

9. William Bogley and Gerald Williams. Efficient finite groups arising in the study of relative asphericity. *Mathematische Zeitschrift*, 284, 2016.

10. William A. Bogley, Martin Edjvet, and Gerald Williams. Aspherical relative presentations all over again. In *Groups St Andrews 2017 in Birmingham*, volume 455 of *London Math. Soc. Lecture Note Ser.*, pages 169–199. Cambridge Univ. Press, Cambridge, 2019.

11. A. M. Brunner. The determination of Fibonacci groups. *Bulletin of the Australian Mathematical Society*, 11:11, 1974.

12. A. Cavicchioli, F. Hegenbarth, and A. C. Kim. A geometric study of Sieradski groups. *Algebra Colloquium*, 5:203–217, 01 1998.

13. Alberto Cavicchioli, Dušan Repovš, and Fulvia Spaggiari. Topological properties of cyclically presented groups. *Journal of Knot Theory and Its Ramifications*, 12:243–268, 2003.

14. Alberto Cavicchioli and Fulvia Spaggiari. The classification of 3-manifolds with spines related to Fibonacci groups. In *Algebraic Topology Homotopy and Group Cohomology*, pages 50–78. Springer Berlin Heidelberg, 1992.

15. Christopher P. Chalk. Fibonacci groups with aspherical presentations. *Communications in Algebra*, 26:1511–1546, 1998.

16. Ian M. Chiswell, Donald J. Collins, and Johannes Huebschmann. Aspherical group presentations. *Mathematische Zeitschrift*, 178:1–36, 1981.

17. J. H. Conway. Advanced problem 5327. *American Mathematical Monthly*, 72:915, 1965.

18. J. H. Conway, J. A. Wenzel, R. C. Lyndon, and Harley Flanders. Solution to advanced problem 5327. *American Mathematical Monthly*, 74:91, 1967.

19. Gabor Csardi and Tamas Nepusz. The igraph software package for complex network research. *InterJournal*, Complex Systems:1695, 2006.

20. M. Edjvet. Equations over groups and a theorem of Higman, Neumann, and Neumann. *Proceedings of the London Mathematical Society*, s3-62:563–589, 1991.

21. Martin Edjvet. On the asphericity of one-relator relative presentations. *Proceedings of the Royal Society of Edinburgh Section A Mathematics*, 124:713–728, 1994.

22. Martin Edjvet and Arye Juhász. The infinite Fibonacci groups and relative asphericity. *Transactions of the London Mathematical Society*, 4:148–218, 2017.

23. D. B. A. Epstein. Projective planes in 3-manifolds. *Proceedings of the London Mathematical Society*, s3-11:469–484, 1961.

24. The GAP Group. *GAP – Groups, Algorithms, and Programming, Version 4.11.0*, 2020.

25. N. D. Gilbert and J. Howie. LOG groups and cyclically presented groups. *Journal of Algebra*, 174:118–131, 1995.

26. I. A. Grushko. Über die basen eines freien produktes von gruppen. *Matematicheskii Sbornik*, 8:169–182, 1940.

27. Richard S. Hamilton. Three-manifolds with positive Ricci curvature. *Journal Of Differential Geometry*, 17:255–306, 1982.

28. Richard S. Hamilton. Non-singular solutions of the Ricci flow on three-manifolds. In C. C. Hsiung and S. T. Yau, editors, *Surveys in Differential Geometry, Vol. 2: Proceedings of the conference on geometry and topology held at Harvard University, April 23-25, 1993*, volume 2, pages 7–136. International Press of Boston, 1995.

29. Richard S. Hamilton. Non-singular solutions of the Ricci flow on three-manifolds. *Communications in Analysis and Geometry*, 7:695–729, 1999.

30. Allen Hatcher. *Algebraic topology*. Cambridge University Press, 2001.

31. George Havas. Computer aided determination of a Fibonacci group. *Bulletin of the Australian Mathematical Society*, 15:297, 1976.

32. H. Helling, A. C. Kim, and J. L. Mennicke. A geometric study of Fibonacci groups. *Journal of Lie Theory*, 8(1):1–23, 1998.

33. John Hempel. *3-Manifolds*. Annals of Mathematics Studies 86. Princeton University Press, 1976.

34. Hugh Hilden, M. Lozano, and Jos Montesinos. On a remarkable polyhedron geometrizing the figure eight knot cone manifolds. *Journal of Mathematical Sciences. The University of Tokyo*, 2:501–561, 01 1995.

35. Hugh Michael Hilden, María Teresa Lozano Imízcoz, and José María Montesinos Amilibia. The arithmeticity of the figure eight knot orbifolds. In Boris Apanasov, Walter D. Neumann, Alan W. Reid, and Laurent Siebenmann, editors, *Topology '90.*, number 1 in Ohio State University Mathematical Research Institute Publications, pages 169–183. Walter de Gruyter & Co, Berlin, 1992. Papers from the Research Semester in Low-dimensional Topology held at Ohio State University, Columbus, Ohio, February–June 1990.

36. Derek F. Holt. An alternative proof that the Fibonacci group $F(2,9)$ is infinite. *Experimental Mathematics*, 4:97–100, 1995.

37. Heinz Hopf. Zum Clifford-Kleinschen raumproblem. *Mathematische Annalen*, 95:313–339, 1926.

38. James Howie. The solution of length three equations over groups. *Proceedings of the Edinburgh Mathematical Society*, 26:89–96, 1983.

39. James Howie and Gerald Williams. Tadpole labelled oriented graph groups and cyclically presented groups. *Journal of Algebra*, 371, 2012.

40. James Howie and Gerald Williams. Fibonacci type presentations and 3-manifolds. *Topology and its Applications*, 215:24–34, 2017.

41. Johannes Huebschmann. Aspherical 2-complexes and an unsettled problem of J. H. C. Whitehead. *Mathematische Annalen*, 258:17–37, 1981.

42. D. L. Johnson. *Topics in the Theory of Group Presentations*. London Mathematical Society Lecture Note Series. Cambridge University Press, 1 edition, 1980.

43. D. L. Johnson and H. Mawdesley. Some groups of Fibonacci type. *Journal of the Australian Mathematical Society*, 20:199–204, 1975.

44. P. H. Kropholler. A note on centrality in 3-manifold groups. *Mathematical Proceedings of the Cambridge Philosophical Society*, 107(2):261–266, 1990.

45. C. Maclachlan. Generalizations of Fibonacci numbers, groups and manifolds. In *Combinatorial and Geometric Group Theory, Edinburgh 1993*, London Mathematical Society Lecture Note Series, pages 233–238. International Press of Boston, 1995.

46. Wilhelm Magnus, Abraham Karrass, and Donald Solitar. *Combinatorial group theory: Presentations of groups in terms of generators and relations*. Dover Books on Mathematics. Dover Publications, 2 revised edition, 2004.

47. Kirk McDermott. *Topological and Dynamical Properties of Cyclically Presented Groups*. PhD thesis, Oregon State University, 2017.

48. Jens L. Mennicke. On Fibonacci groups and some other groups. In *Groups — Korea 1988: Proceedings of a Conference on Group Theory, held in Pusan, Korea, August 15–21, 1988*.

49. Matthias C. Merzenich. A program for finding reduced relative spherical pictures. Oregon State University. https://doi.org/10.7267/6395wf63g, 2020.

50. B. H. Neumann. On the number of generators of a free product. *Journal of the London Mathematical Society*, s1-18:12–20, 1943.

51. M. F. Newman. Proving a group infinite. *Archiv der Mathematik*, 54:209–211, 1990.

52. Grigori Perelman. The entropy formula for the Ricci flow and its geometric applications, 2002.

53. Grigori Perelman. Finite extinction time for the solutions to the Ricci flow on certain three-manifolds, 2003.

54. Grigori Perelman. Ricci flow with surgery on three-manifolds, 2003.

55. Matveî I. Prishchepov. Aspherisity, atorisity and simmetrically presented groups. *Communications in Algebra*, 23:5095–5117, 1995.

56. R Core Team. *R: A Language and Environment for Statistical Computing.* R Foundation for Statistical Computing, Vienna, Austria, 2018.

57. Allan J. Sieradski. Combinatorial squashings, 3-manifolds, and the third homology of groups. *Inventiones mathematicae*, 84:121–139, 1986.

58. J. H. C. Whitehead. Combinatorial homotopy. I. *Bulletin of the American Mathematical Society*, 55:213–246, 1949.

59. J. H. C. Whitehead. Combinatorial homotopy. II. *Bulletin of the American Mathematical Society*, 55:453–497, 1949.

60. Gerald Williams. The aspherical Cavicchioli-Hegenbarth-Repovš generalized Fibonacci groups. *Journal of Group Theory*, 12, 2009.

61. Gerald Williams. Groups of Fibonacci type revisited. *International Journal of Algebra and Computation*, 22:1240002, 2012.

APPENDIX

A   APPENDIX   Some Additional Spherical Pictures

In this appendix we collect the program output for a few additional relative presen-tations. These presentations have the form

$$\mathcal{J}_n(m, k) = \langle G, x \mid x^{m-k} g^3 x^k g^2 \rangle.$$

where $n \in \{4, 6\}$ and G is the cyclic group of order n generated by g. When $(m, k) = 1$, the groups defined by these presentations are finite [9, Theorem B(c)]. Orders for the groups considered here are listed explicitly in [9], and a picture for $\mathcal{J}_6(3, 1)$ is given in [9, Fig. 1]

Since these groups are finite, we have by Theorem 2.2.1 that the presentations are not aspherical. Thus they provided a useful testing ground for our program. We construct the explicit spherical pictures for $\mathcal{J}_4(5, 1)$ and $\mathcal{J}_4(5, 2)$. We give only the program output for $\mathcal{J}_4(4, 1)$ and $\mathcal{J}_6(4, 1)$. If a constraint such as `maxVertices` is not given as part of our input, it is assumed to be large enough that it does not influence the search. `symmetry` and `startWord` can be deduced from the output.

A.1 $\mathcal{J}_4(4, 1)$

Let $\mathcal{P} = \langle G, x \mid xaxbxcxd \rangle$ where $a = b = 1$, $c = g^3$, $d = g^2$, and $|g| = 4$. This is equivalent to $\mathcal{J}_4(4, 1)$. We use the input

- `maxFaces = 14`

- `maxHalfEdges = 8`

- `maxNewVertices = 2`

and get the following output:

0001 aD (x2)	0006 bA (hop)	0011 aDcD cD
0002 dC bC	0007 aDcB cB	0012 bCdC
0003 Ab (hop)	0008 aB (hop)	0013 aB
0004 aBcB cD	0009 dAdA	0014 Ad (x2)
0005 dC bC	0010 bA (hop)	

A.2 $\mathcal{J}_4(5, 1)$

Let $\mathcal{P} = \langle G, x \mid xaxbxcxdxe \rangle$ where $a = b = c = 1$, $d = g^3$, $e = g^2$, and $|g| = 4$. This is equivalent to $\mathcal{J}_4(5, 1)$. We use the input

- `maxHalfEdges = 12`

- `maxNewVertices = 4`

and get the following output:

0001 cD (x4)	0005 dEdC	0009 Ab
0002 bC	0006 cB	0010 Bc
0003 aB	0007 bA	0011 dC (x4)
0004 eA eDeD	0008 EaEa	

An explicit construction of this picture is given in Figure A.1.

A.3 $\mathcal{J}_4(5, 2)$

Let $\mathcal{P} = \langle G, x \mid xaxbxcxdxe \rangle$ where $a = b = d = 1$, $c = g^3$, $e = g^2$, and $|g| = 4$. This is equivalent to $\mathcal{J}_4(5, 2)$. We use the input

- `maxHalfEdges = 10`

- `maxNewVertices = 2`

and get the following output:
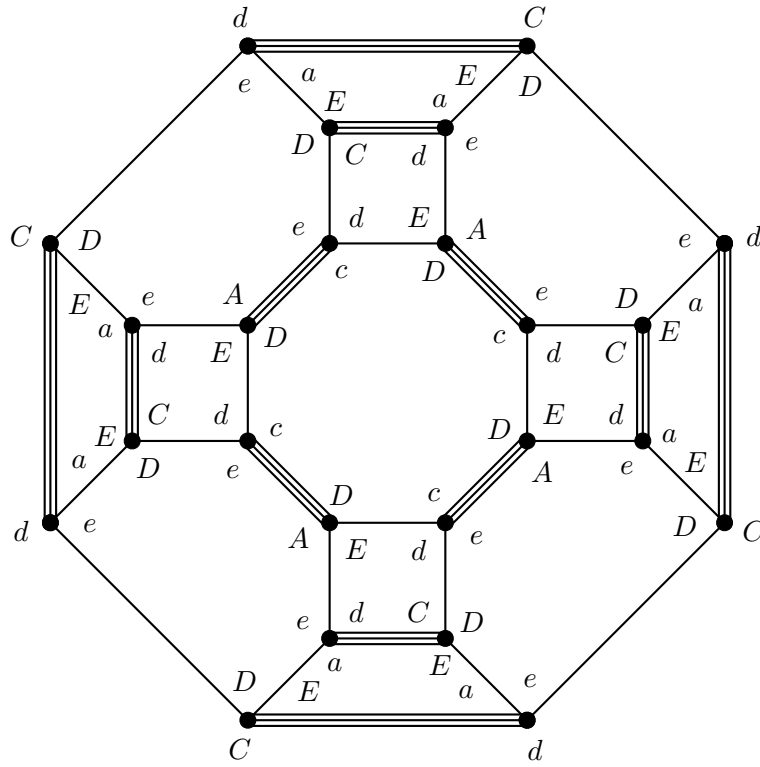
FIGURE A.1: A reduced spherical picture over $\mathcal{J}_4(5,1)$

0001	aC (x4)	0005	dA (hop)	0009	eCaC
0002	eB eB	0006	cEcE bE	0010	dB
0003	dA	0007	bD	0011	Ac (x4)
0004	Db (hop)	0008	aD (hop)		

An explicit construction of this picture is given in Figure A.2.

A.4 $\mathcal{J}_6(4,1)$

Let $\mathcal{P} = \langle G, x \mid xaxbxcxd \rangle$ where $a = b = 1$, $c = g^3$, $d = g^2$, and $|g| = 6$. This is equivalent to $\mathcal{J}_6(4,1)$. We use the input

- maxHalfEdges = 8

- maxNewVertices = 4
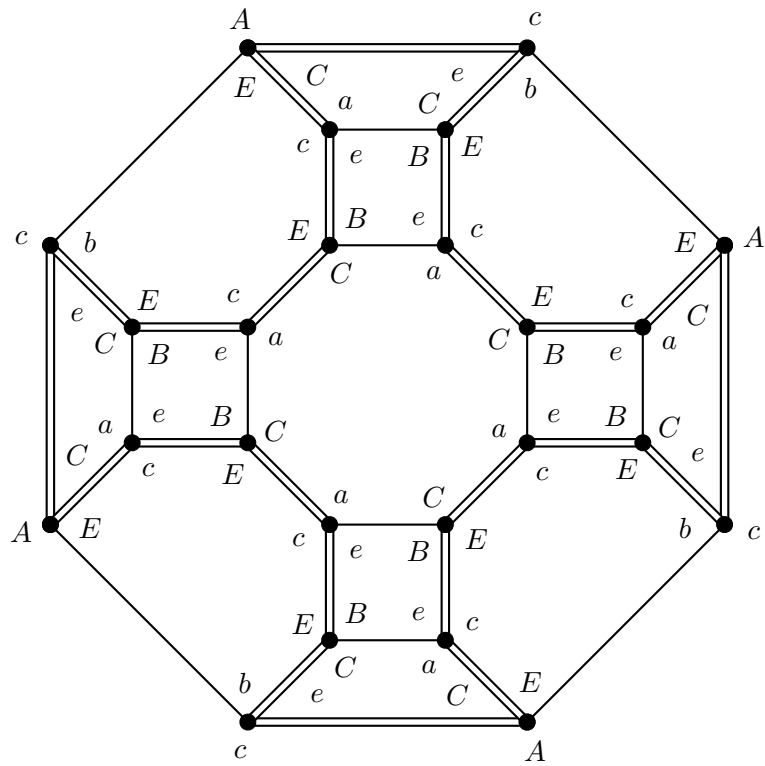
FIGURE A.2: A reduced spherical picture over $\mathcal{J}_4(5,2)$

and get the following output:

0001	dC (x6)	0007	Ab (hop)	0013	Ba
0002	cB cB	0008	cBcA	0014	Ba (hop)
0003	bA	0009	bD cDcD	0015	CbCb
0004	bA (hop)	0010	bCaC	0016	cD (x6)
0005	aDaD aD	0011	aB		
0006	dCdC dB	0012	AdAd Ad		

INDEX